AIRES Pty Ltd

Watching Volcanic Eruptions From Space:

How we use Satellites to Warn Aviation of the Threat from Ash Clouds

Dr Fred Prata
Director AIRES Pty Ltd
Visiting Professor, Curtin University, Western Australia

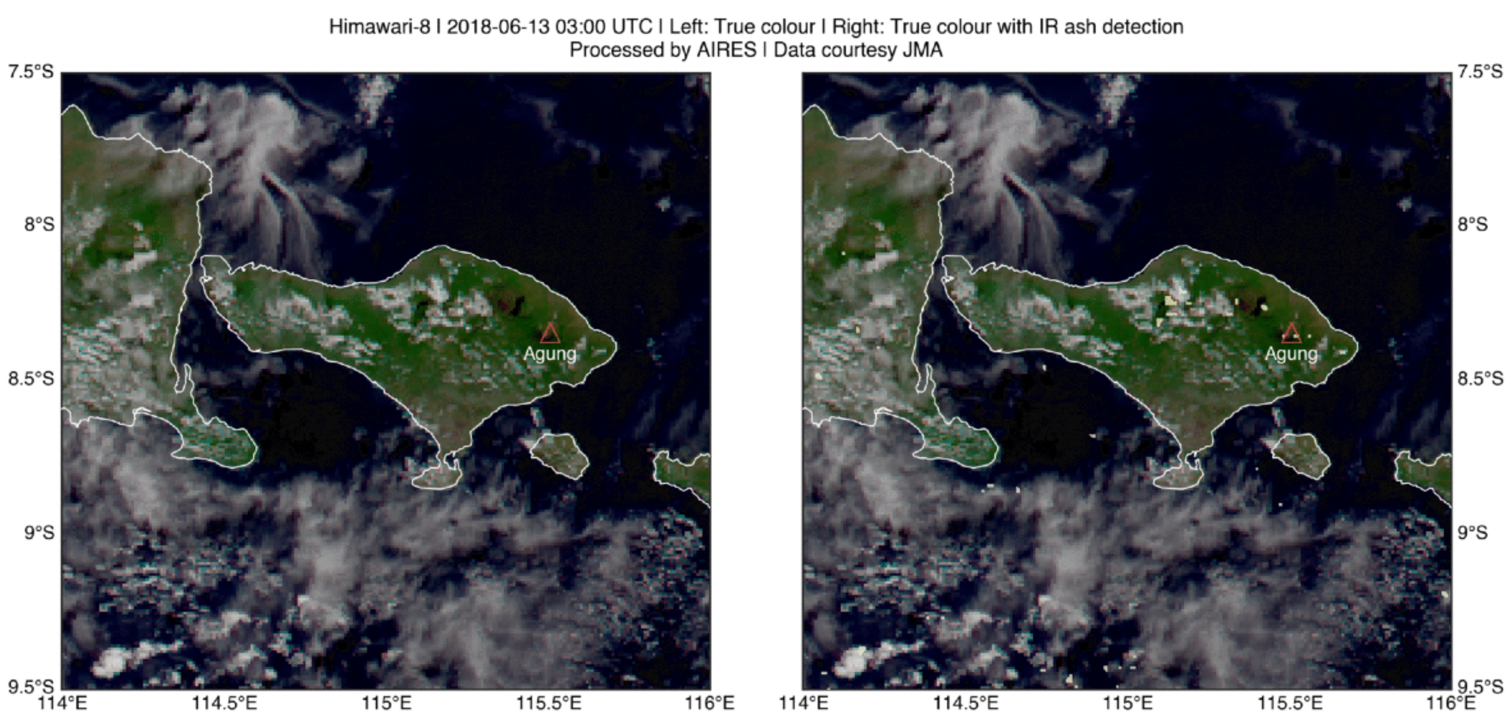

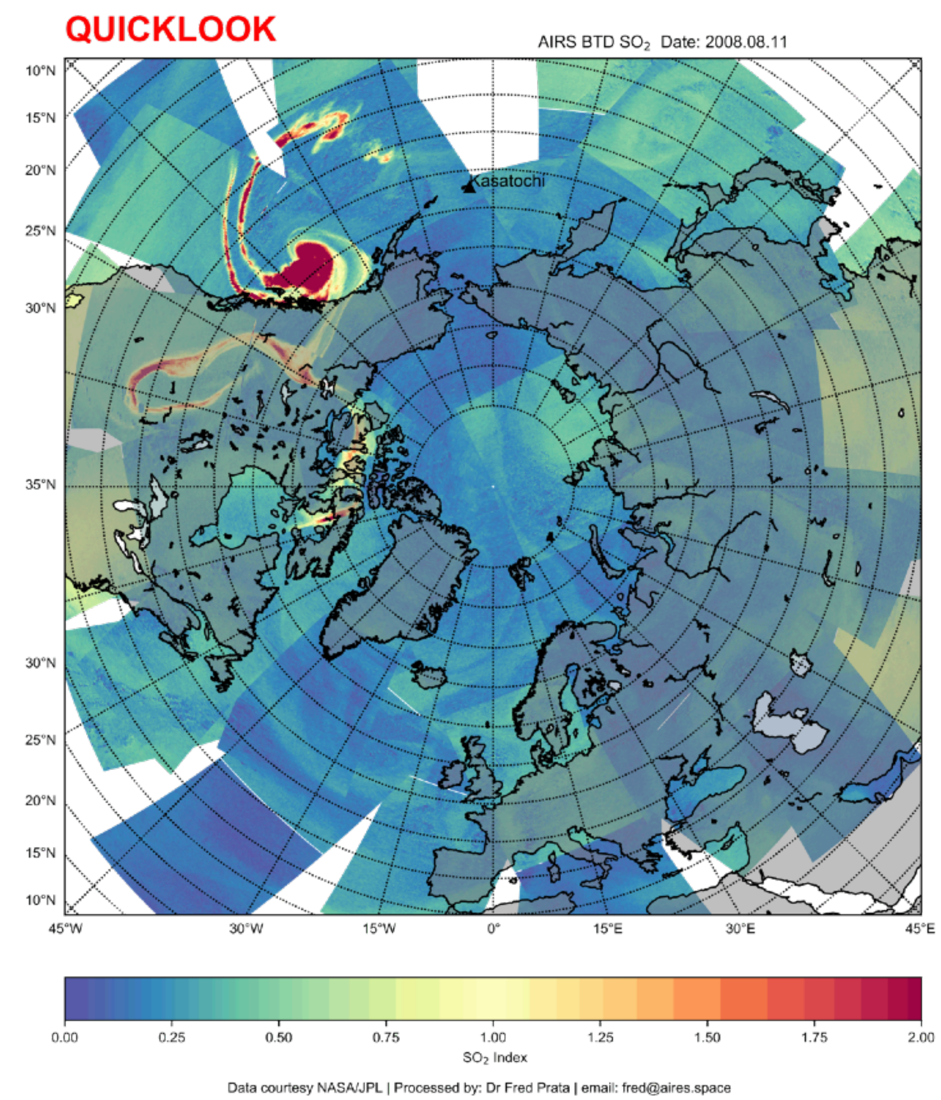

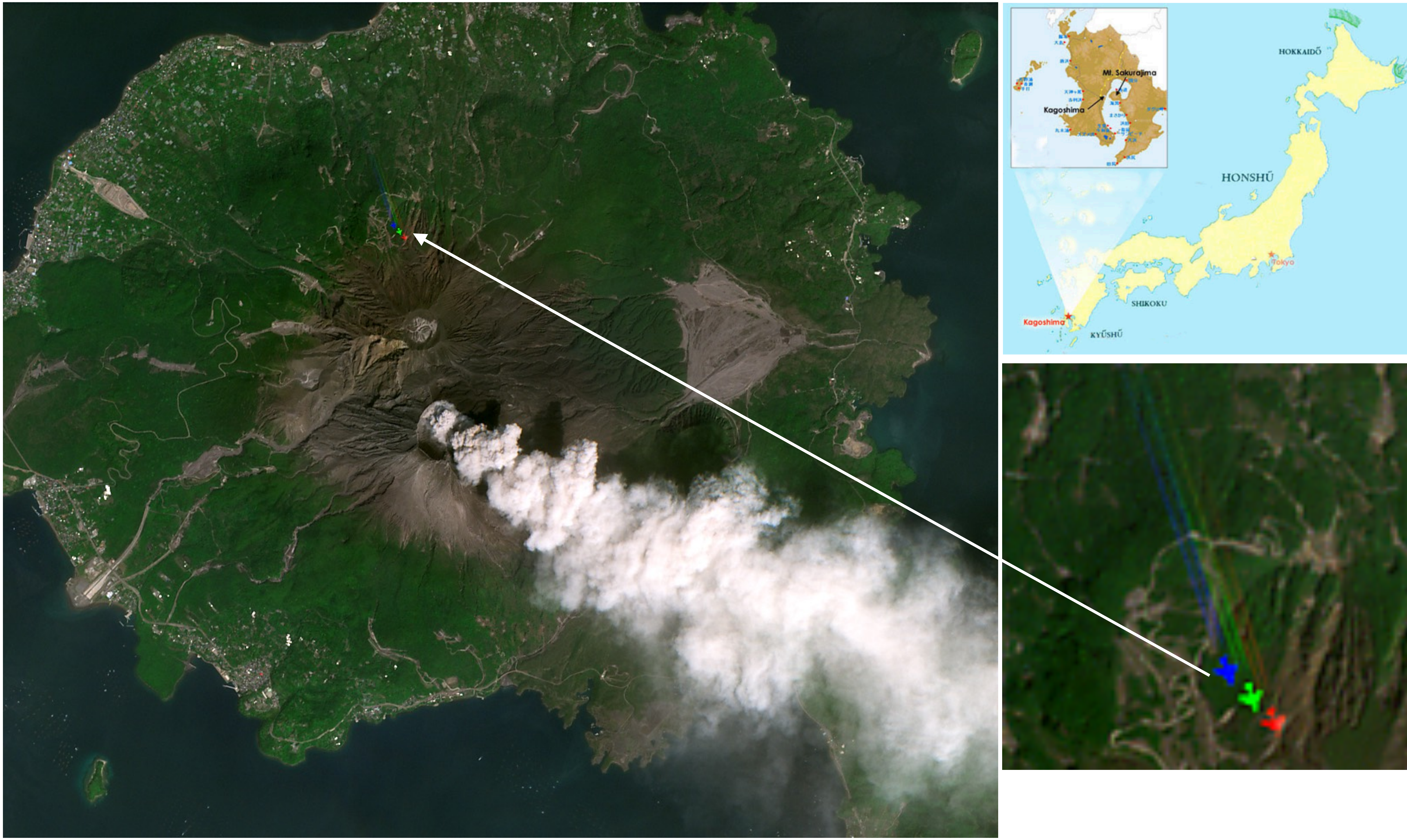

Sentinel-2 True-colour (RGB) image ~10 m resolution

Synopsis

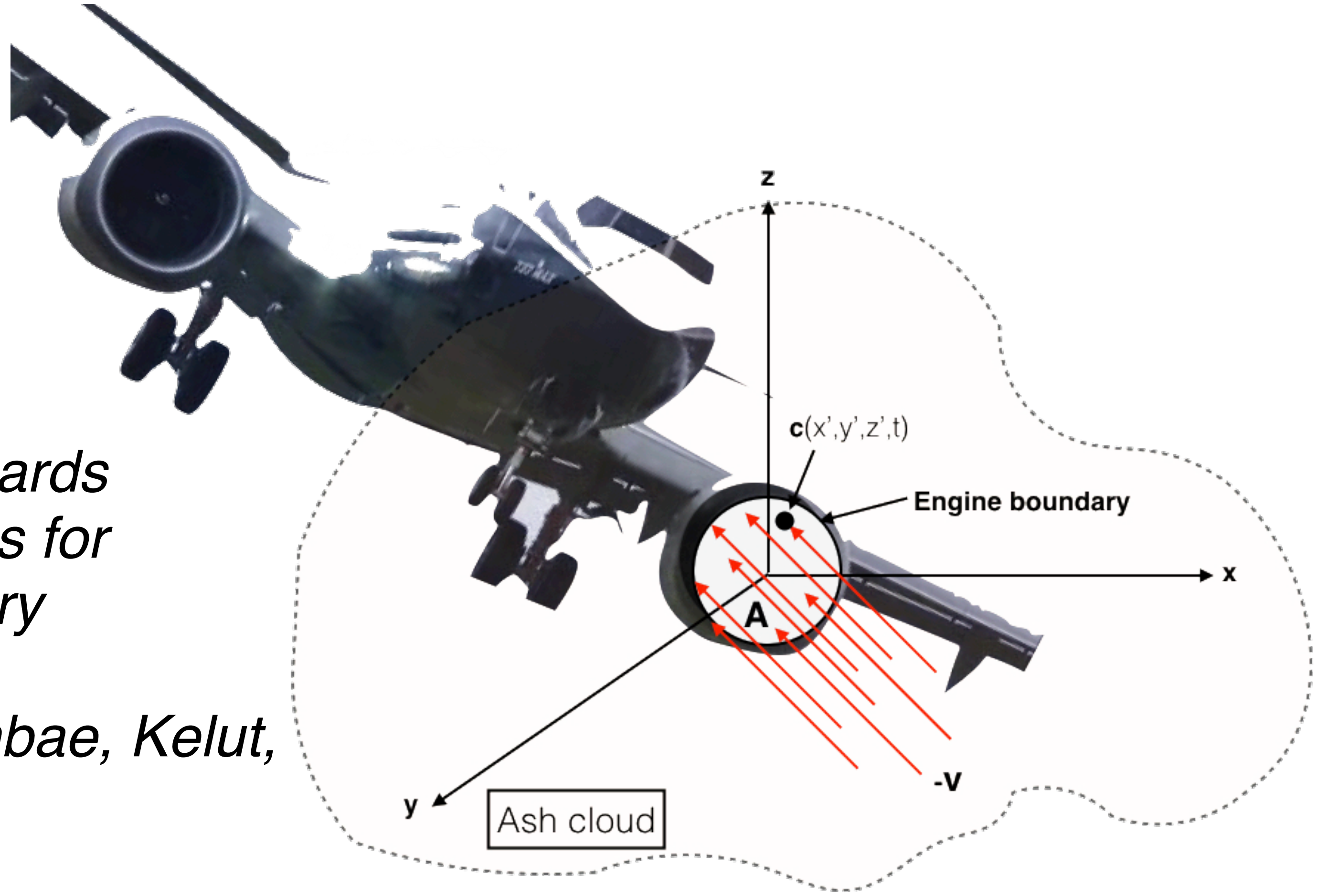

- Volcanoes: distribution, eruptions and hazards
- Satellites: polar and geostationary systems for watching volcanoes–how to use the imagery
- Infrared imagery: ash and gas detection
- Some examples: Eyjafjallajökull, Aoba/Ambae, Kelut, and others
- Cloud height and eruption rate

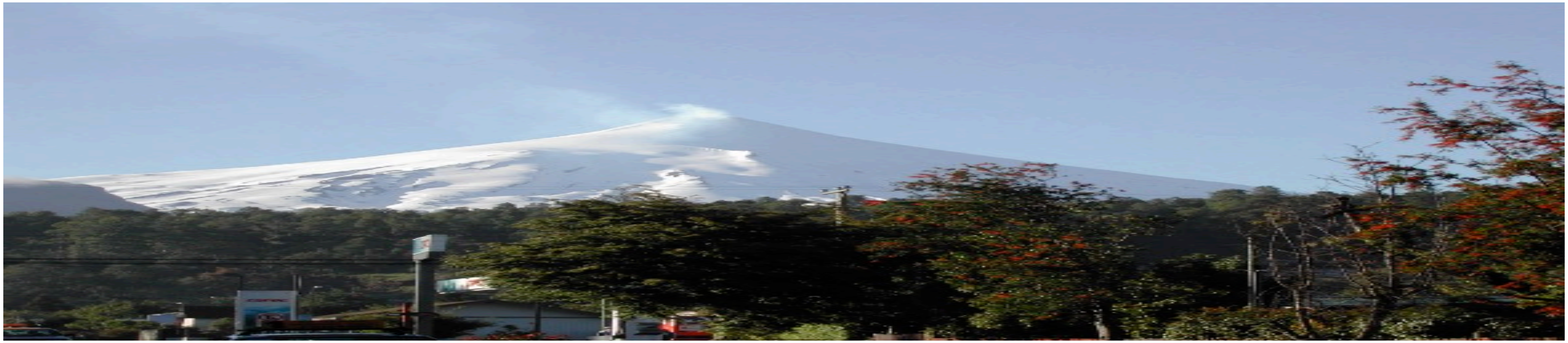

Volcanoes: distribution, eruptions and hazards

- Distribution
- Historic Eruptions
- Recent Eruptions
- Hazards

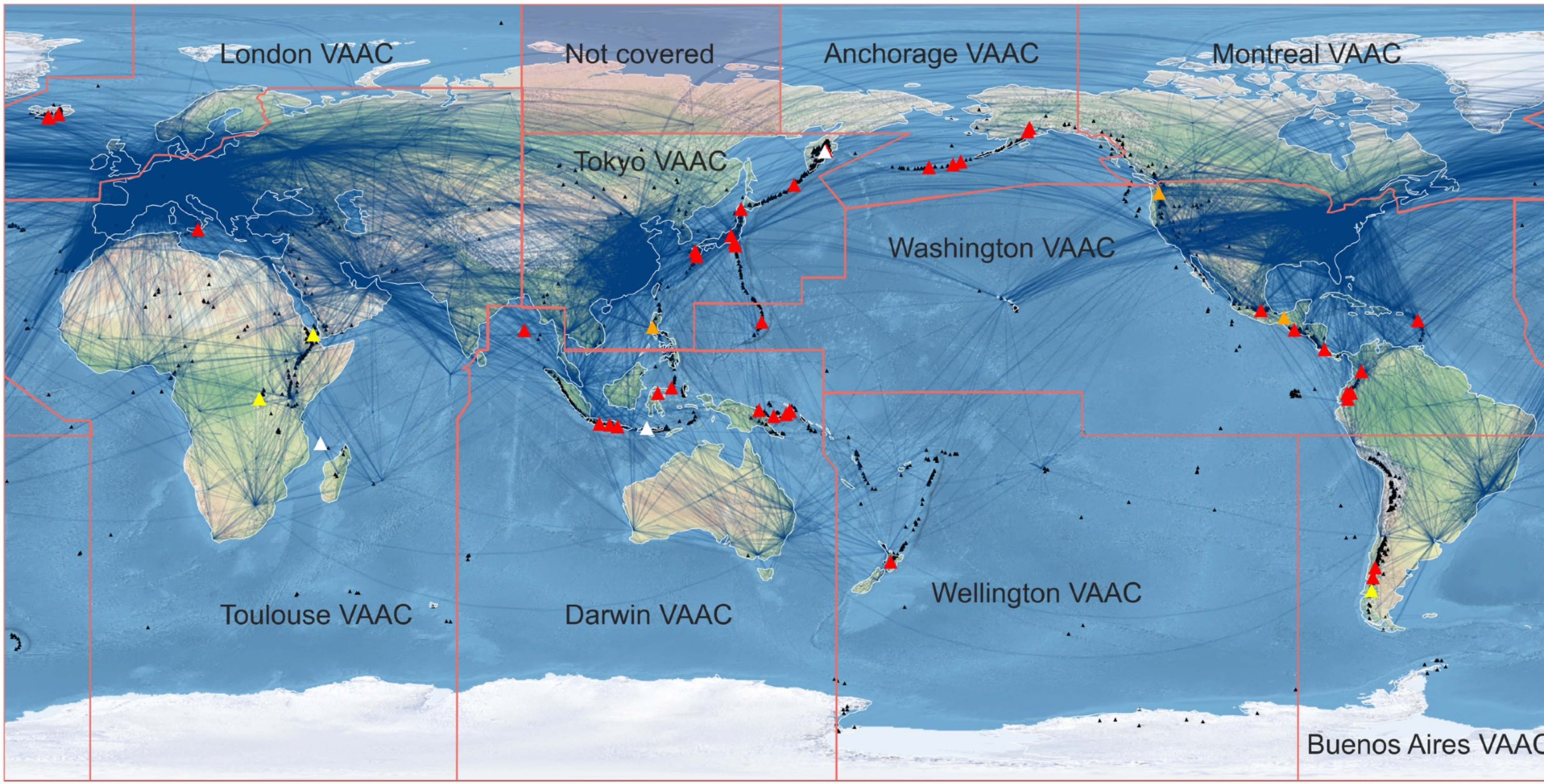

Rolls-Royce Duration of Exposure v Ash Concentration Chart

Clarkson et al., (2016)
Prata, A. J. and W. I. Rose (2016)
Encyclopedia of Volcanoes 2nd Edition

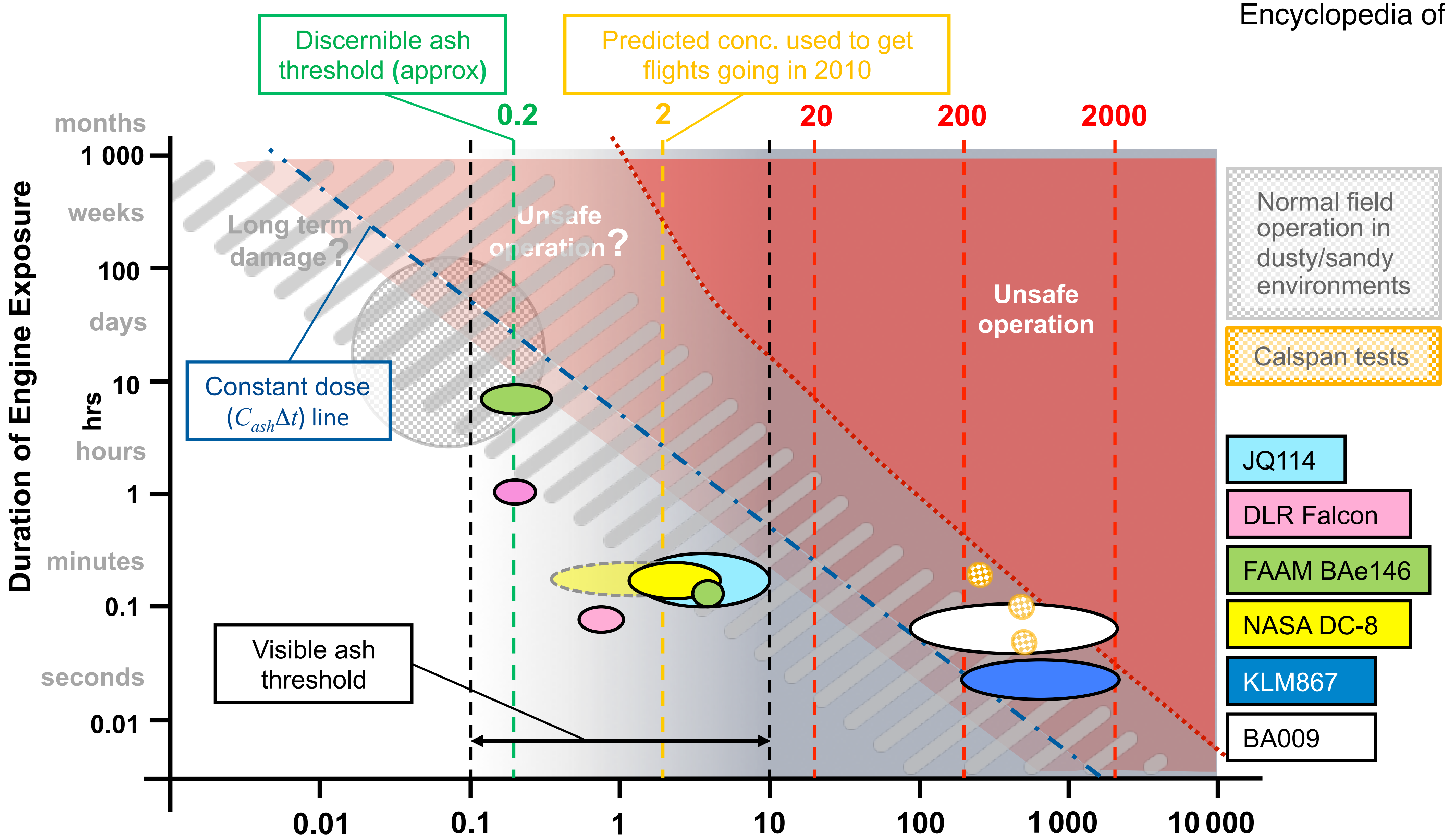

(UK MoD Requested & Funded)

Move towards ash mass loadings rather than concentrations (maybe this will become “law”)
Conclusion 7/16 — Definitions of visible ash and discernible ash for operational use. That:

Visible ash be defined as:

“volcanic ash observed by the human eye and not be defined quantitatively by the observer”

Discernible ash be defined as:

“volcanic ash detected by defined impacts on/in aircraft or by agreed in-situ and/or remote-sensing techniques”

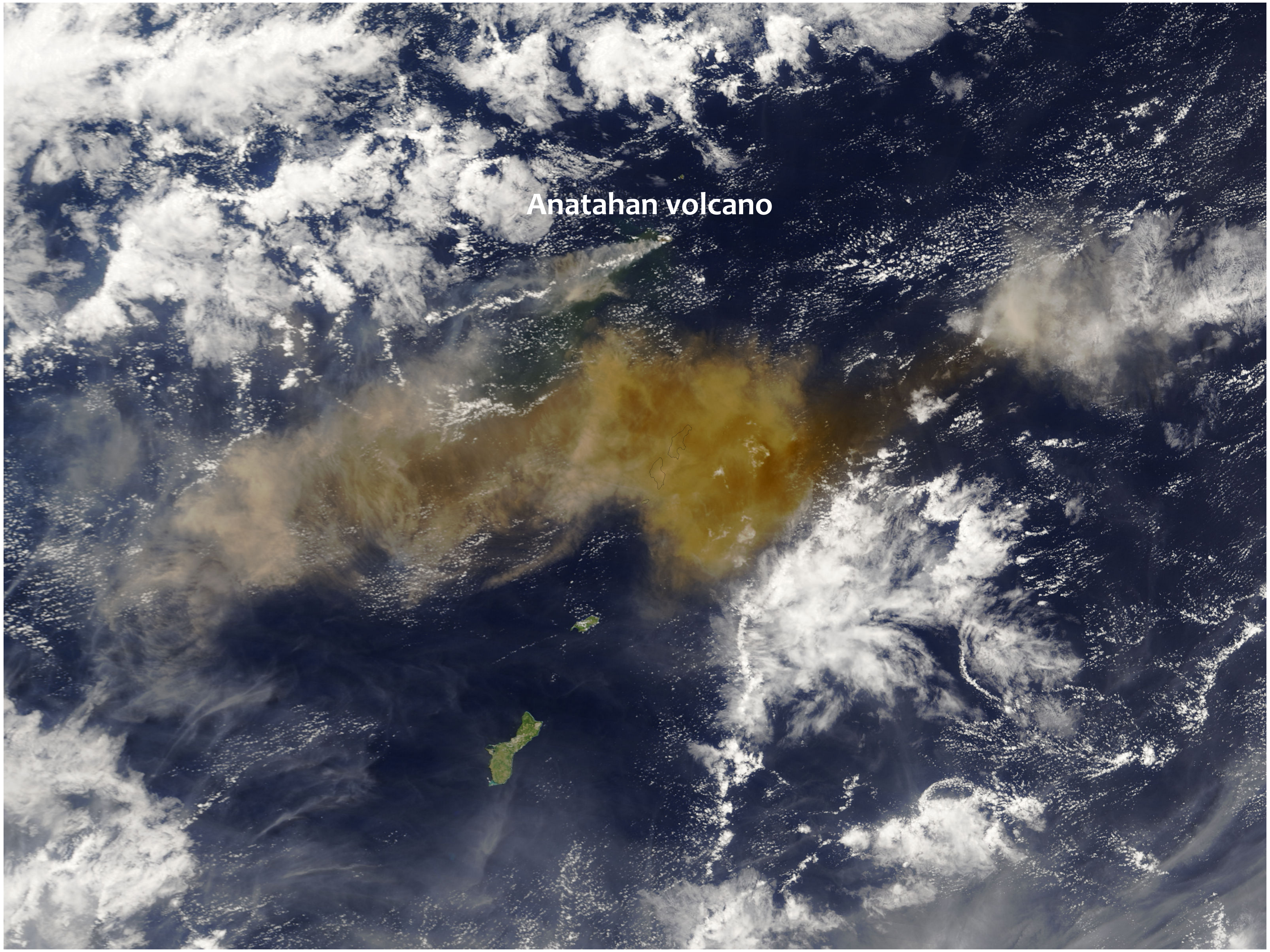

Volcanic ash cloud appearance in MODIS True-colour imagery

Brightness Temperature Differences

How do you identify volcanic eruptions in satellite data?

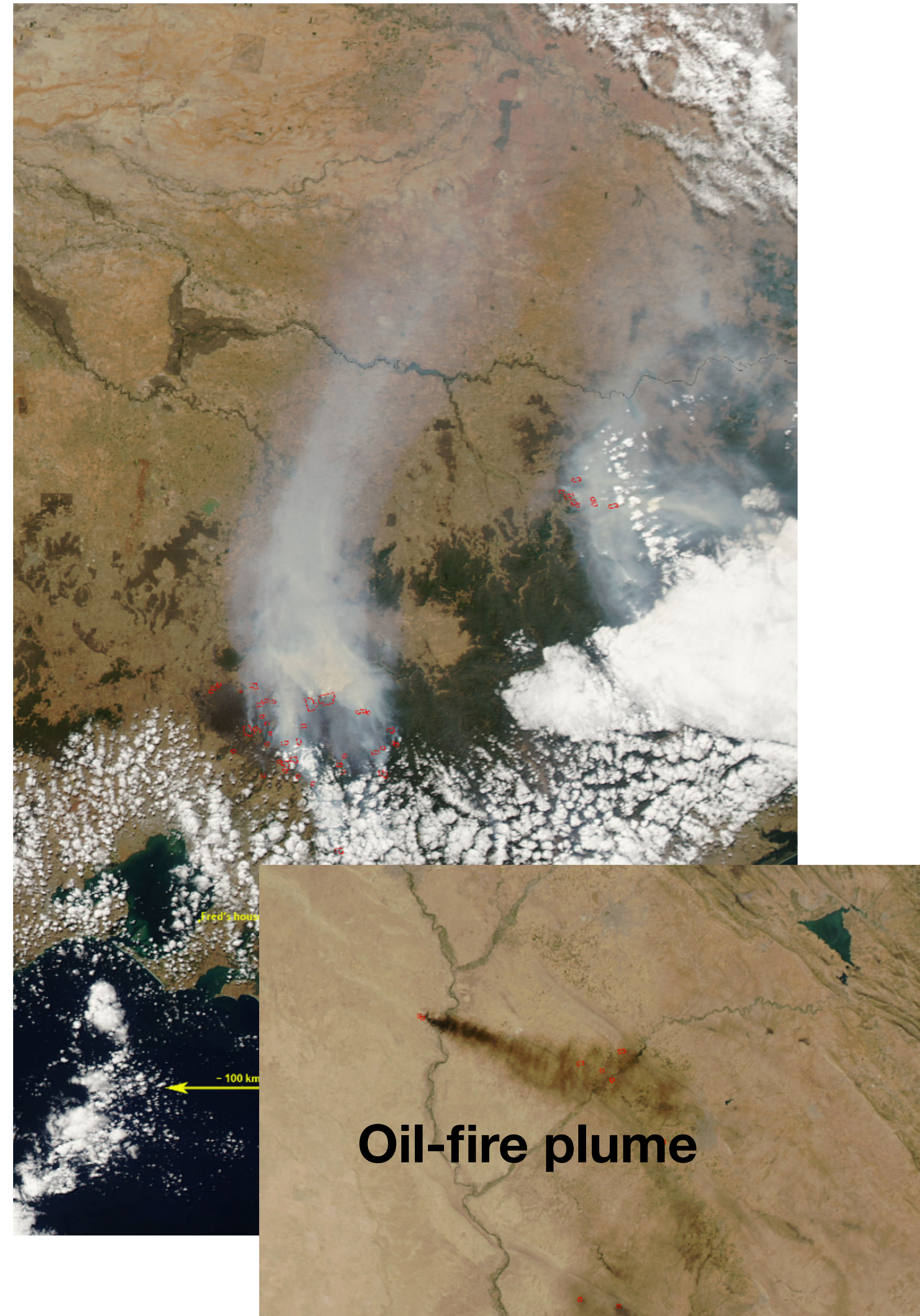

The appearance of a plume that is discoloured and appearing to come from a point source is suggestive. These are fires.

Context is important

Examples

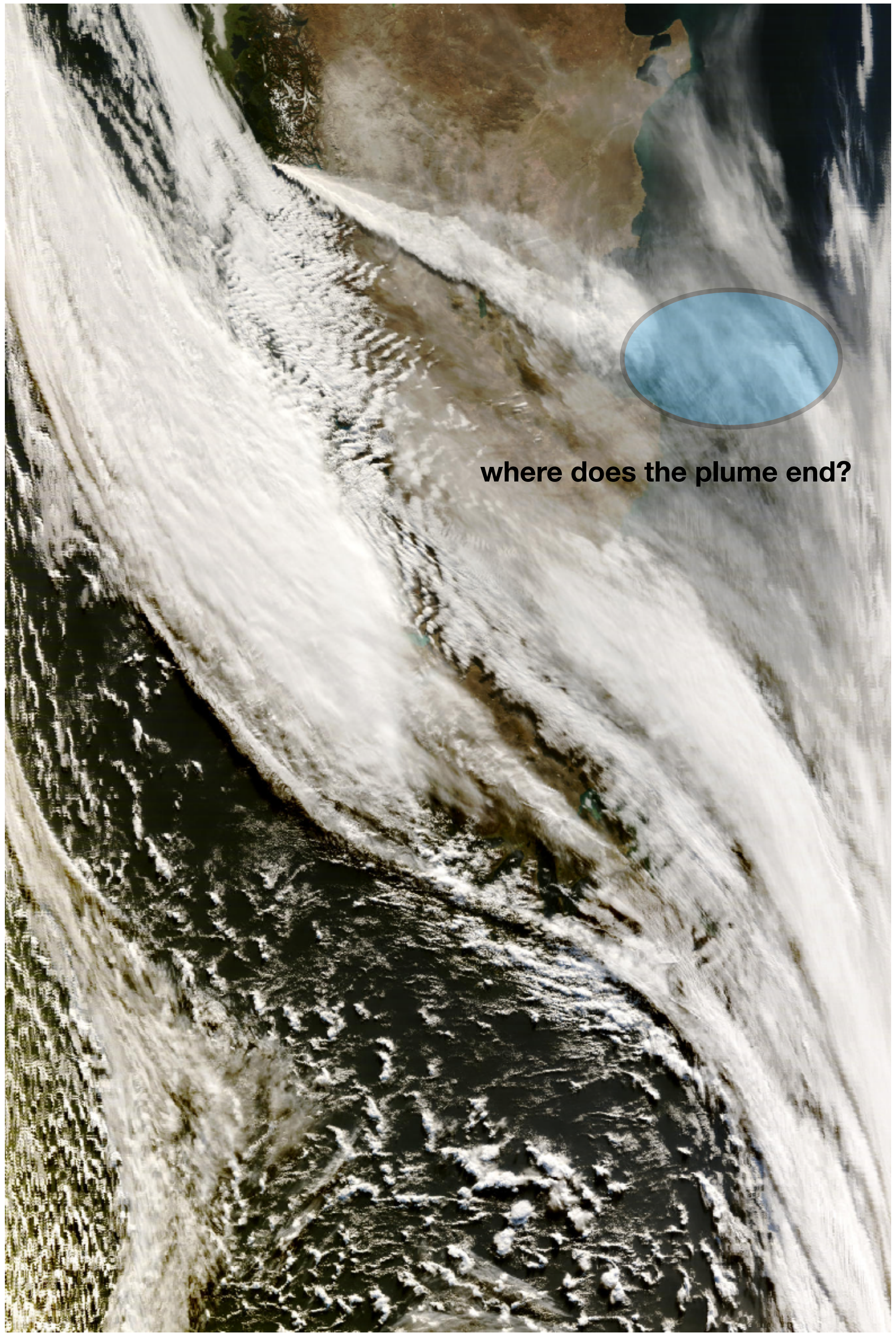

This image shows a volcanic plume from Chaiten, southern Chile.

The plume appears "white" – similar to surrounding meteorological cloud but from this "true-colour" MODIS image it is difficult to judge how much of the plume is volcanic

Properties of Volcanic Ash

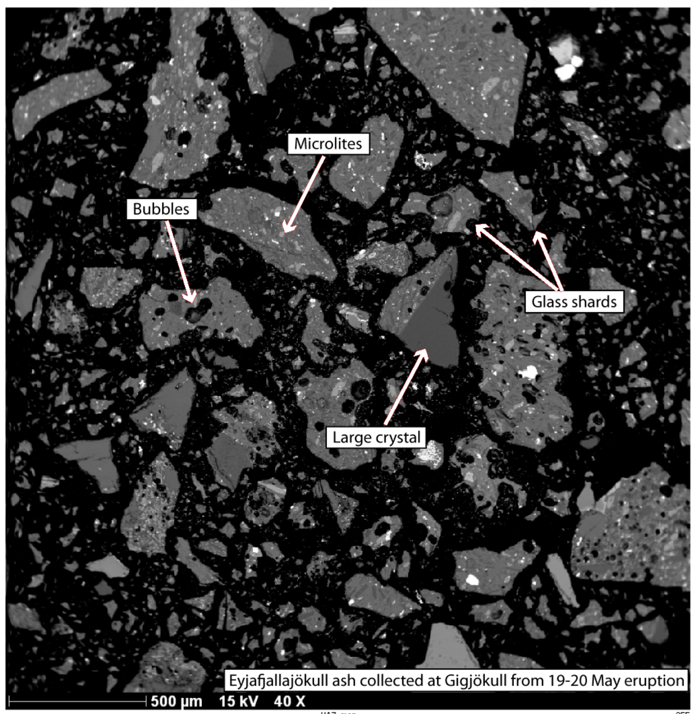

Courtesy: G. Prata, U of Oxford

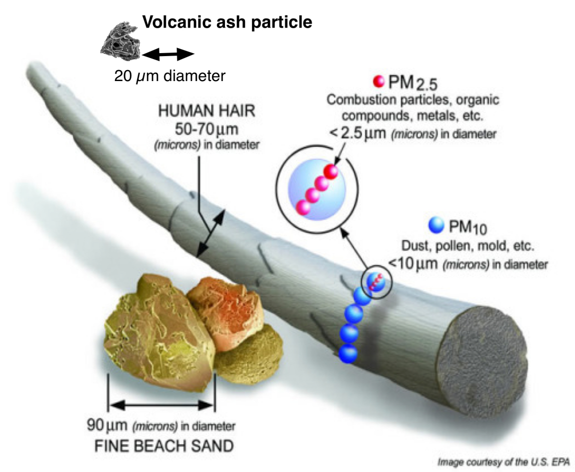

Mt Redoubt ash

Mineral	%Mass
SiO_2	69.9
Al_2O_3	10.4
CaO	8.4
FeO	5.0
Na_2O	4.3
MgO	0.5
K_2O	0.3

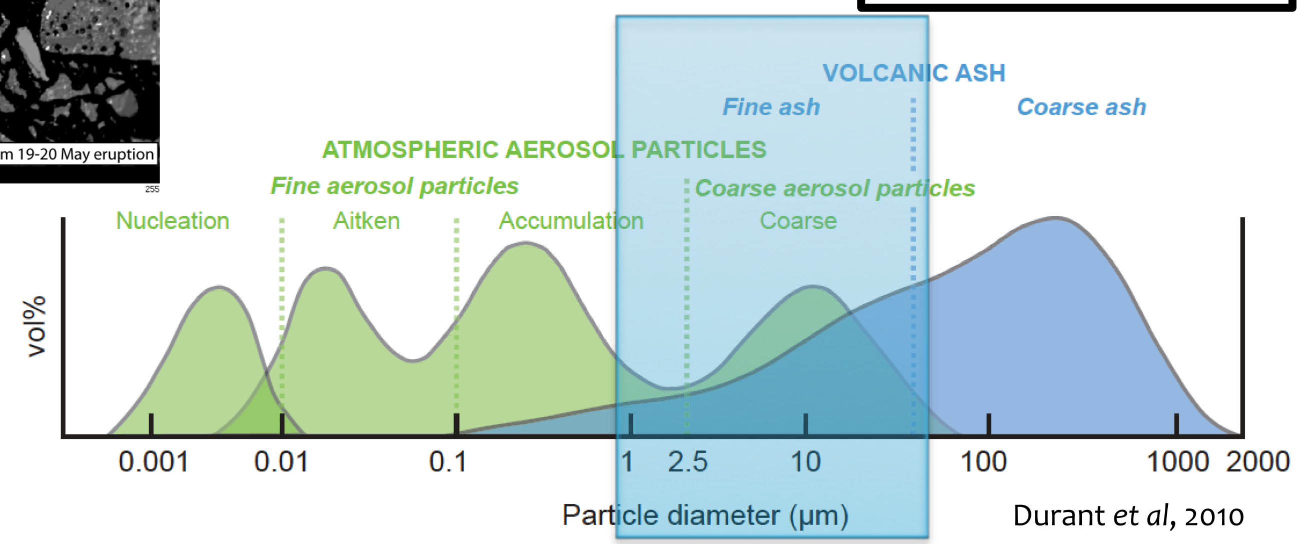

Durant *et al*, 2010

Examples

Using spectral IR data helps

AVHRR visible channel

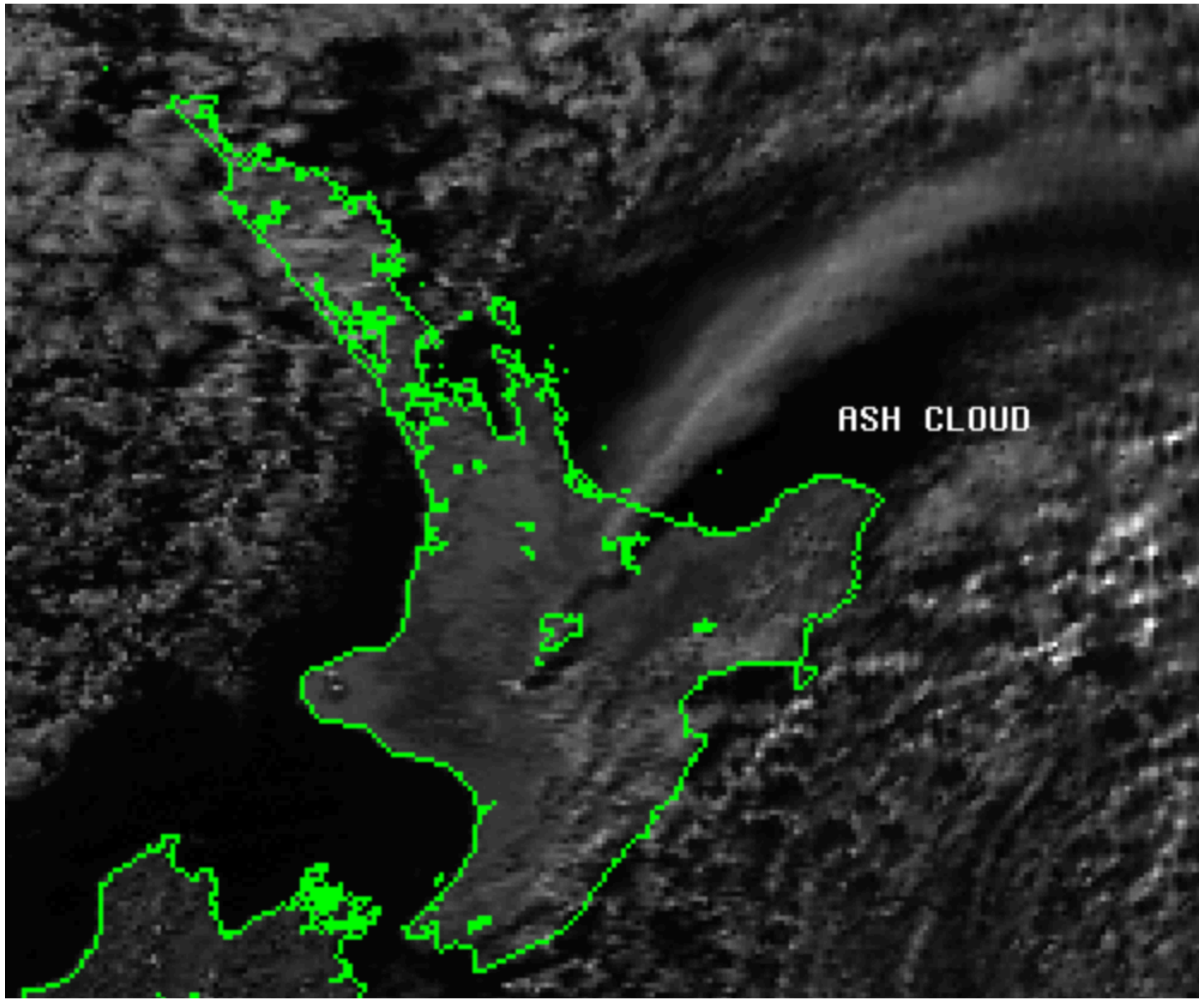

True-colour with BTD overlay

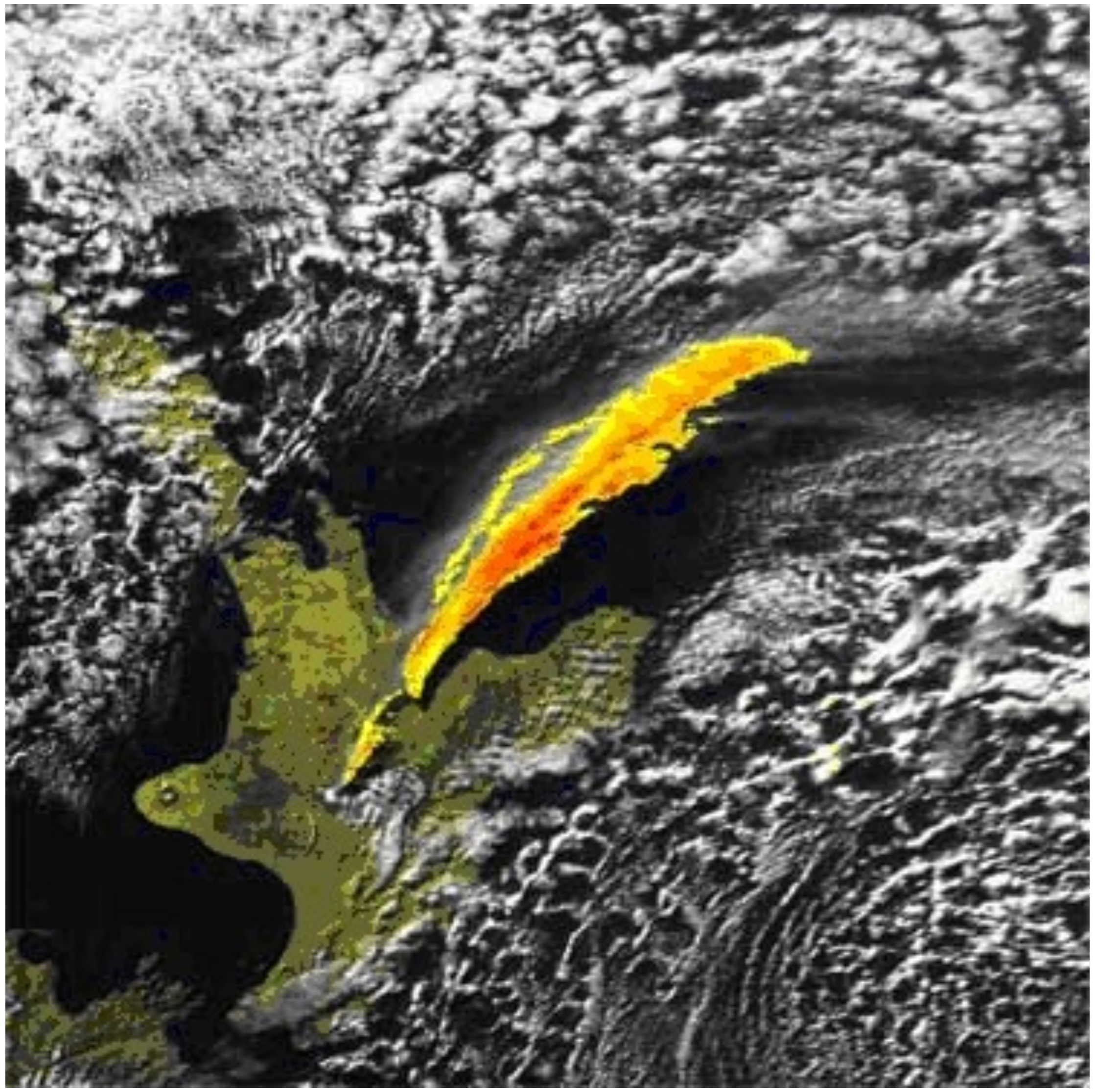

Mt Ruapehu eruption, 17 June 1996

Context helps but if this eruption occurred at night then visible cues are not available

Examples

Brightness temperature difference - the ‘reverse’ absorption effect

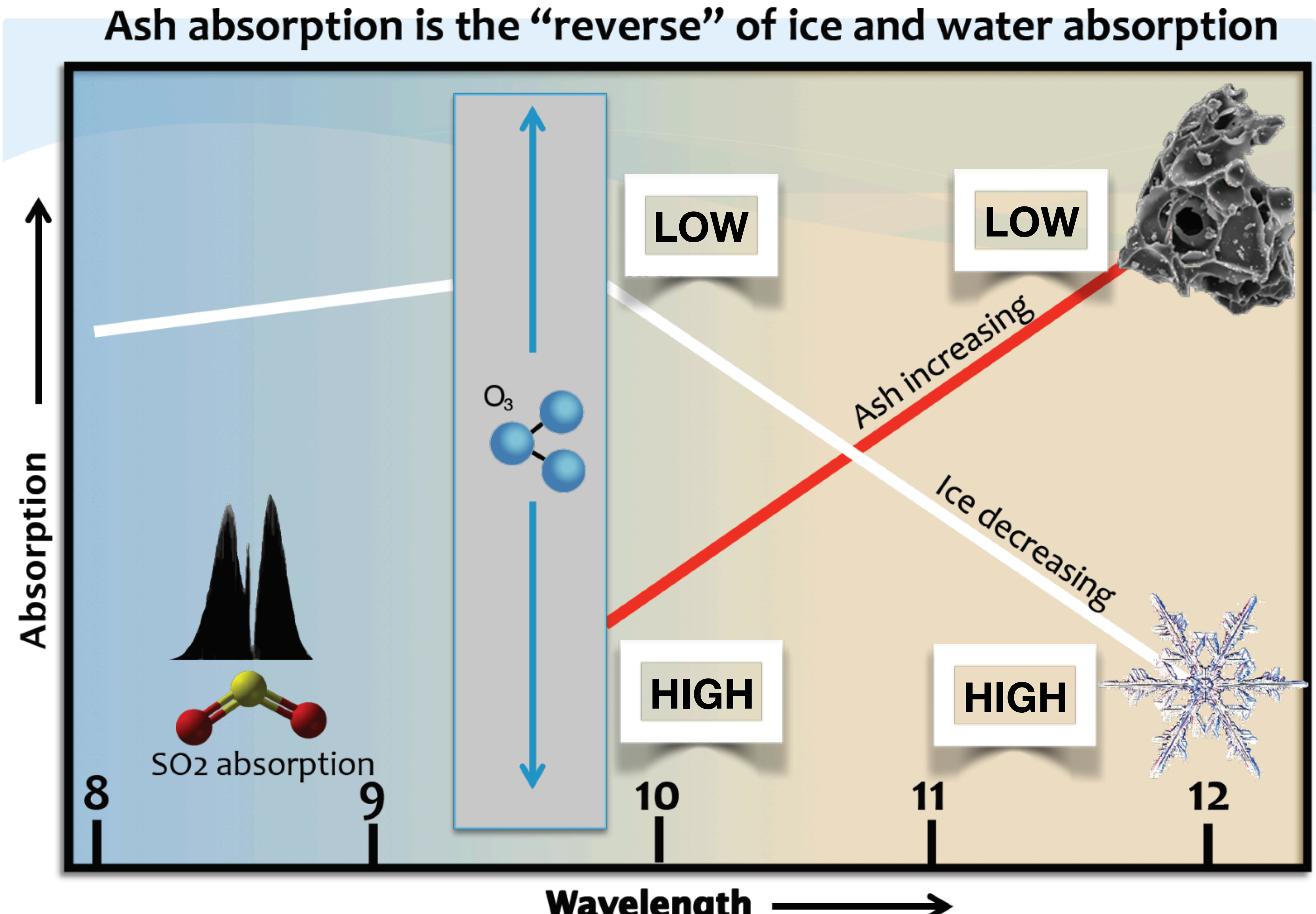

Smoke from forest fires or oil fires or industrial plumes ***DO NOT*** show the reverse absorption effect

Examples

What causes the effect?

The SiO_2 molecule exhibits internal crystal lattice vibrations that preferentially absorb radiation at certain infrared wavelengths. These are the restrahlen and Christiansen frequencies. The effects and locations of the vibrational frequencies are best seen in refractive index measurements.

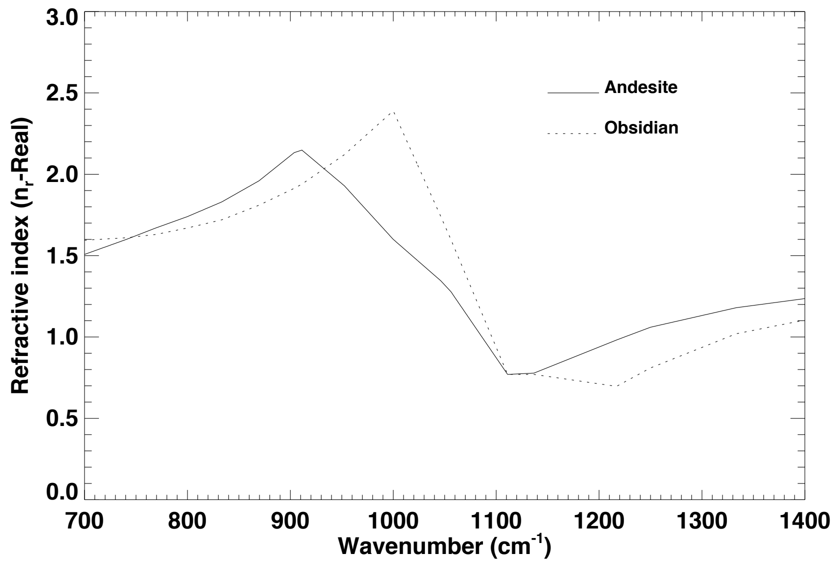

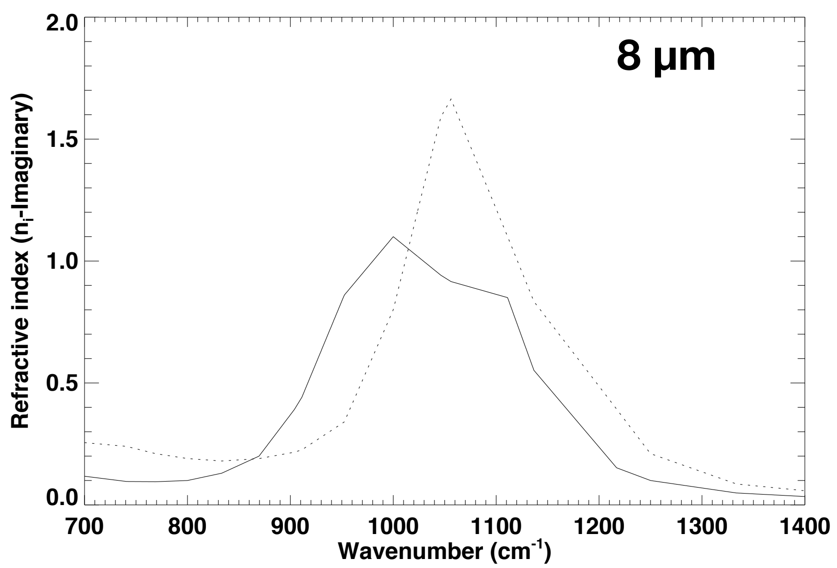

Peak in imaginary part of the refractive index implies greater absorption there

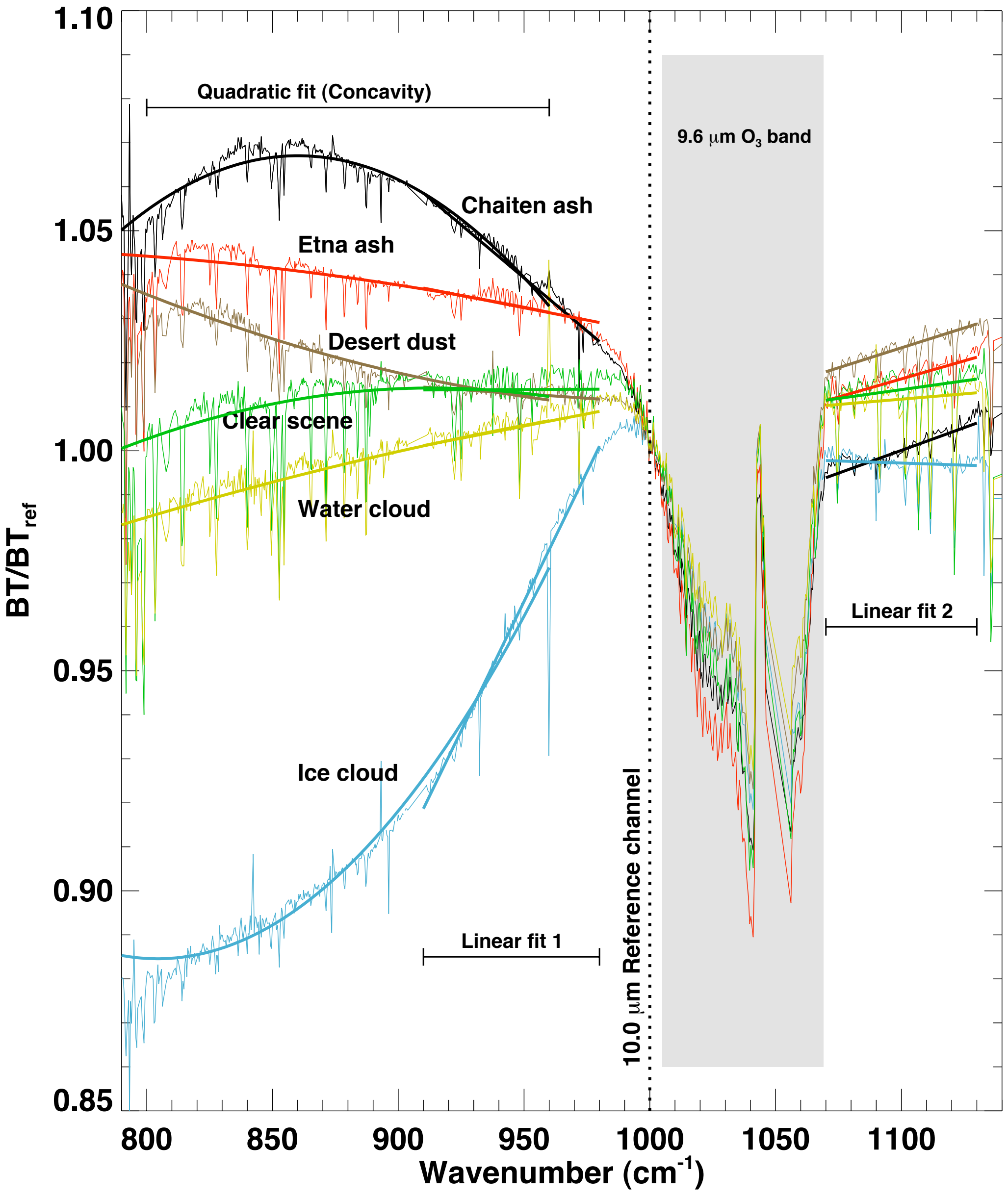

Examples

There is a strong particle size and compositional effect

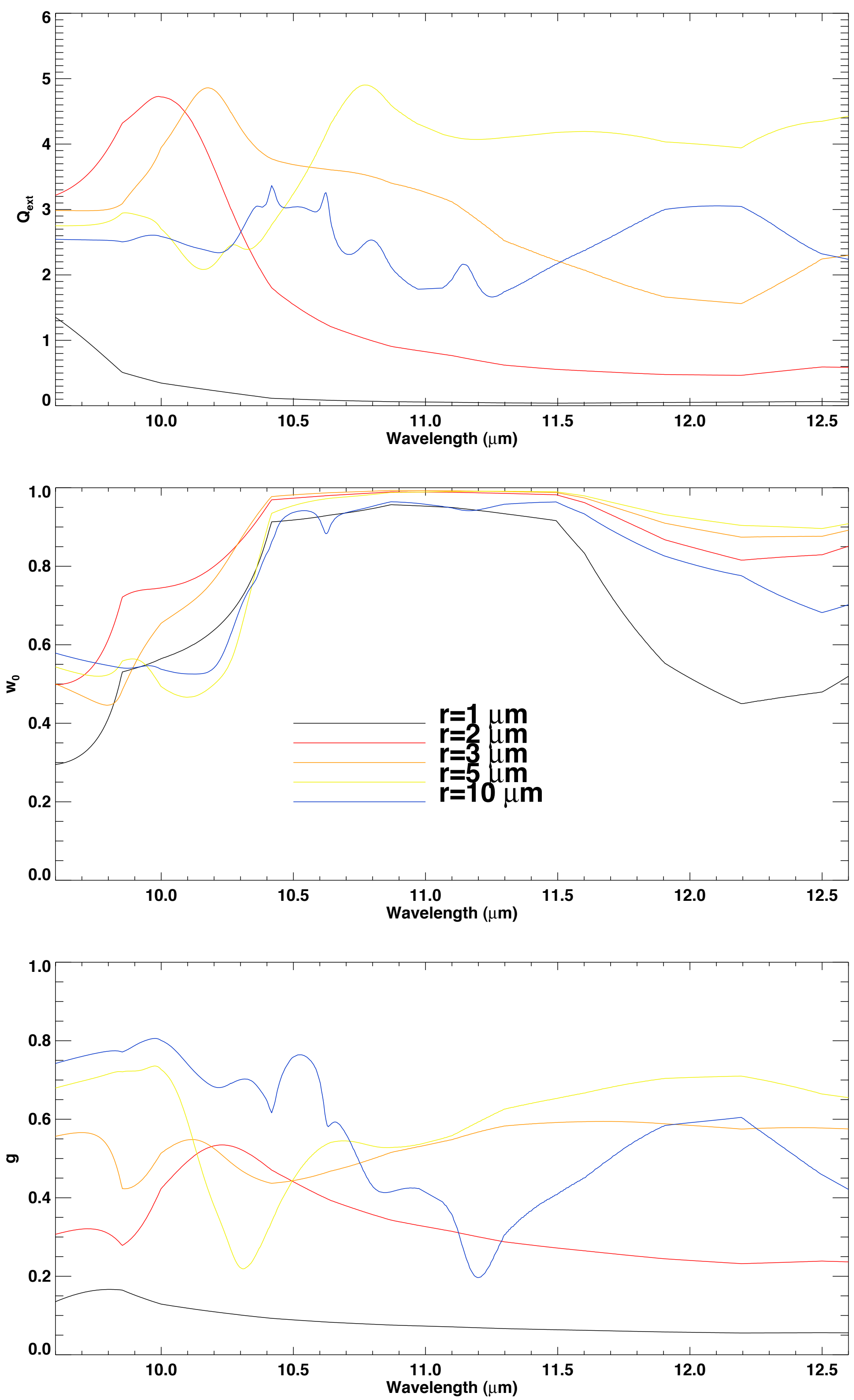

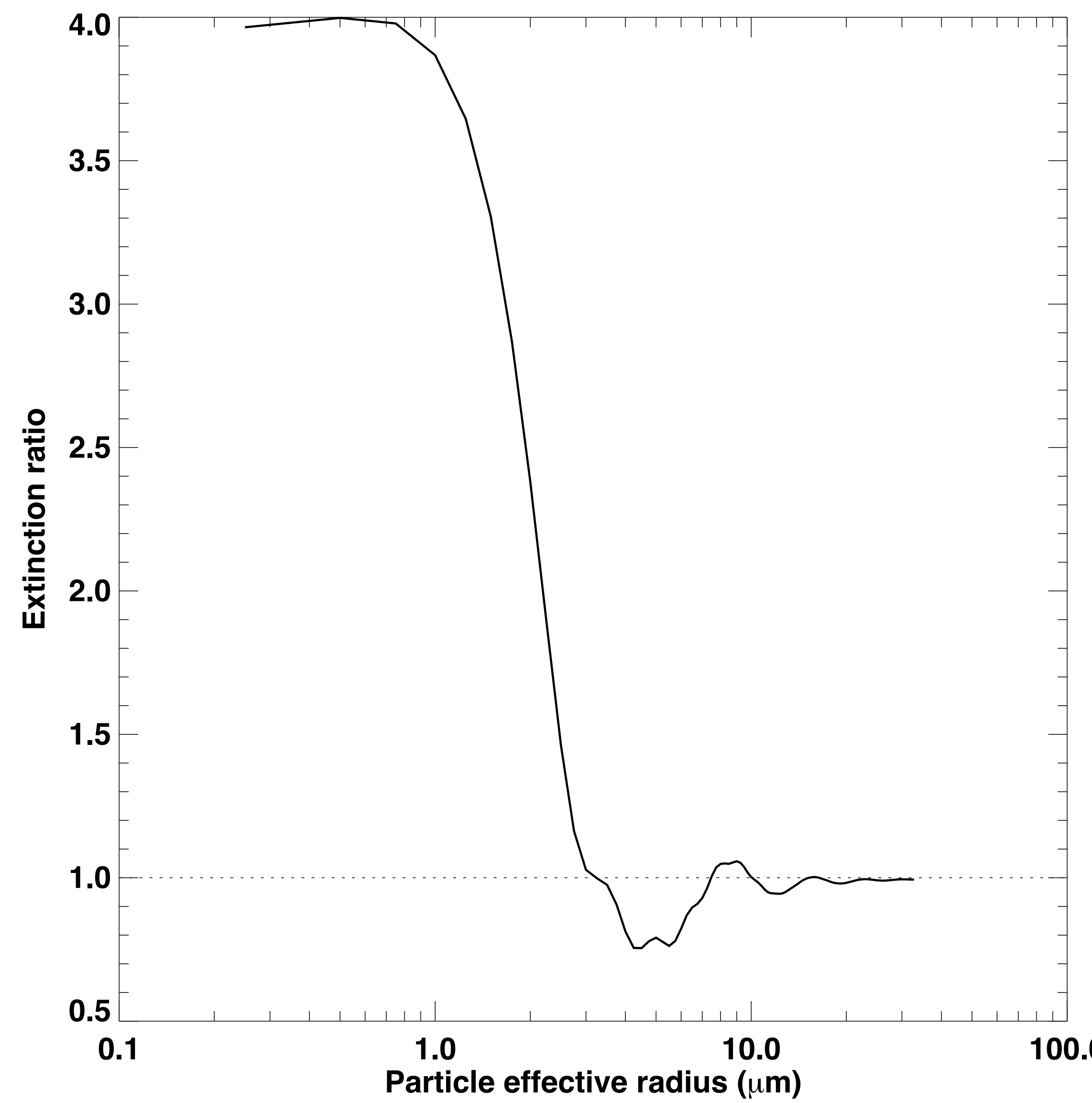

Hyperspectral Infrared

AIRS and IASI provide 100s of channels in the IR and suggest the possibility of deriving new quantitative aspects of volcanic emissions

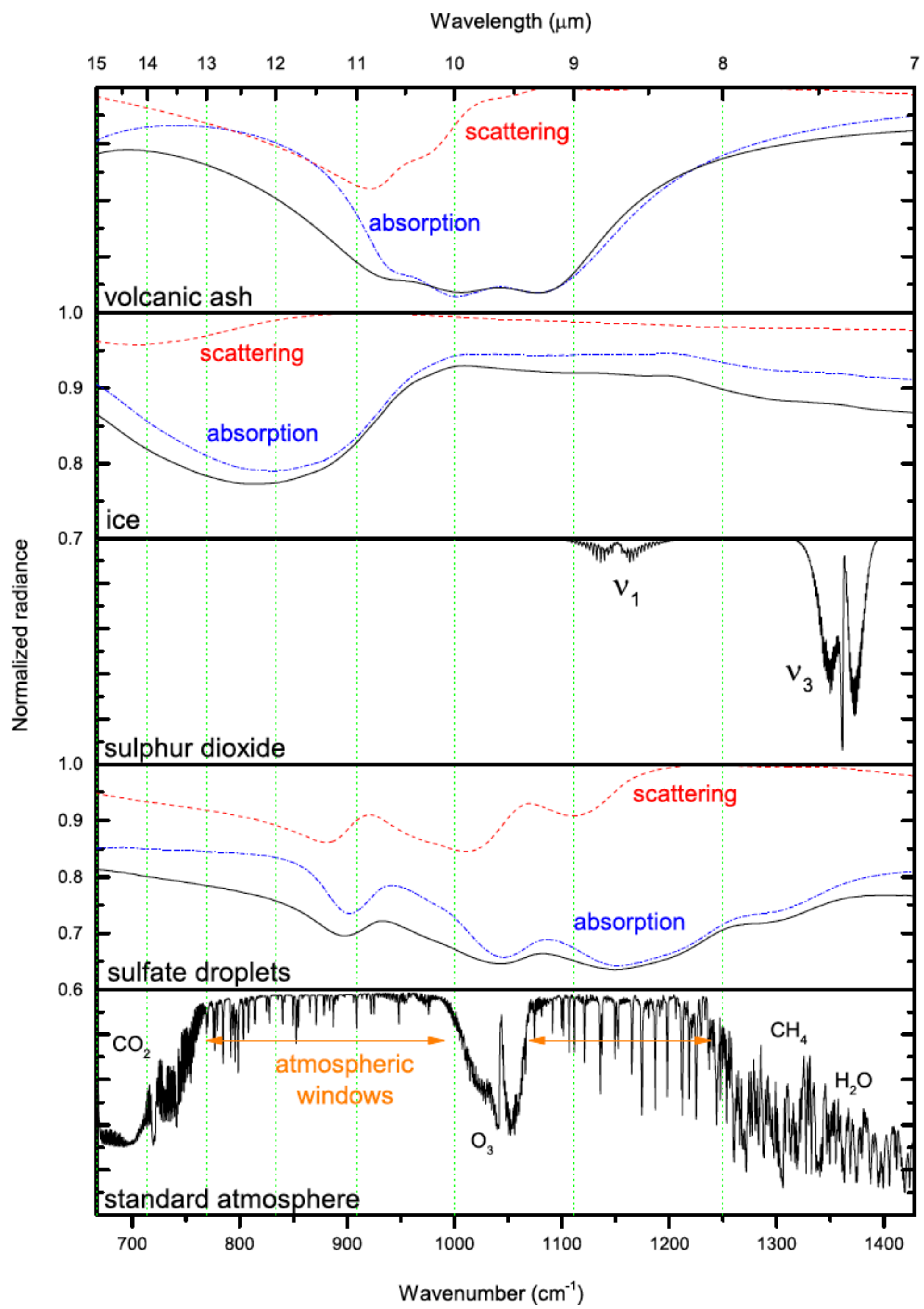

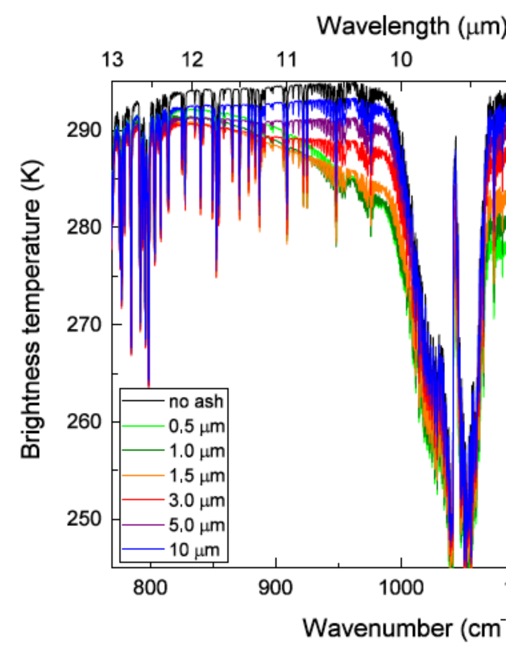

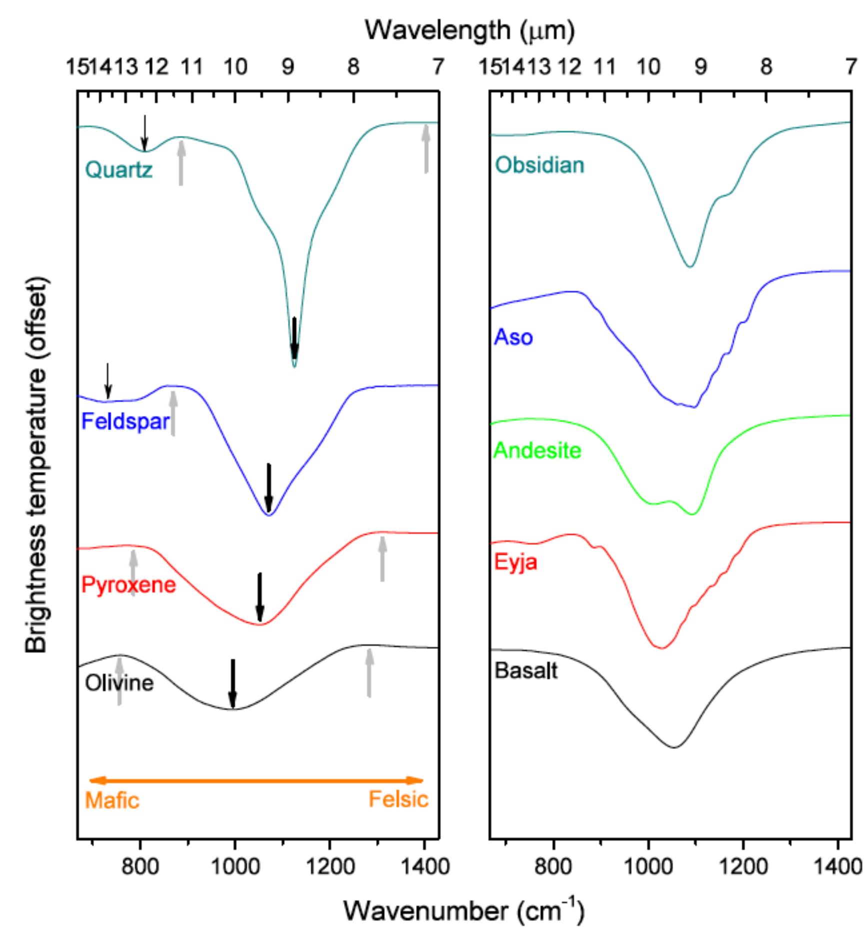

AIRES Pty Ltd

Examples

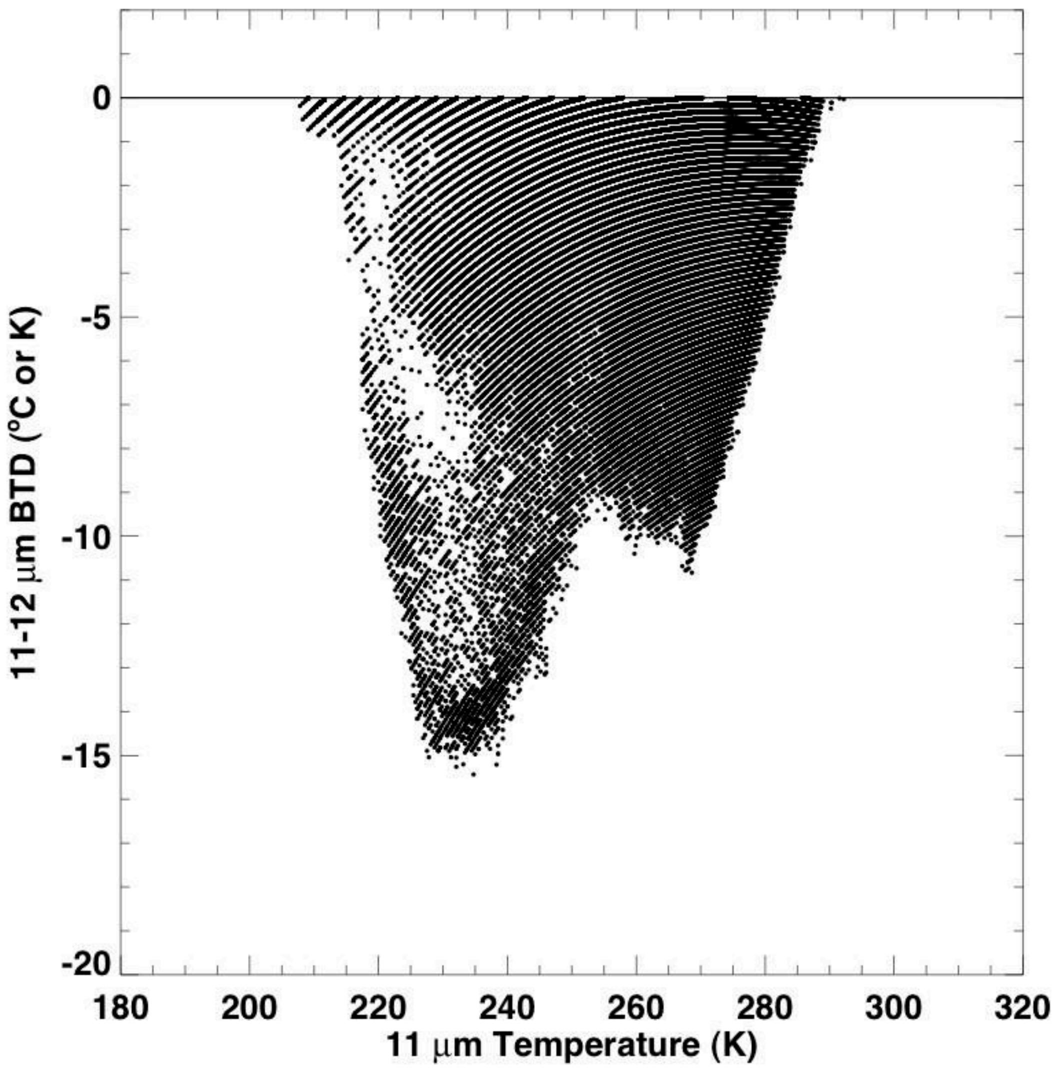

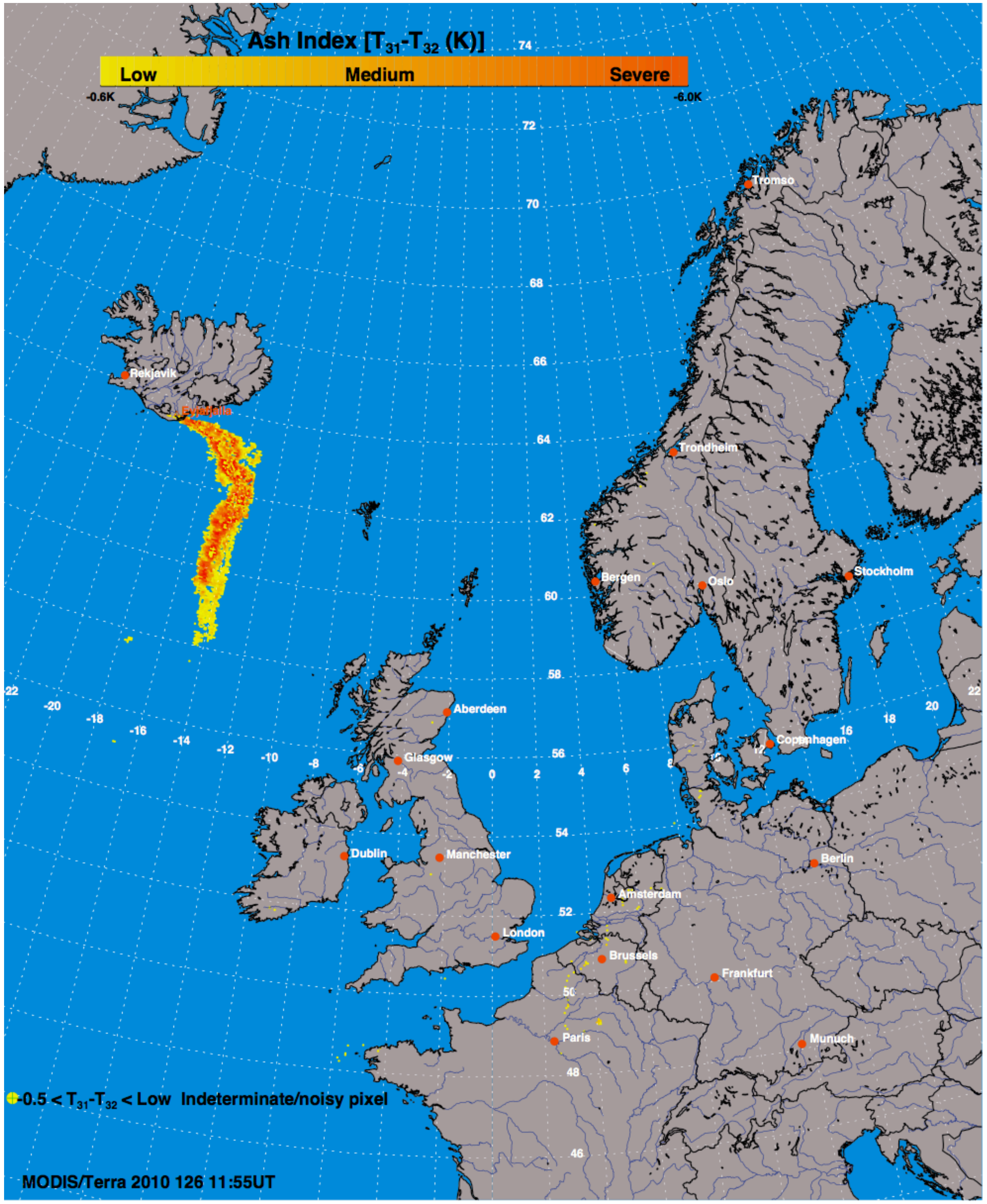

Method:

Plot T_{11} vs BTD (T_{11}-T_{12})

Identify ash as all pixels with BTD<ΔT

Examples
(Setting the threshold)

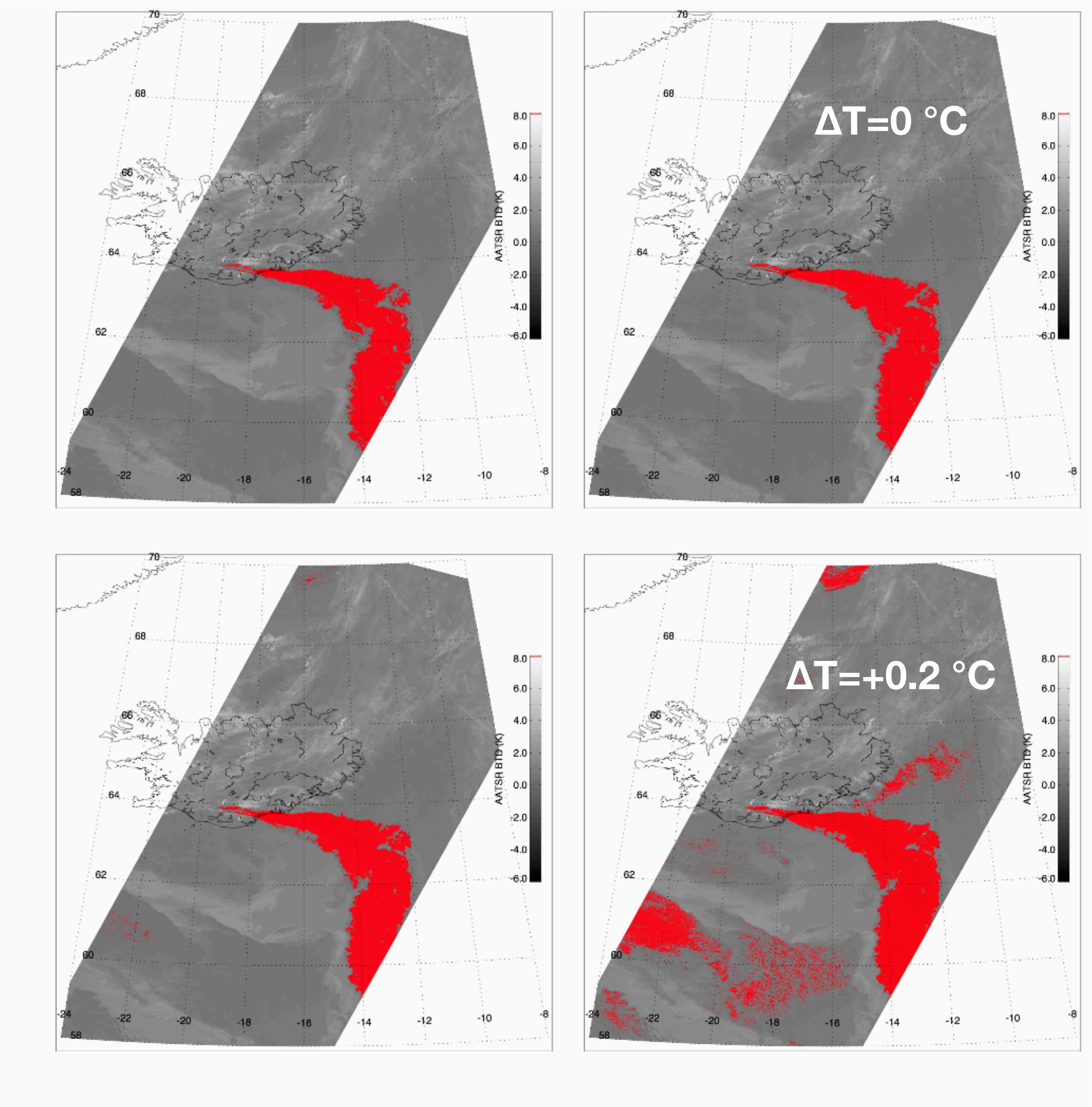

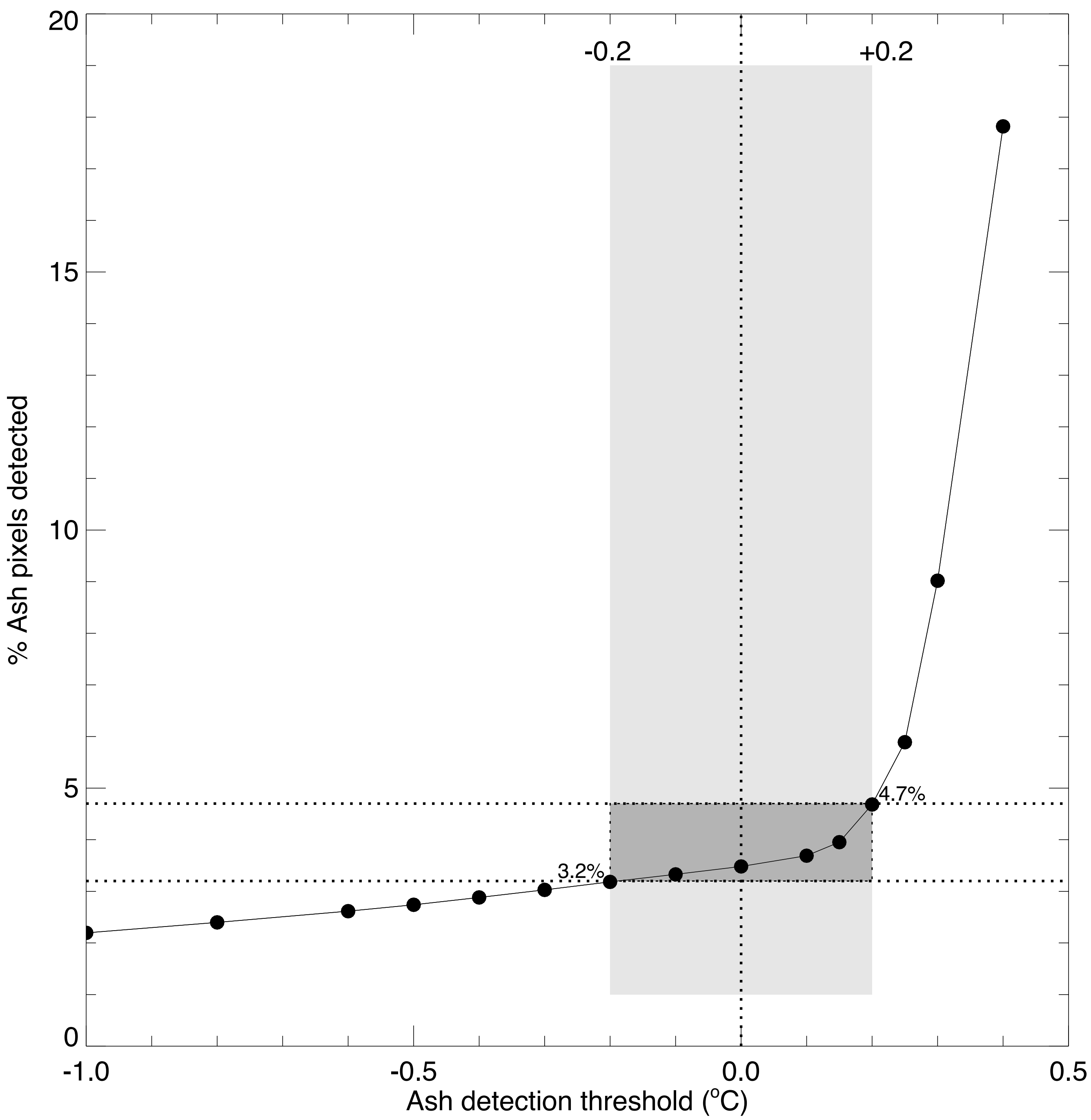

MODIS True-colour image – Eyjafjallajökull

Eyja

17 May 2010
13:25 UT

Mass loadings

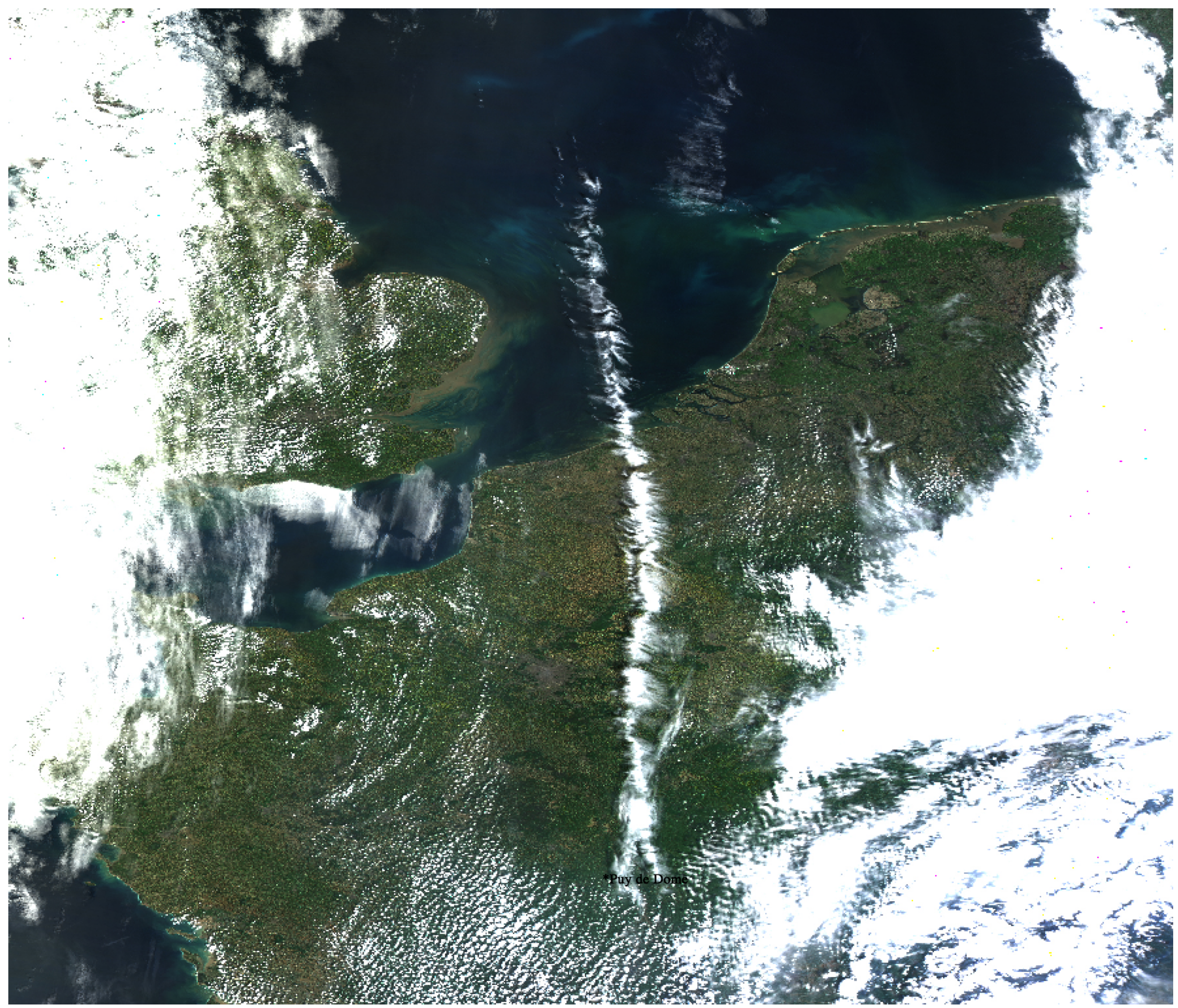

Eyja

17 May 2010
13:25 UT

Mass loadings

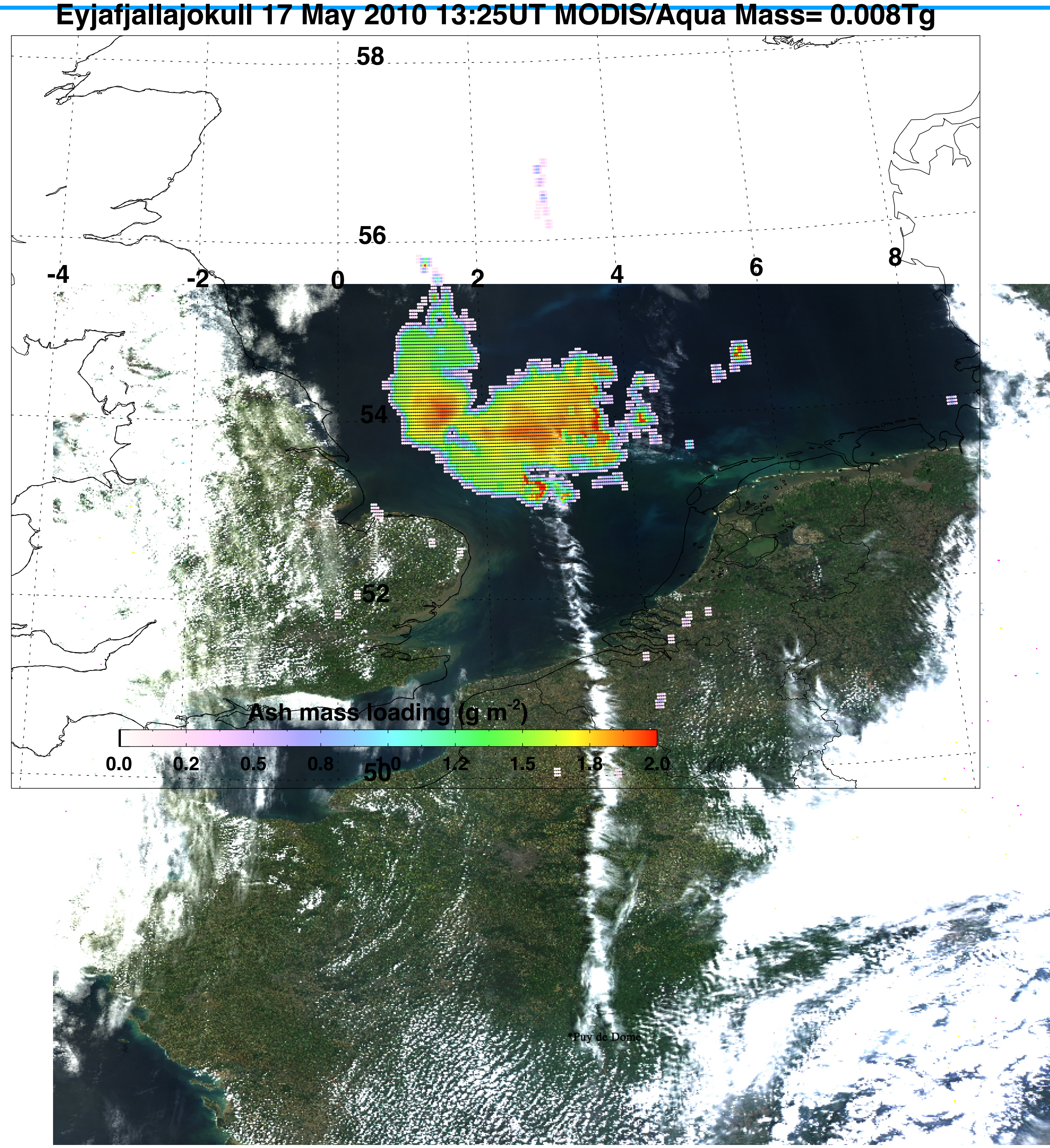

Large Eruptions

Pinatubo eruption June 1991

No MODIS
No AIRS
No IASI
No OMI

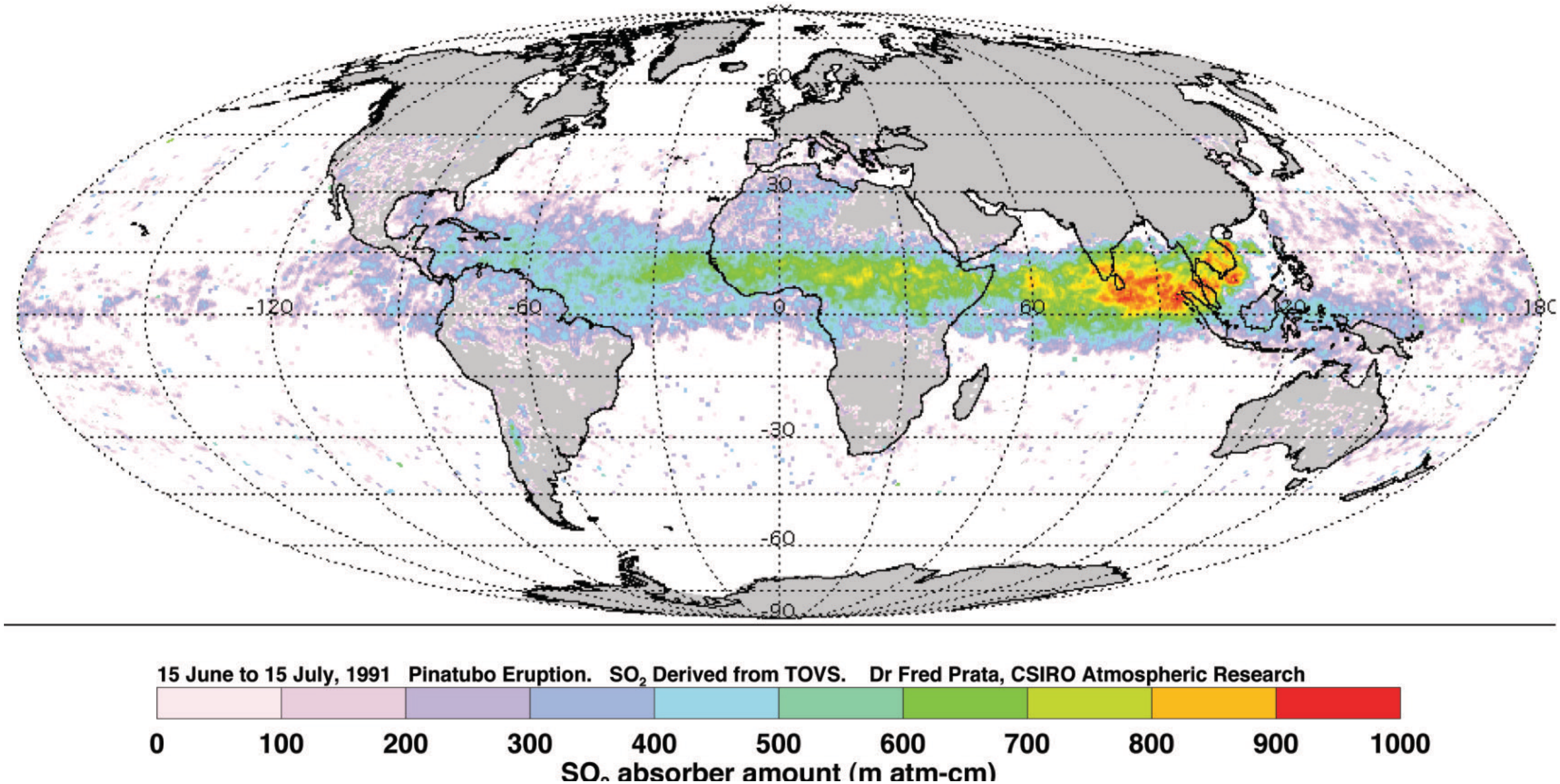

Large eruptions

G. M. Miles et al.: Retrieval of volcanic SO_2 from HIRS/2 using optimal estimation

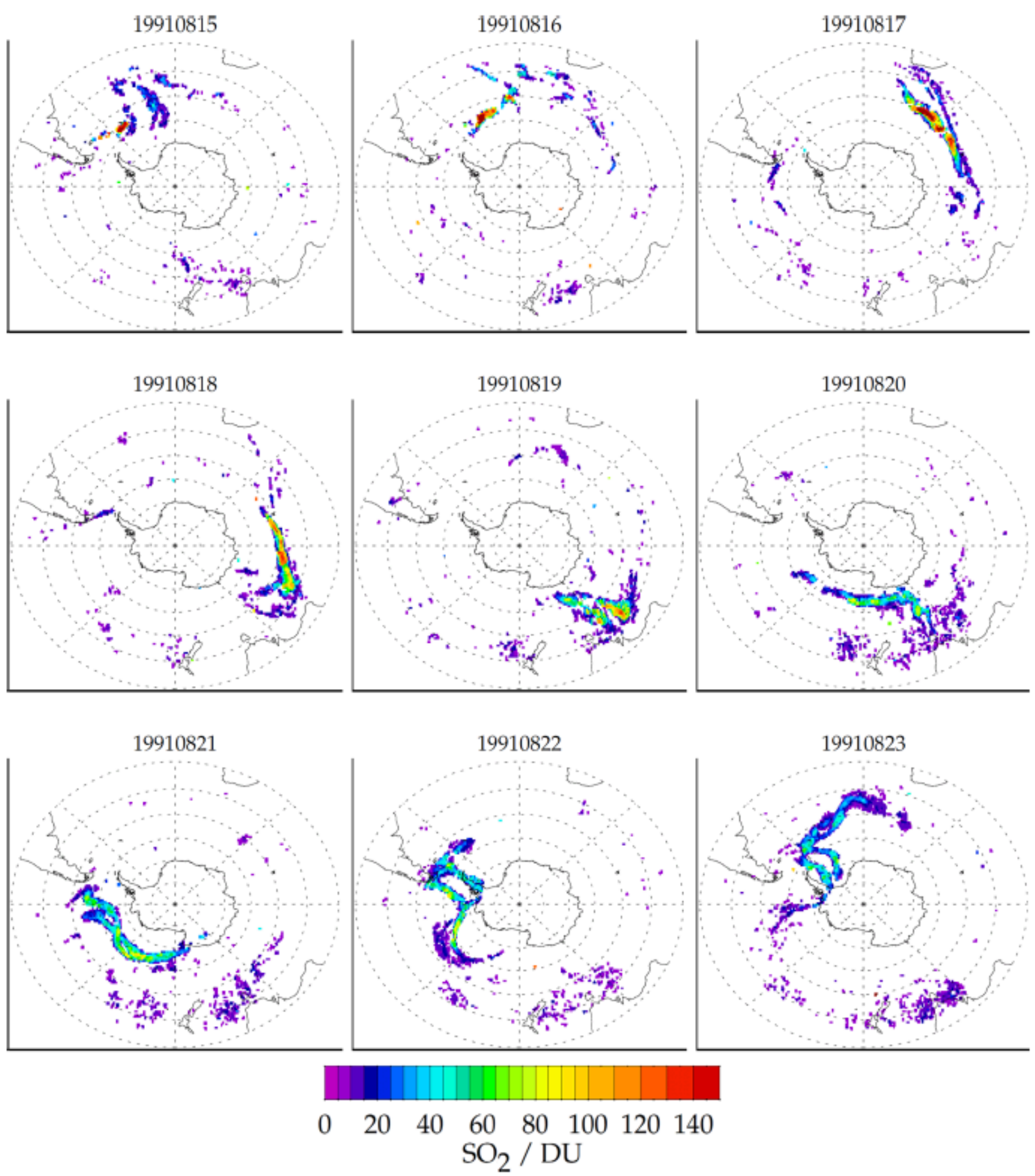

Figure 8. Progression of main erupted plume from 15 August 1991, using all orbits (day and night) from HIRS/2 NOAA 11. The eruption began with smaller amounts emitted from 8 August, which are apparent on the 15th and disassociated from the main plume. The plume's transport between observations is evident, particularly from 21 August, where it is captured multiple times by multiple swaths. Data have been screened at the 3σ level (8.1 DU) for clarity of the main plume.

Table 3. Total erupted SO_2 rounded estimates for Cerro Hudson.

Eruptive phase	TOMS SO_2^1	TOMS SO_2^2	HIRS/2 Prata fit[3]	HIRS/2 OE[4]
8–9 August	700 kT	–	300 kT	500 ± 150 kT
12 August	600 kT	–	400 kT	300 ± 90 kT
15 August	2700 kT	2000 kT	1200 kT	1500 ± 400 kT

[1] Constantine et al. (2000), with errors estimated to be circa 30 %. [2] This work, based on updated TOMS algorithm, for total mass as observed on 16 August (as region was poorly observed on the 15th) with consideration of pixel overlap within orbit. [3] After Prata et al. (2003), but data reproduced and sampled as OE HIRS/2 product is herein. [4] This work, with retrieved error.

https://www.atmos-meas-tech.net/10/2687/2017/

Hudson, Chile. August 1991
Probably 3rd* largest SO_2
emission in the satellite era

*Pinatubo ~18Tg
El Chichon ~6Tg
Hudson ~4Tg
Nabro ~4Tg
Kasatochi ~2Tg

AIRES Pty Ltd

Large Eruptions

For large eruptions weather satellite data from 1979 onwards can be used to determine SO_2 mass loadings based on a channel at 7.3 µm. This has implications for analysing the effects of volcanic emissions on climate.

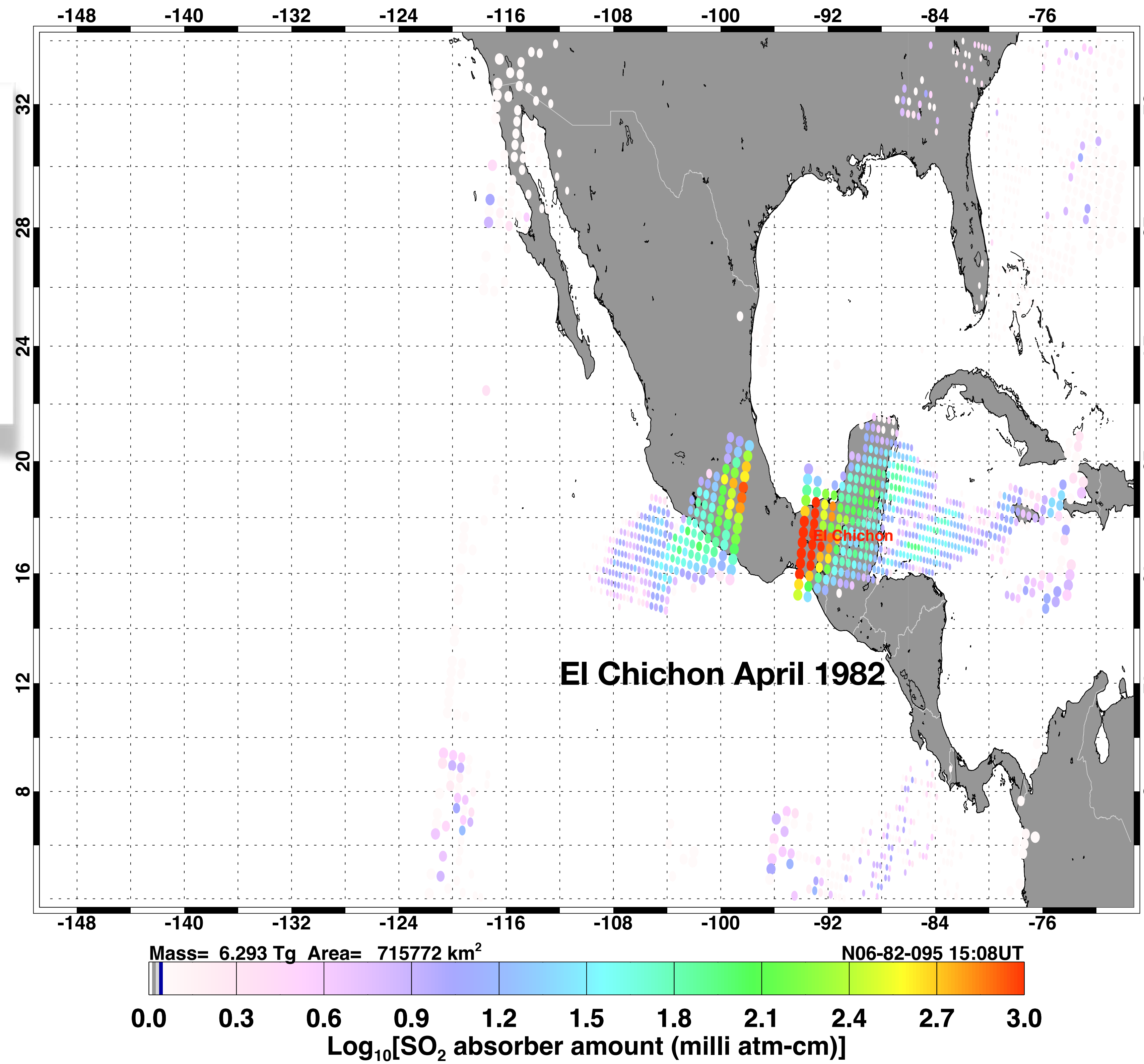

Large eruptions

Table 1
Volcanic gases measured or potentially detectable from space.

Sensor[a]	H_2O	CO_2	CO	SO_2	H_2S	HCl	BrO	OClO	CH_3Cl	Timespan	Reference(s)[b]
	Volatile species										
TOMS*				Red						1978–2005	1, 2
SBUV* (P)				Red						1978–present	3, 4
HIRS*				Red						1978–present	5
GOME	Light gray			Red			Light gray	Light gray		1995–2003	6, 7, 8, 9
MODIS*	Light gray			Red						1999–present	10, 11
ASTER				Red						1999–present	12, 13, 14
MOPITT			Red							1999–present	15
SCIAMACHY (L)	Light gray	Light gray	Light gray	Red			Red	Red		2002–2012	8, 16, 17, 18
MIPAS (L)	Light gray			Red						2002–2012	19
AIRS	Light gray	Light gray	Light gray	Red						2002–present	20, 21
ACE (L)	Light gray	Light gray	Light gray	Red		Light gray			Light gray	2003–present	22
SEVIRI				Red						2004–present	23
OMI				Red			Red	Red		2004–present	18, 24, 25, 26
MLS* (L)	Light gray		Light gray	Red		Red	Light gray	Light gray	Red	1991–2001; 2004–present	27, 28, 29, 30
TES (P)	Light gray		Light gray	Red						2004–present	31
GOME-2*	Light gray			Red			Red	Red		2006–present	18, 32, 33, 34
IASI*	Light gray	Light gray	Red	Red	Red					2006–present	15, 35, 36
OMPS*				Red			Light gray	Light gray		2011–present	37
VIIRS				Red						2011–present	38
CrIS				Light gray						2011–present	39
AHI				Light gray						2015–present	40
GOSAT (P)		Light gray		Light gray						2009–present	41
OCO-2		Light gray								2014–present	42

Red = detected in a volcanic cloud; *Light gray* = potentially detectable but not yet proven in a volcanic context and/or not viable for routine volcanic measurements (e.g., due to background interference).

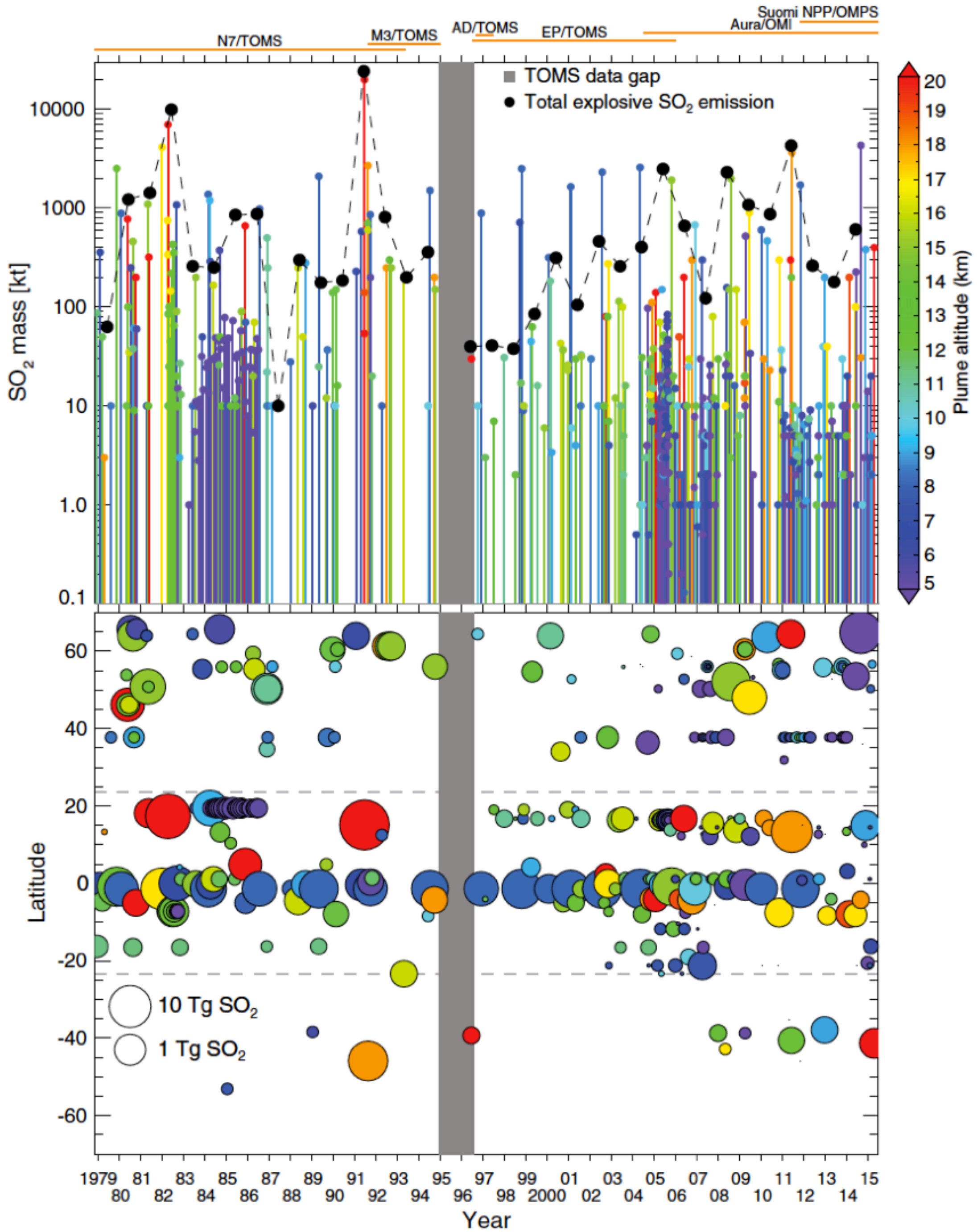

Journal of Volcanology and Geothermal Research
Volume 311, 1 February 2016, Pages 99-134

Review
Multi-decadal satellite measurements of global volcanic degassing

S.A. Carn [a, b], L. Clarisse [c], A.J. Prata [d]

https://www.sciencedirect.com/science/article/pii/S0377027316000032

Large eruptions - Kelut

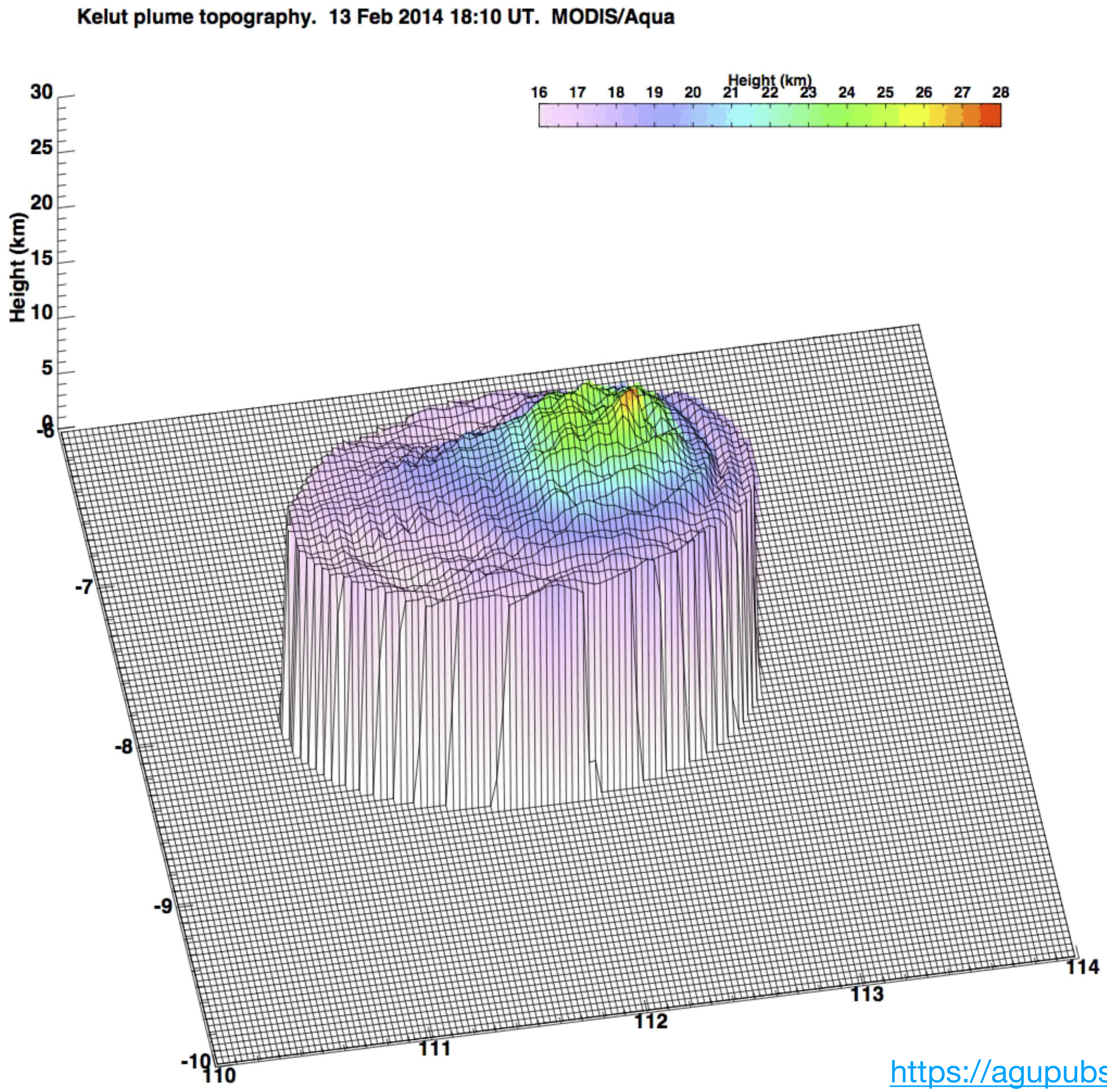

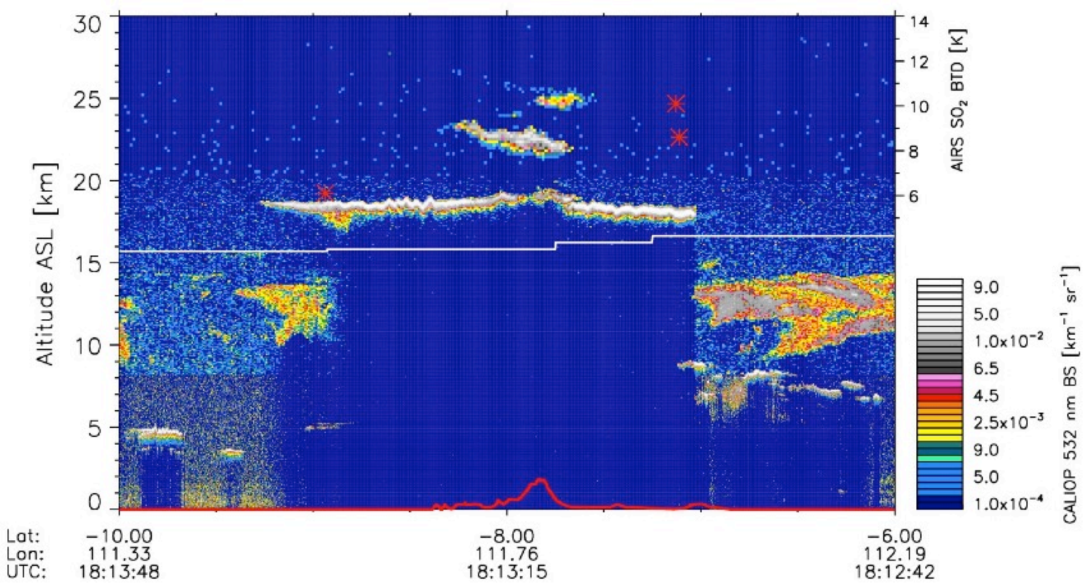

https://agupubs.onlinelibrary.wiley.com/doi/abs/10.1002/2014GL062307

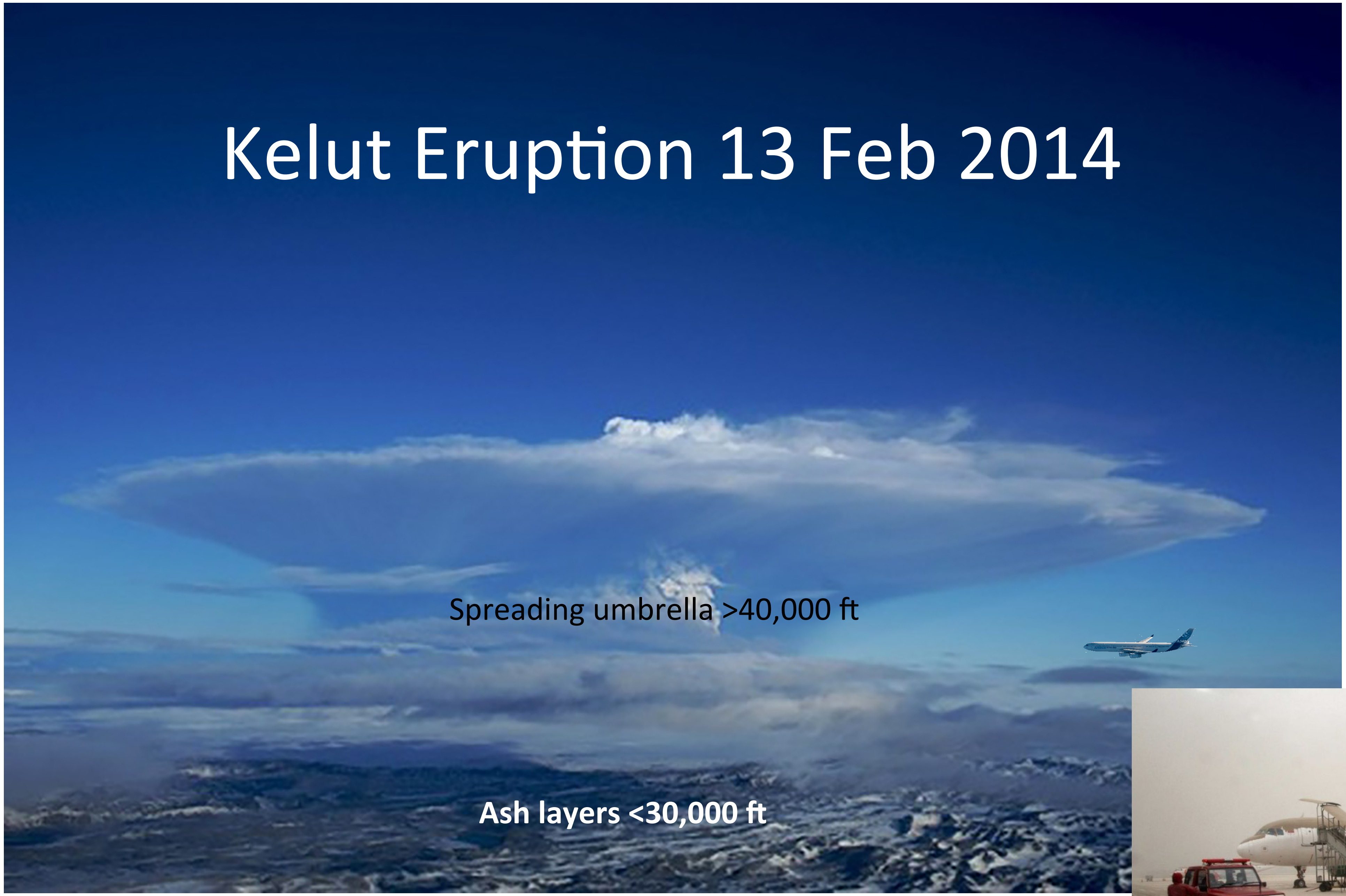
Kelut Eruption 13 Feb 2014
Spreading umbrella >40,000 ft
Ash layers <30,000 ft

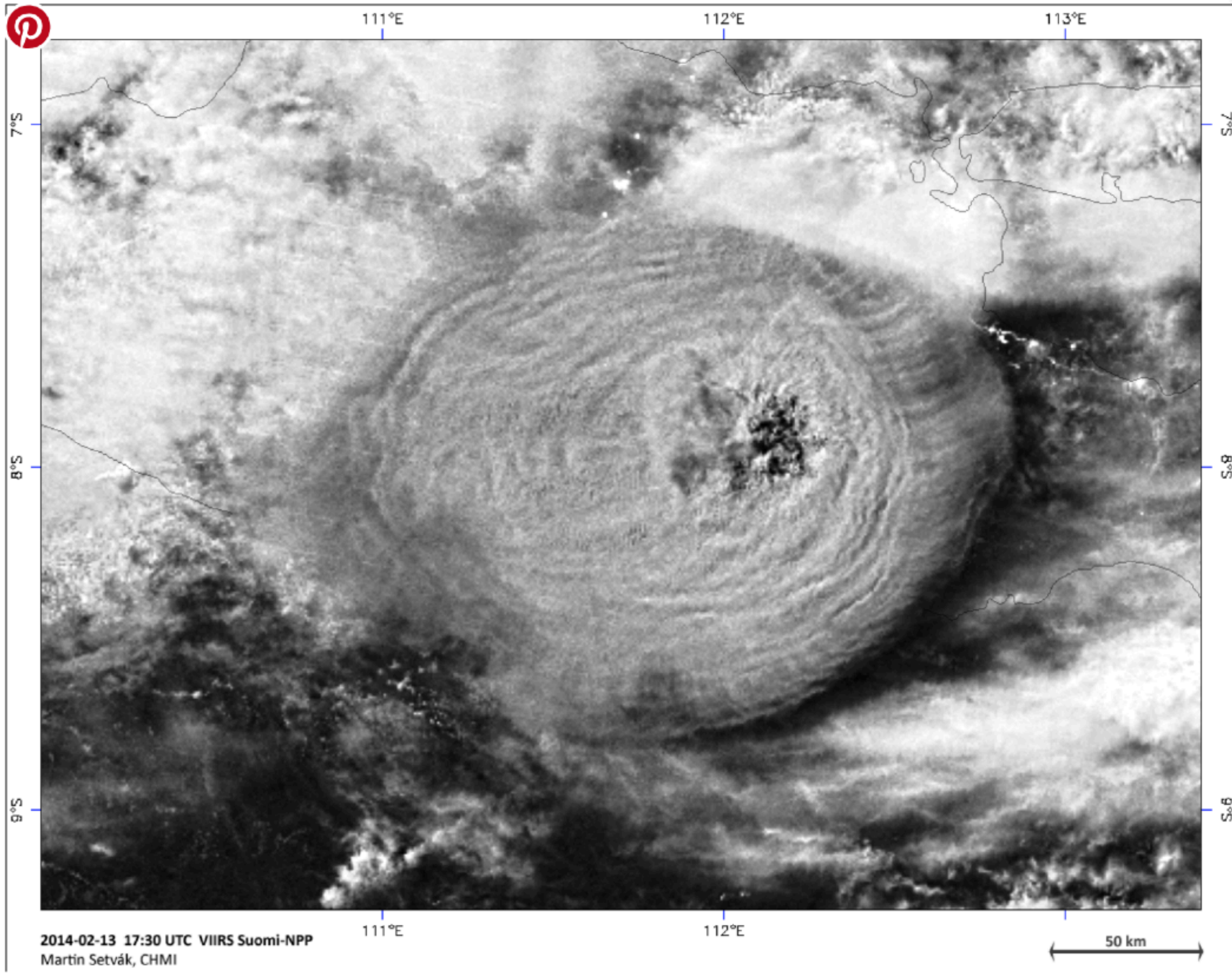

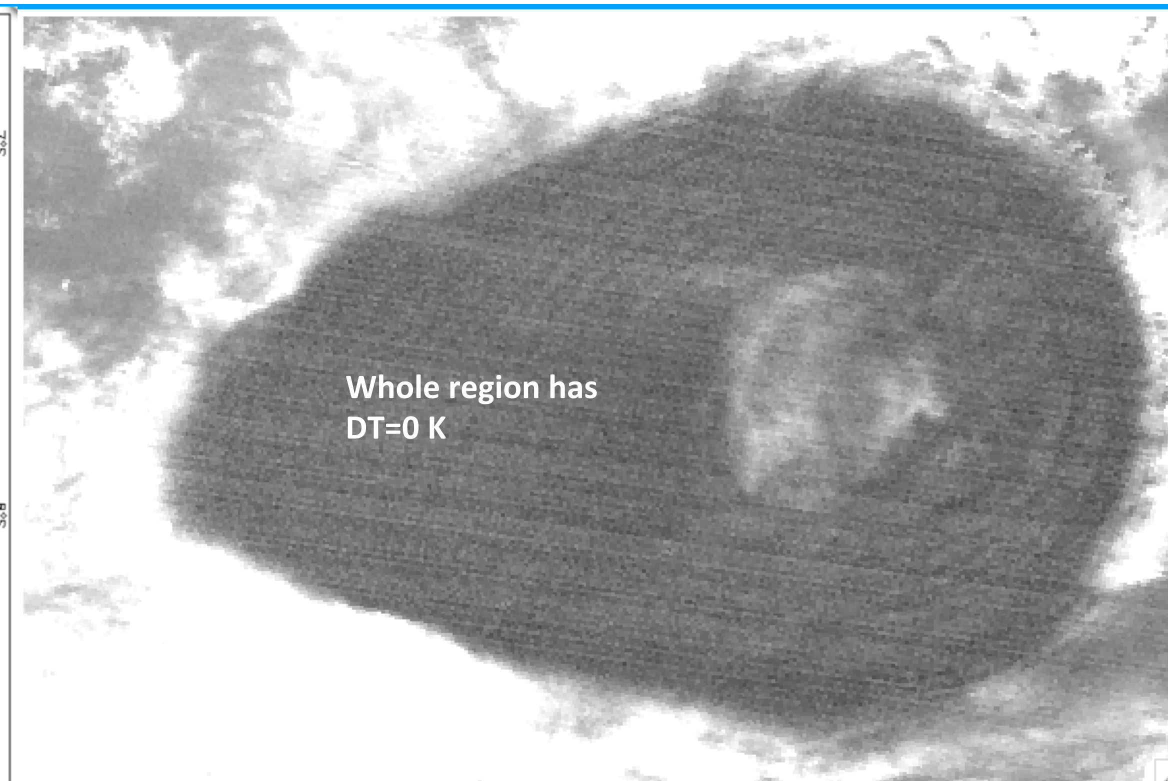

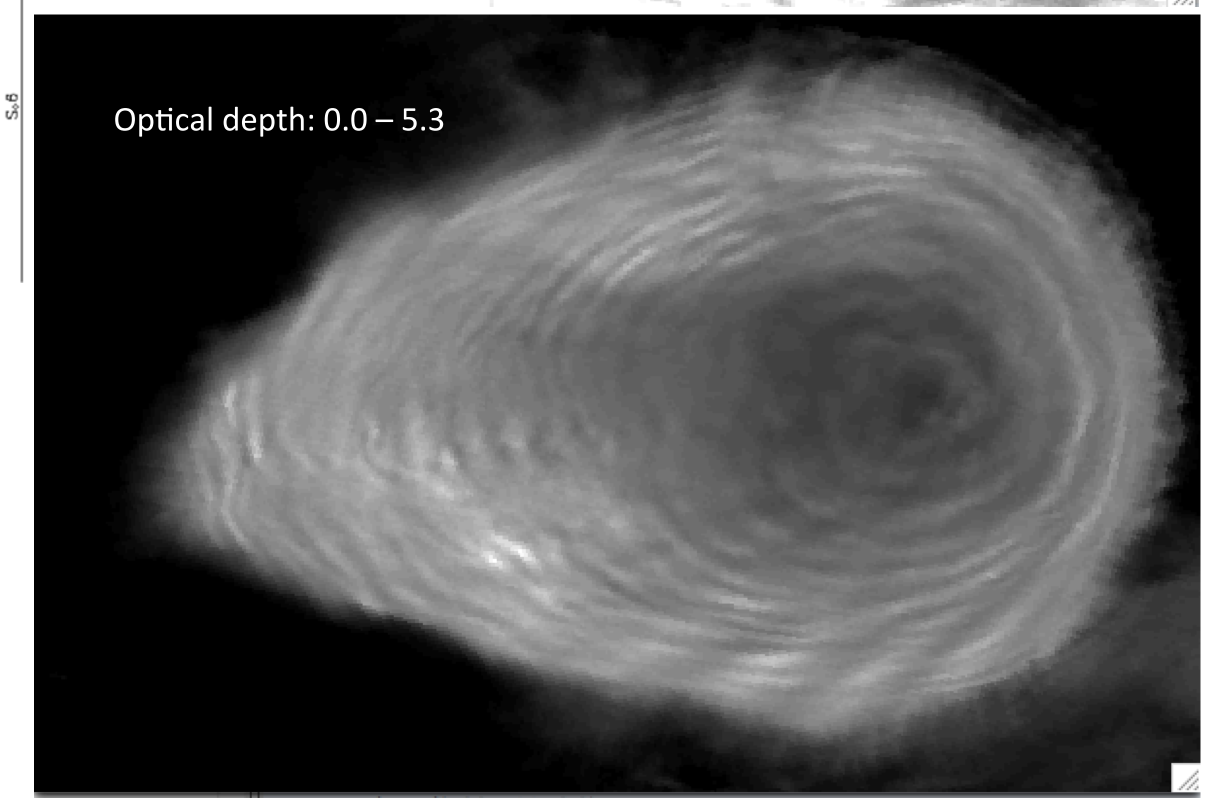

Mt Kelut eruption, Java. 13 February 2014

https://www.eumetsat.int/website/home/Images/ImageLibrary/DAT_2169181.html

Ash mass loadings remain high > 4 g m^{-2} 12 hours later

AVHRR N18 07:15UTC 14 February 2014.

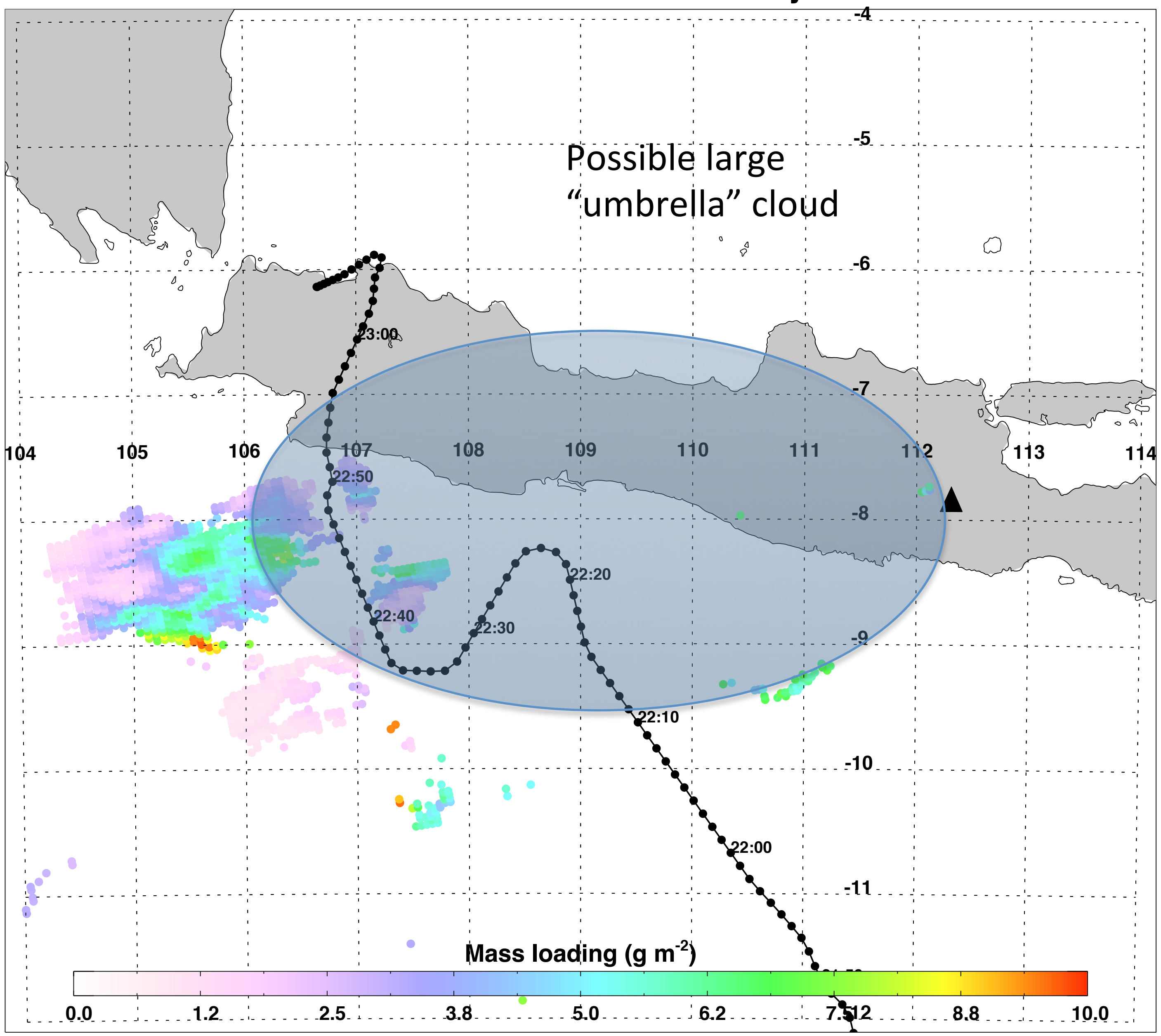

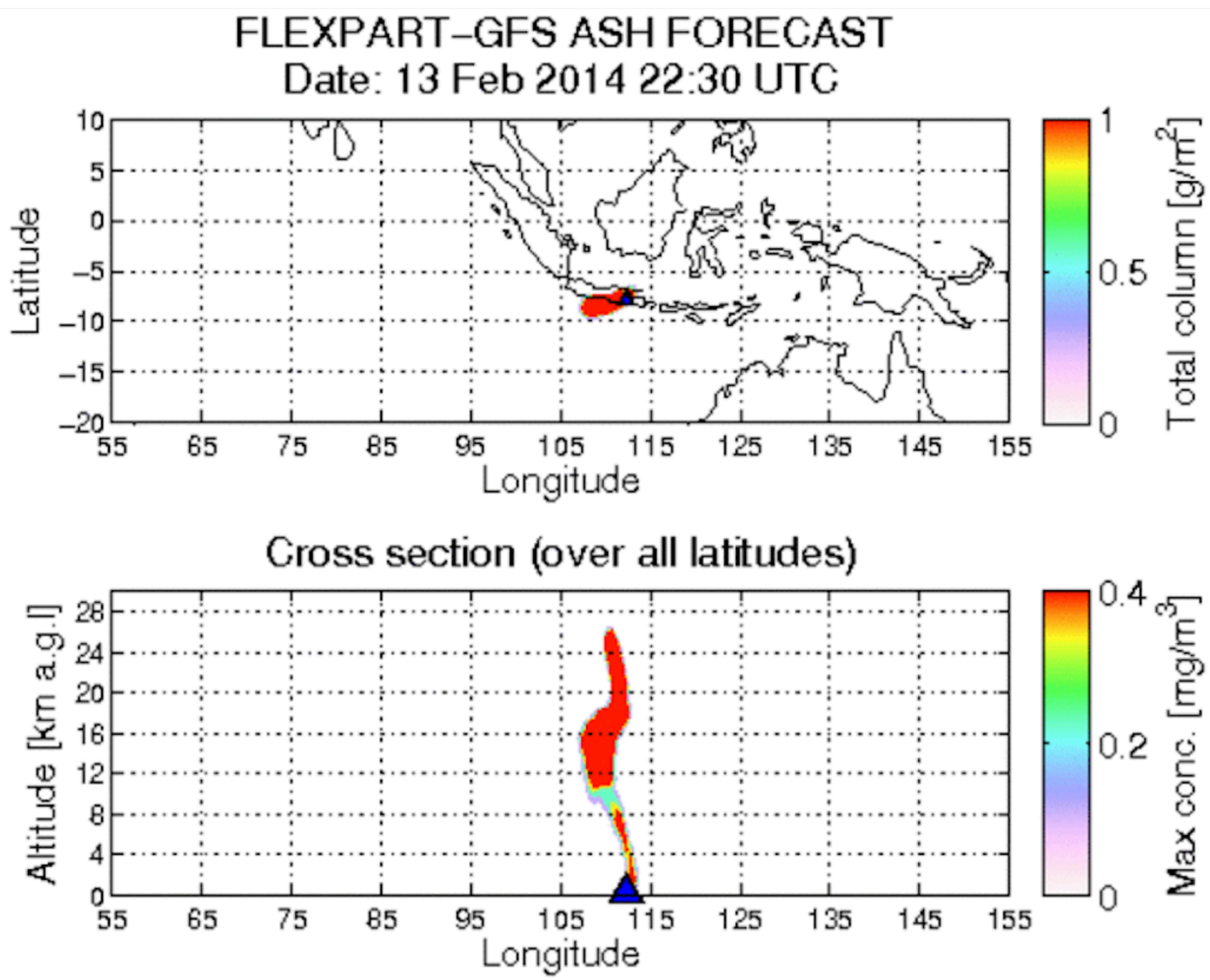
FLEXPART–GFS ASH FORECAST
Date: 13 Feb 2014 22:30 UTC
Latitude
Longitude
Total column [g/m^2]
Cross section (over all latitudes)
Altitude [km a.g.l]
Longitude
Max conc. [mg/m^3]

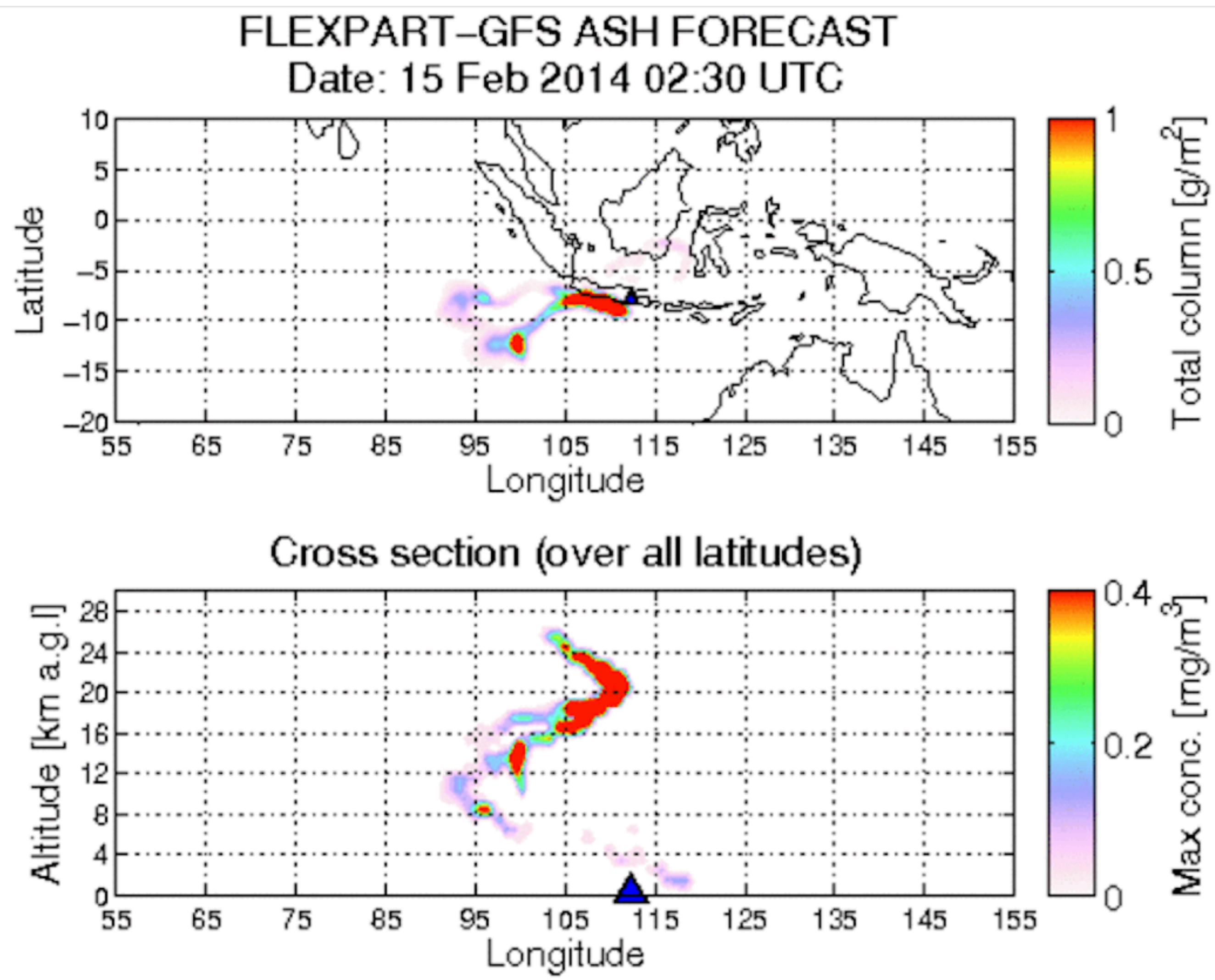
FLEXPART–GFS ASH FORECAST
Date: 15 Feb 2014 02:30 UTC
Latitude
Longitude
Total column [g/m^2]
Cross section (over all latitudes)
Altitude [km a.g.l]
Longitude
Max conc. [mg/m^3]

FLEXPART-GFS MODEL SIMULATION
13 Feb 2014 22:30 - 23:30 UTC

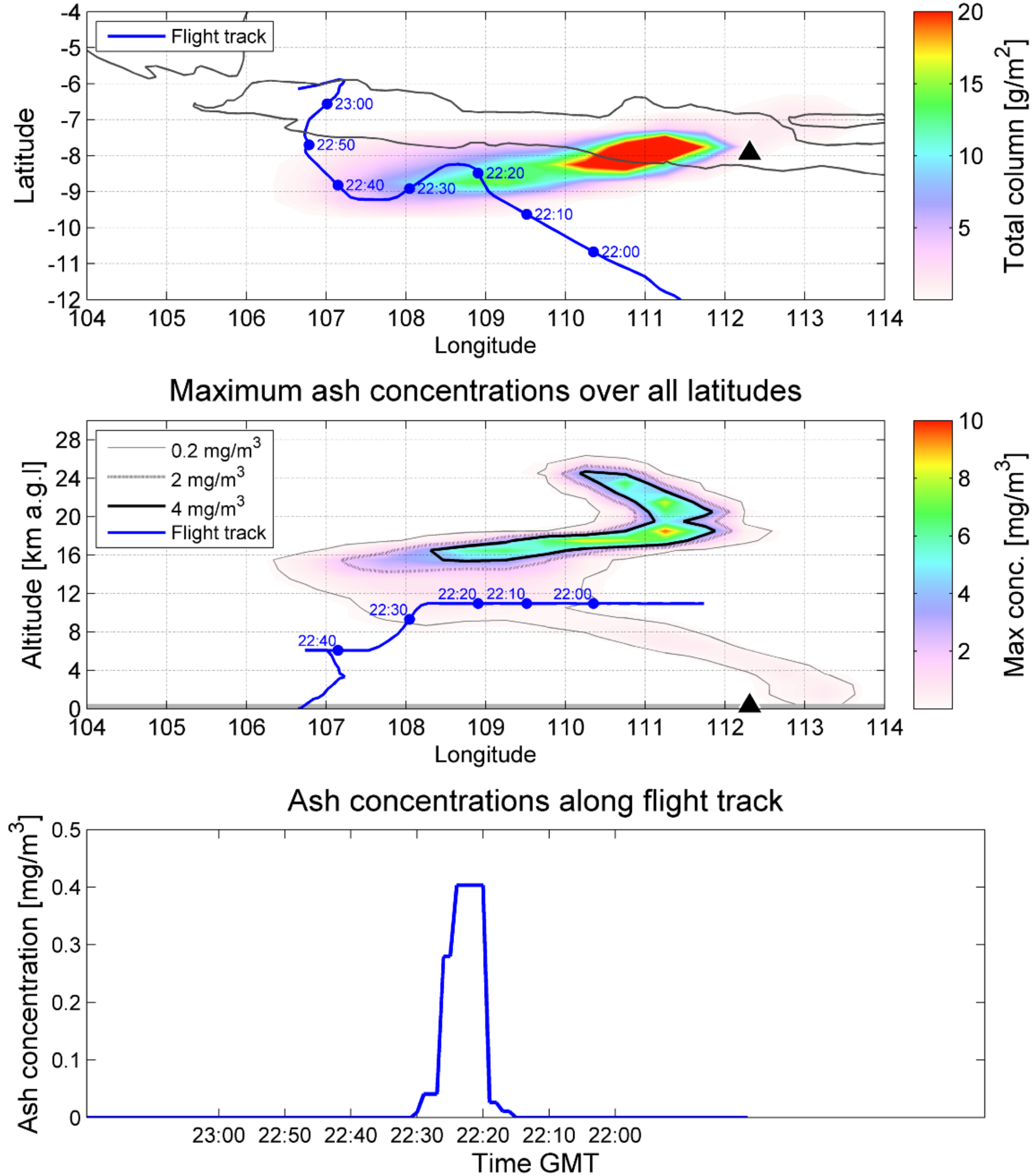

How to use satellite imagery: Estimation of cloud height

Some current methods

Radiative Transfer	Cloud-top Temperature + Radiosonde profile	Cloud slicing	Optimal Estimation
Geometrical	Cloud shadow	Stereoscopy	
Direct Measurement	Lidar	Radiosonde	Radar
Model	Plume position and dispersion	Inverse modelling	

Cloud shadow

e.g. Prata and Grant (2001)

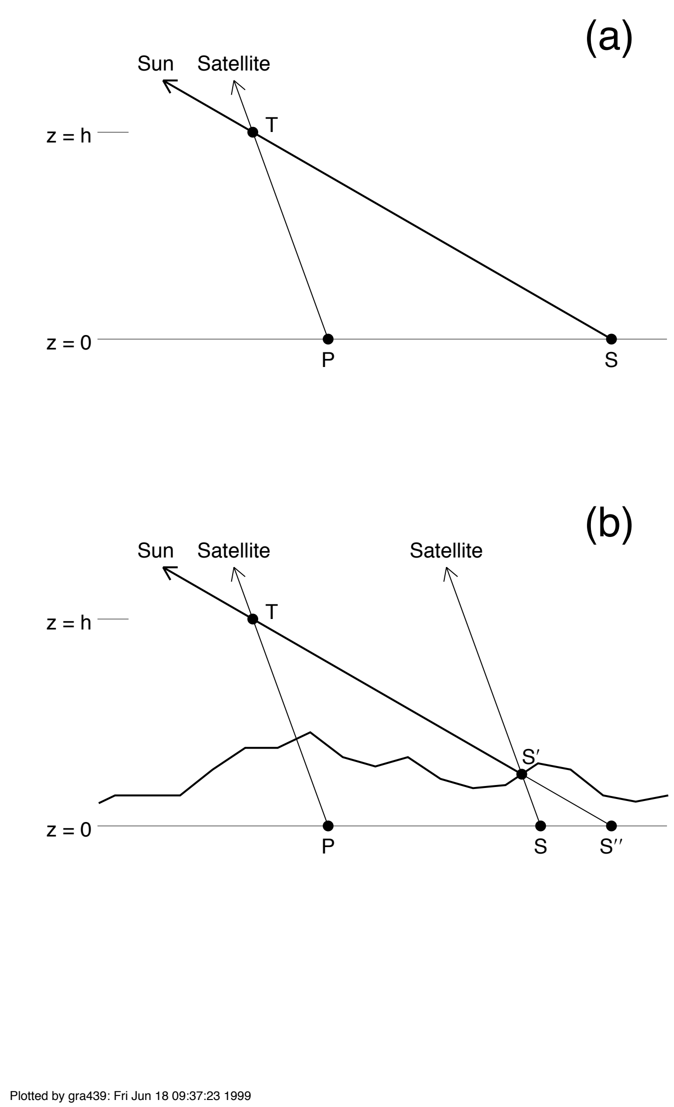

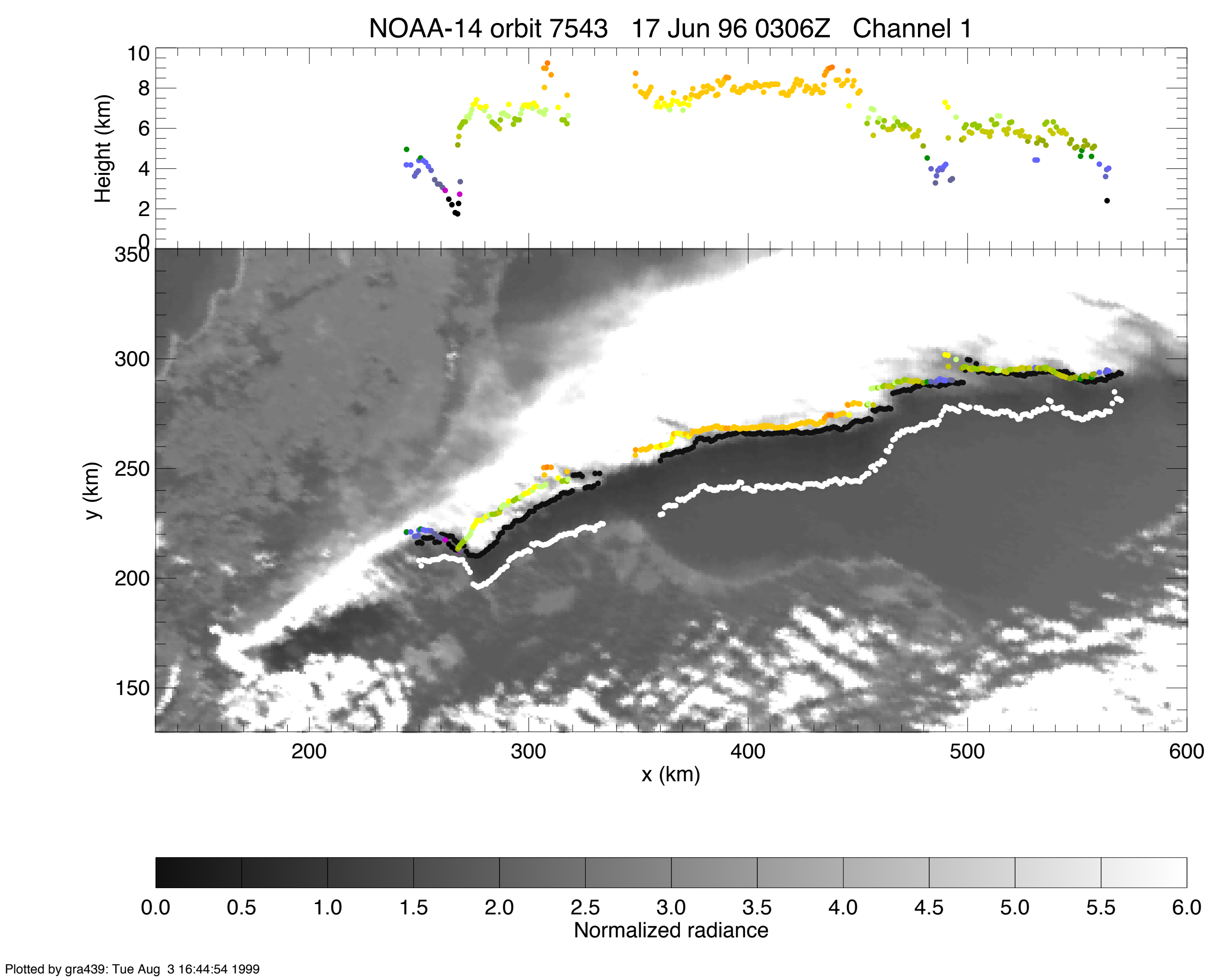

Reference: Prata, A. J. and I. F. Grant (2001) Retrieval of microphysical and morphological properties of volcanic ash plumes from satellite data: Application to Mt. Ruapehu, New Zealand., *Quarterly journal of the Royal Meteorological Society*, 127 (576B), 2153-2179.

Geometry: Parallax from two satellites

e.g. Merucci, L., Klemen Zakšek, K., Carboni, E. and S. Corradini (2016)

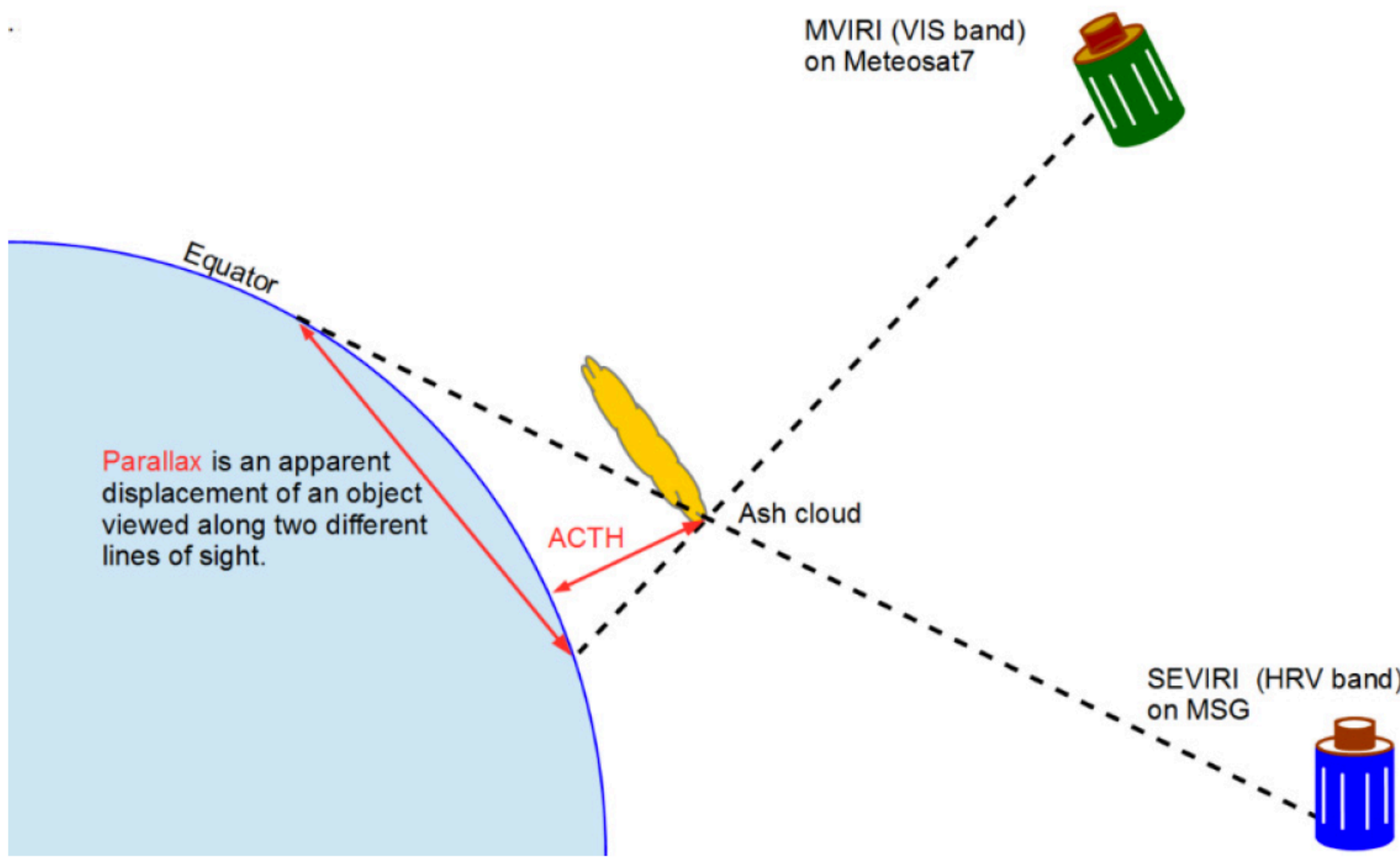

Reference: Merucci et al. (2016), Stereoscopic Estimation of Volcanic Ash Cloud-Top Height from Two Geostationary Satellites,Remote Sens., 8, 206; doi:10.3390/rs8030206

Other methods

Inversion:
Stohl, A., Prata, A.J., Eckhardt, S., Clarisse, L., Durant, A., Henne, S., Kristiansen, N.I., Minikin, A., Schumann, U., Seibert, P. et al. **(2011).** Determination of time- and height-resolved volcanic ash emissions and their use for quantitative ash dispersion modeling: The 2010 Eyjafjallajökull eruption. *Atmos. Chem. Phys.*, 11, 4333–4351.

Optimal Estimation:
Francis, P.N., Cooke, M.C. and Saunders, R.W., **(2012).** Retrieval of physical properties of volcanic ash using Meteosat: A case study from the 2010 Eyjafjallajökull eruption. *Journal of Geophysical Research: Atmospheres*, *117*(D20).

Cloud-slicing:
Holz, R.E., Ackerman, S., Antonelli, P., Nagle, F., Knuteson, R.O., McGill, M., Hlavka, D.L. and Hart, W.D., **(2006).** An improvement to the high-spectral-resolution CO_2-slicing cloud-top altitude retrieval. *Journal of Atmospheric and Oceanic Technology*, *23*(5), pp.653-670.

MISR Stereo:
Flower, V.J. and Kahn, R.A., **(2017).** Assessing the altitude and dispersion of volcanic plumes using MISR multi-angle imaging from space: Sixteen years of volcanic activity in the Kamchatka Peninsula, Russia. *Journal of Volcanology and Geothermal Research*, *337*, pp.1-15.

Cloud-top/radiosonde:
Woods, A.W. and Self, S., **(1992).** Thermal disequilibrium at the top of volcanic clouds and its effect on estimates of the column height. *Nature*, *355*(6361), p.628.

AIRES Pty Ltd

Stereoscopy from ATSR/ATSR-2/AATSR/SLSTR

e.g. Prata and Turner (1997)

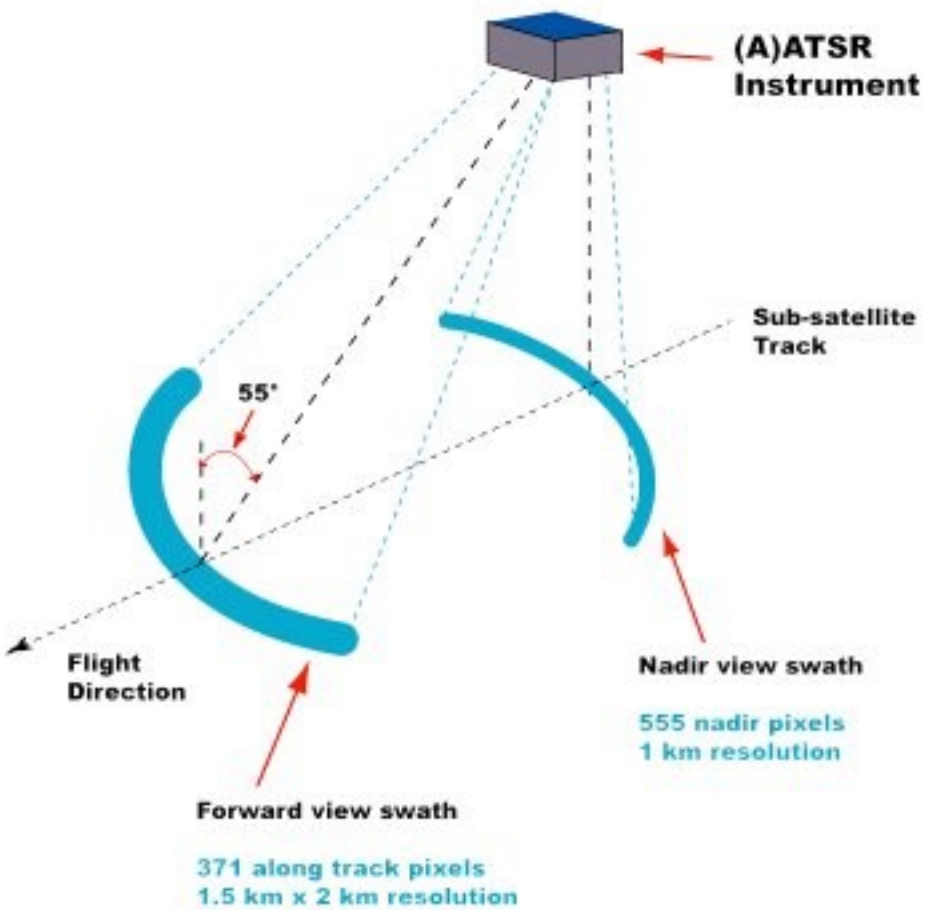

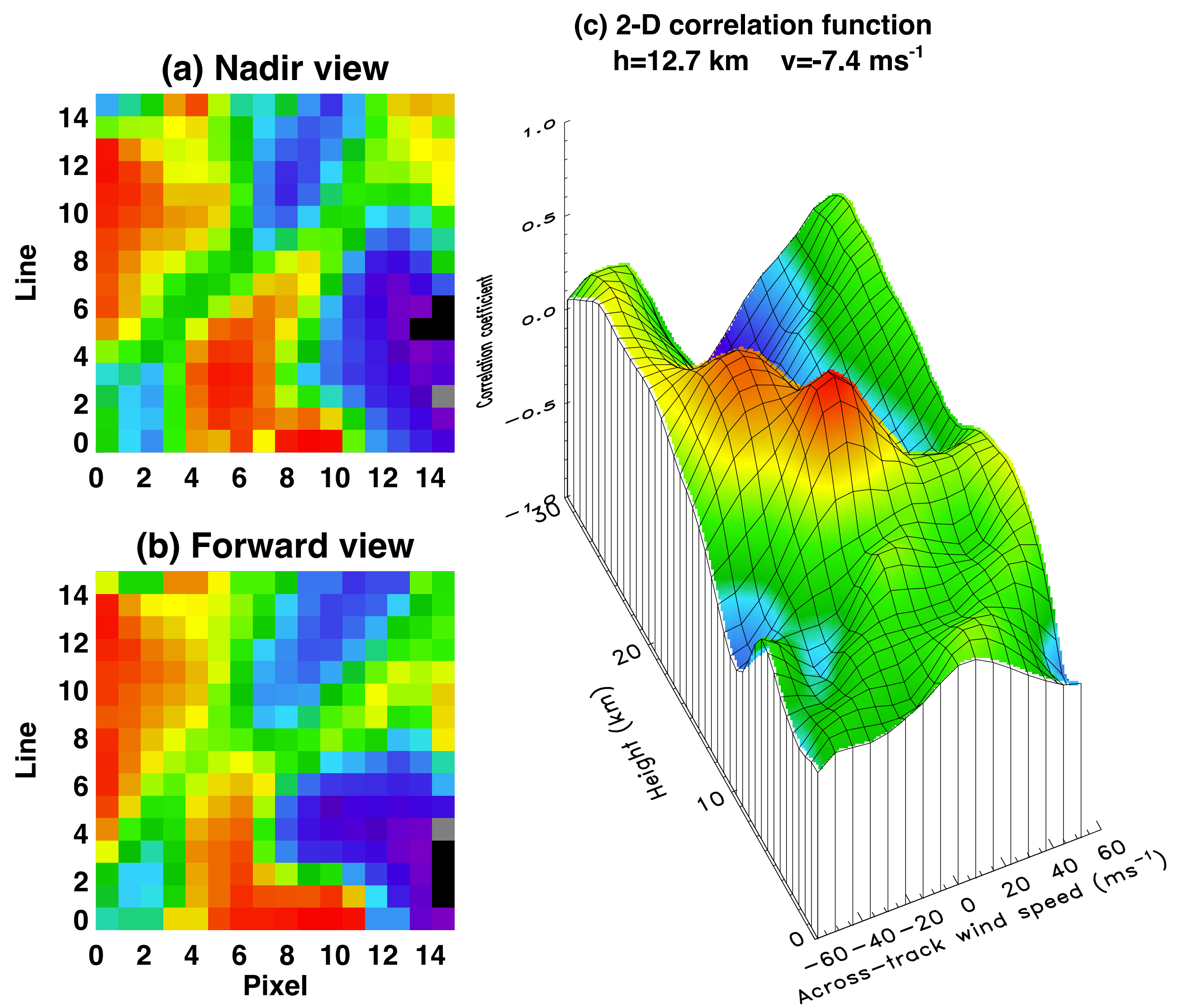

Lascar eruption

ATSR-2 Stereo Pairs

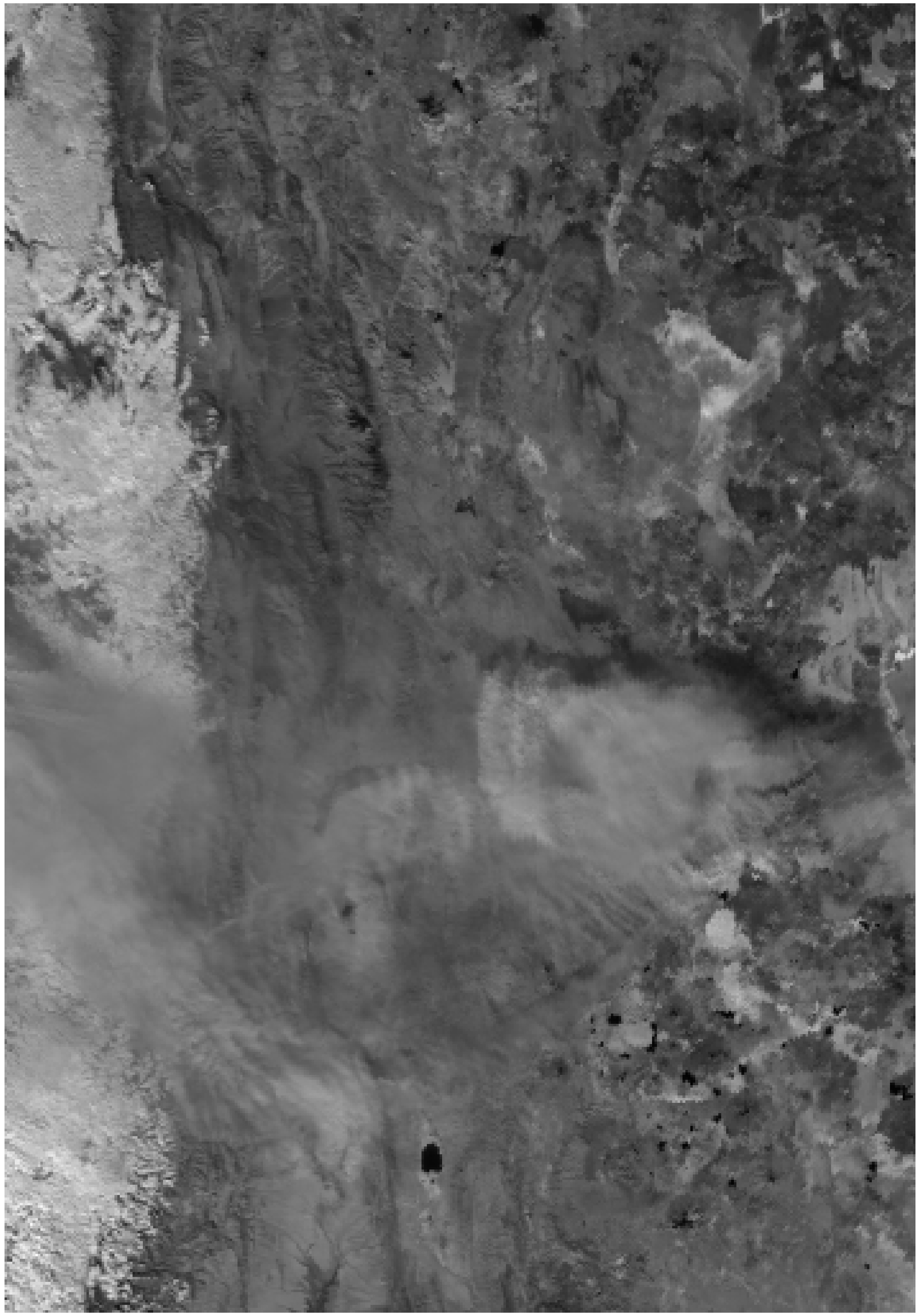

Nadir view

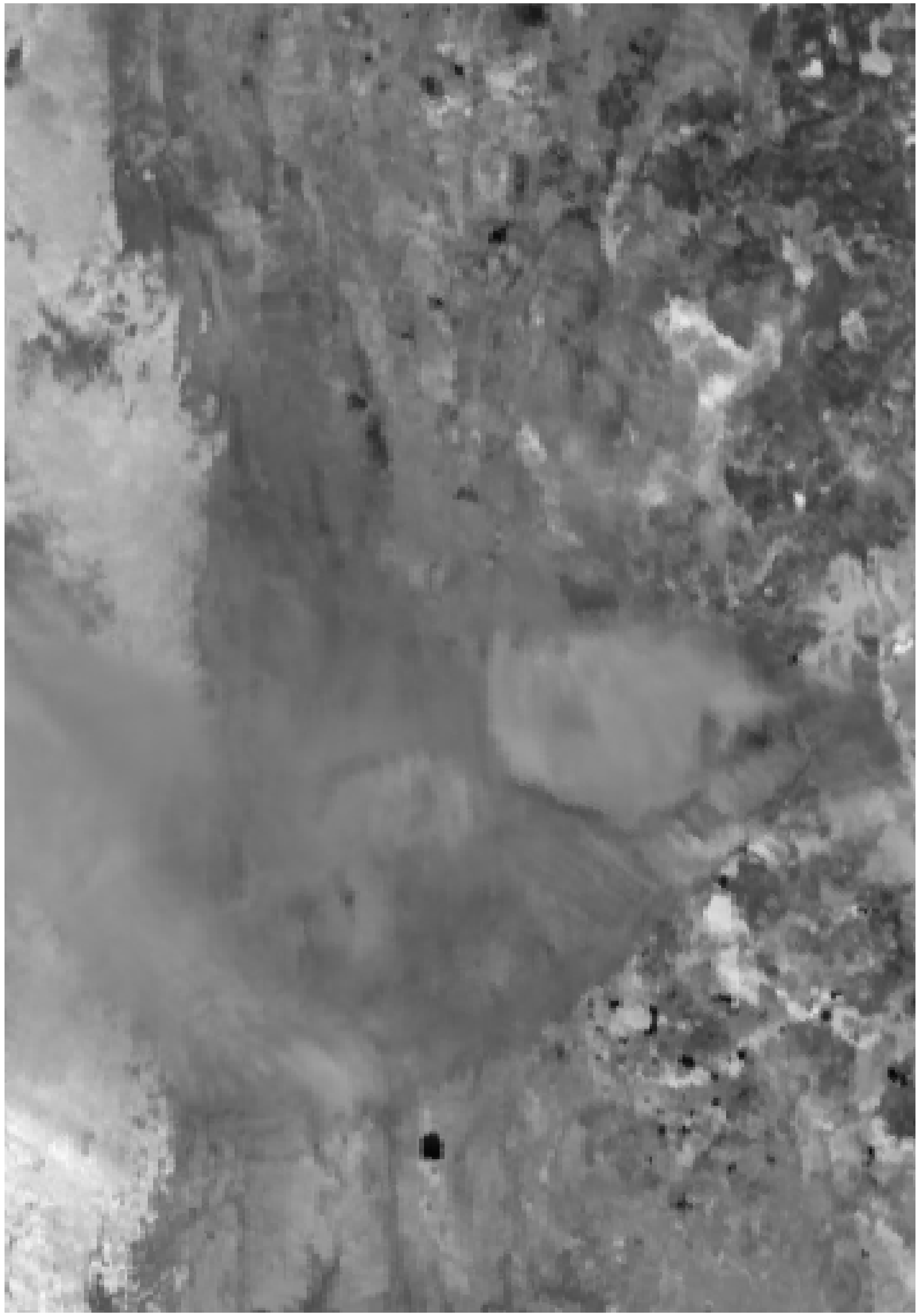

Forward view

AIRES Pty Ltd

Example: Eyjafjallajökull

8-May 2010 Highly dispersed ash cloud over ocean (>36 hrs old)

FLEXPART (model)

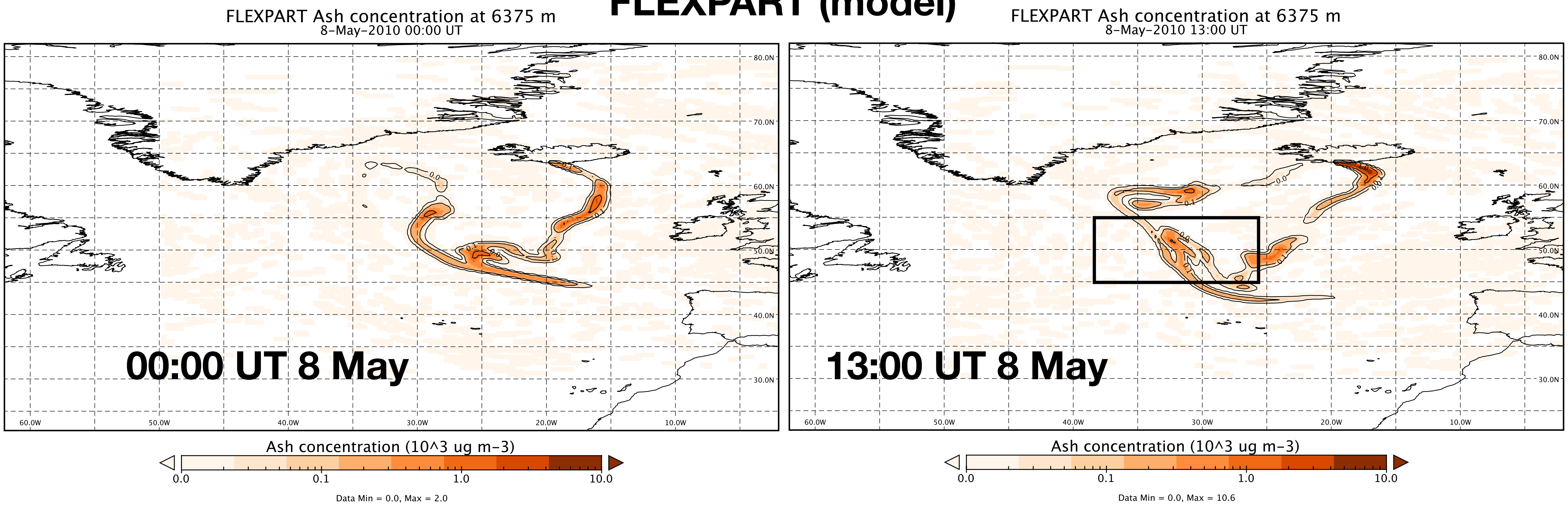

SEVIRI (actual measurements)

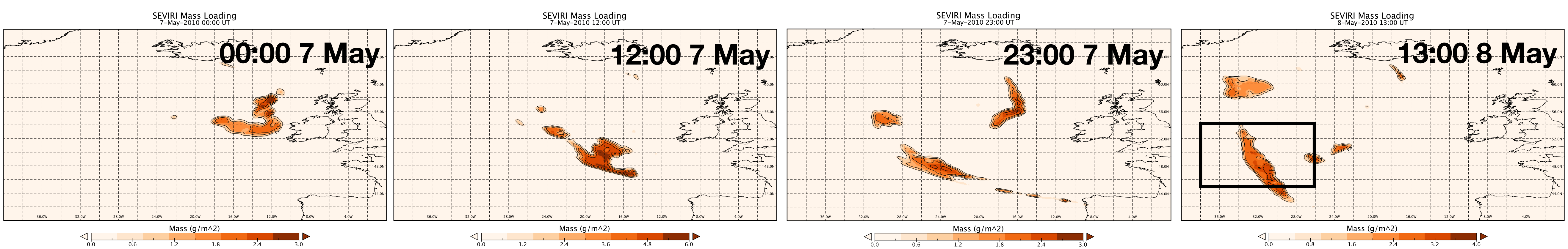

AATSR

BTD=T_{11}(nadir)-T_{12}(nadir)

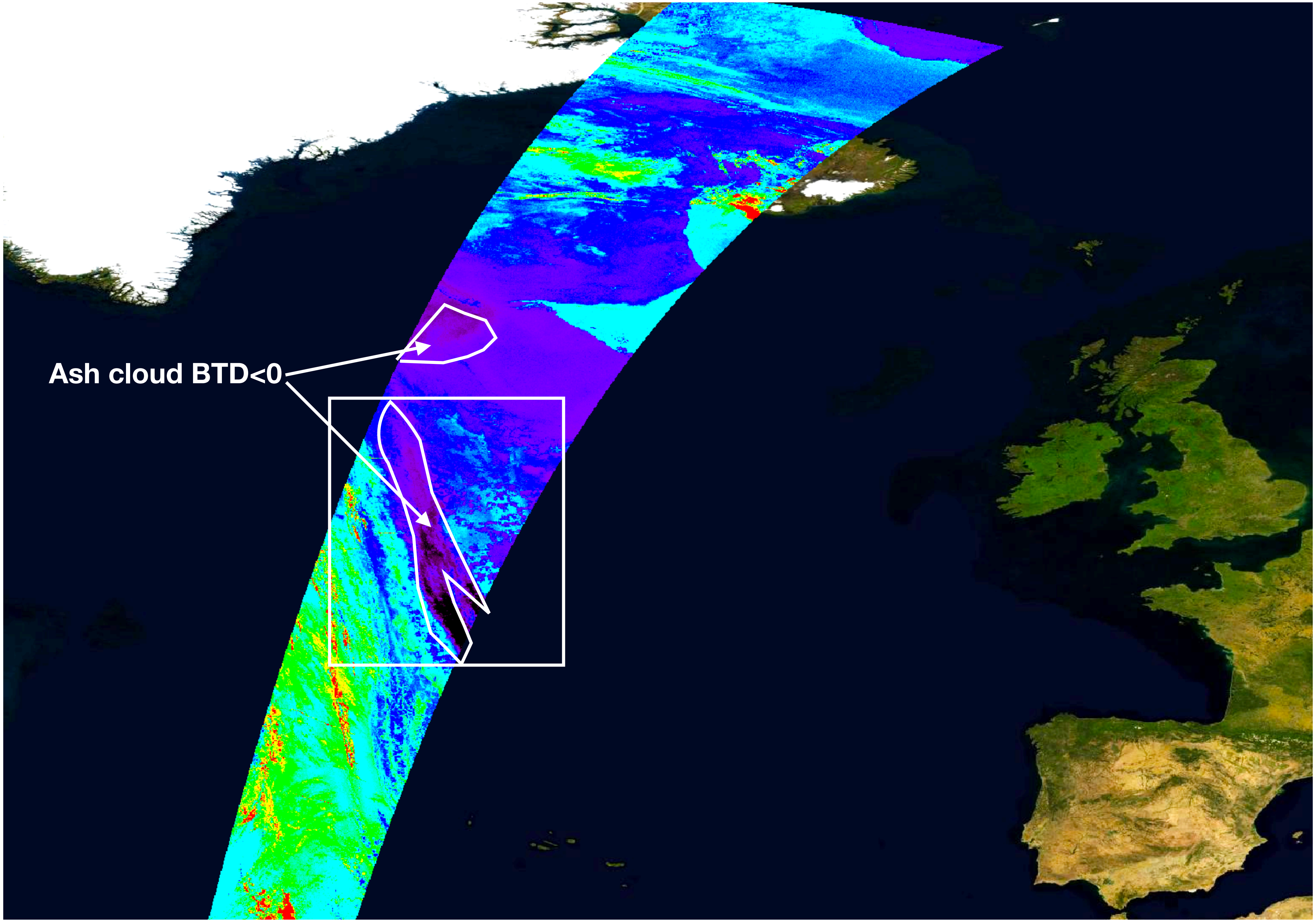

Stare at the image until a third *stereo* image appears between the pair (you may need to go "cross-eyed")

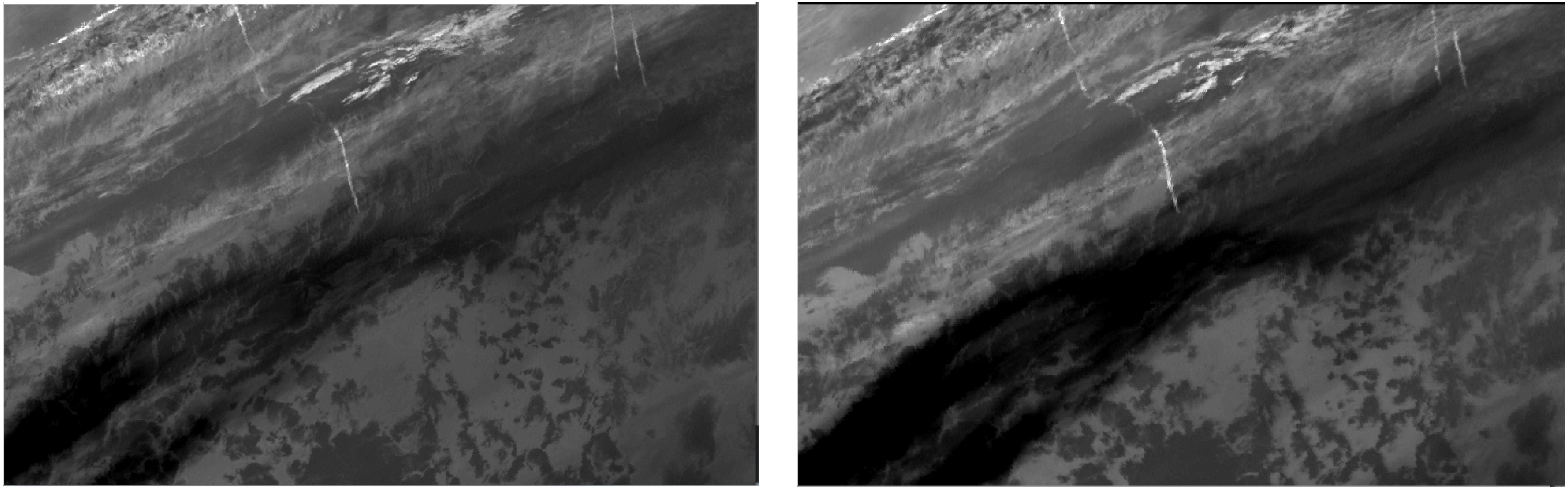

There is a thin veil of high cloud running across the top-left corner of the image
The aircraft contrails are below this
The ash cloud (dark) is below both

AIRES Pty Ltd

Height retrieval

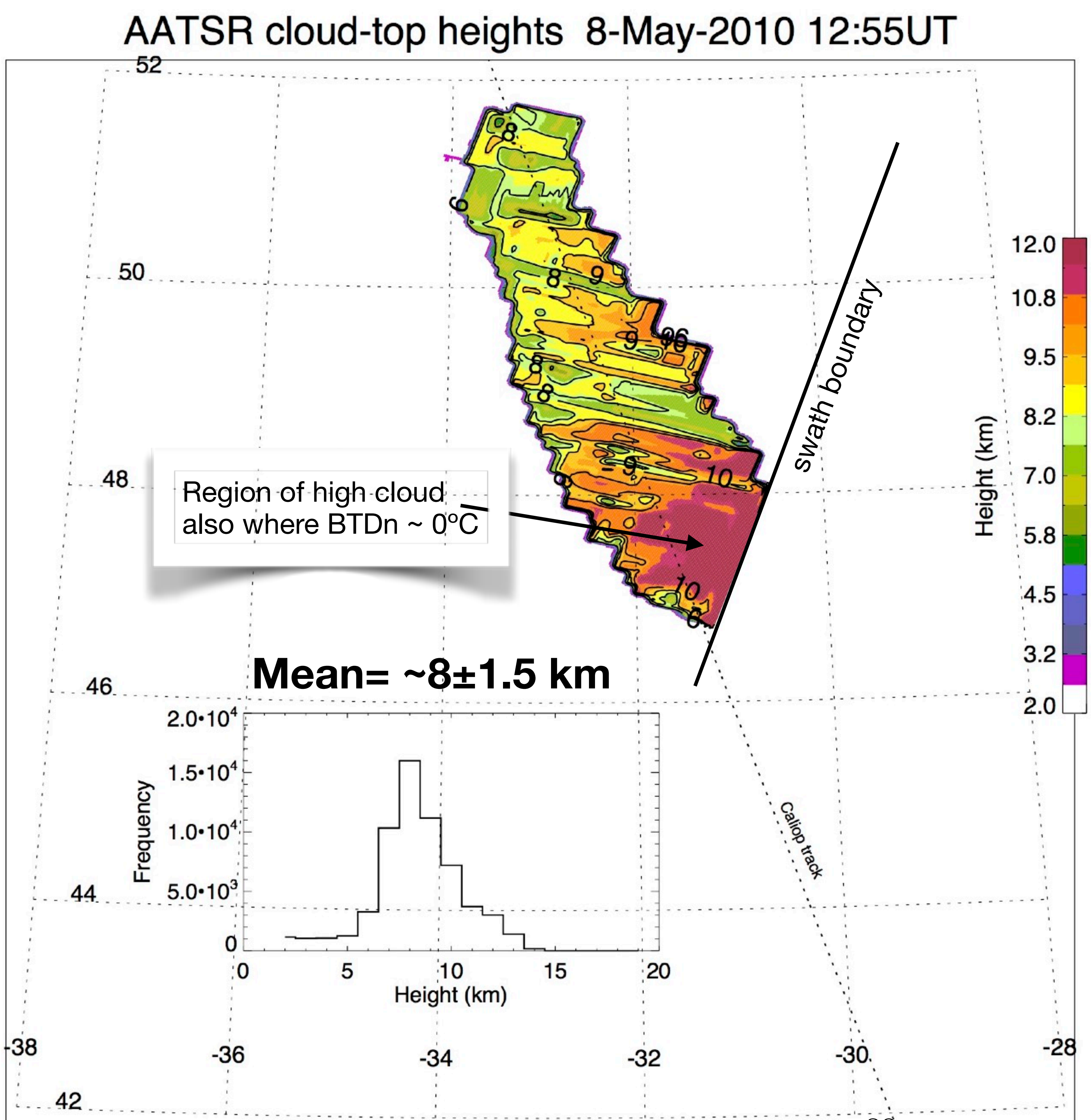

Method

Use 1.6 µm reflectance nadir and forward views. Only process pixels where $BTD_n<0$. The r^2 correlation between parts of the image is calculated in 8x8 pixel chunks. Some smoothing is applied for graphical representation.

AIRES Pty Ltd

Validation–Caliop/AIRS

Mean=7.86±1.8 km

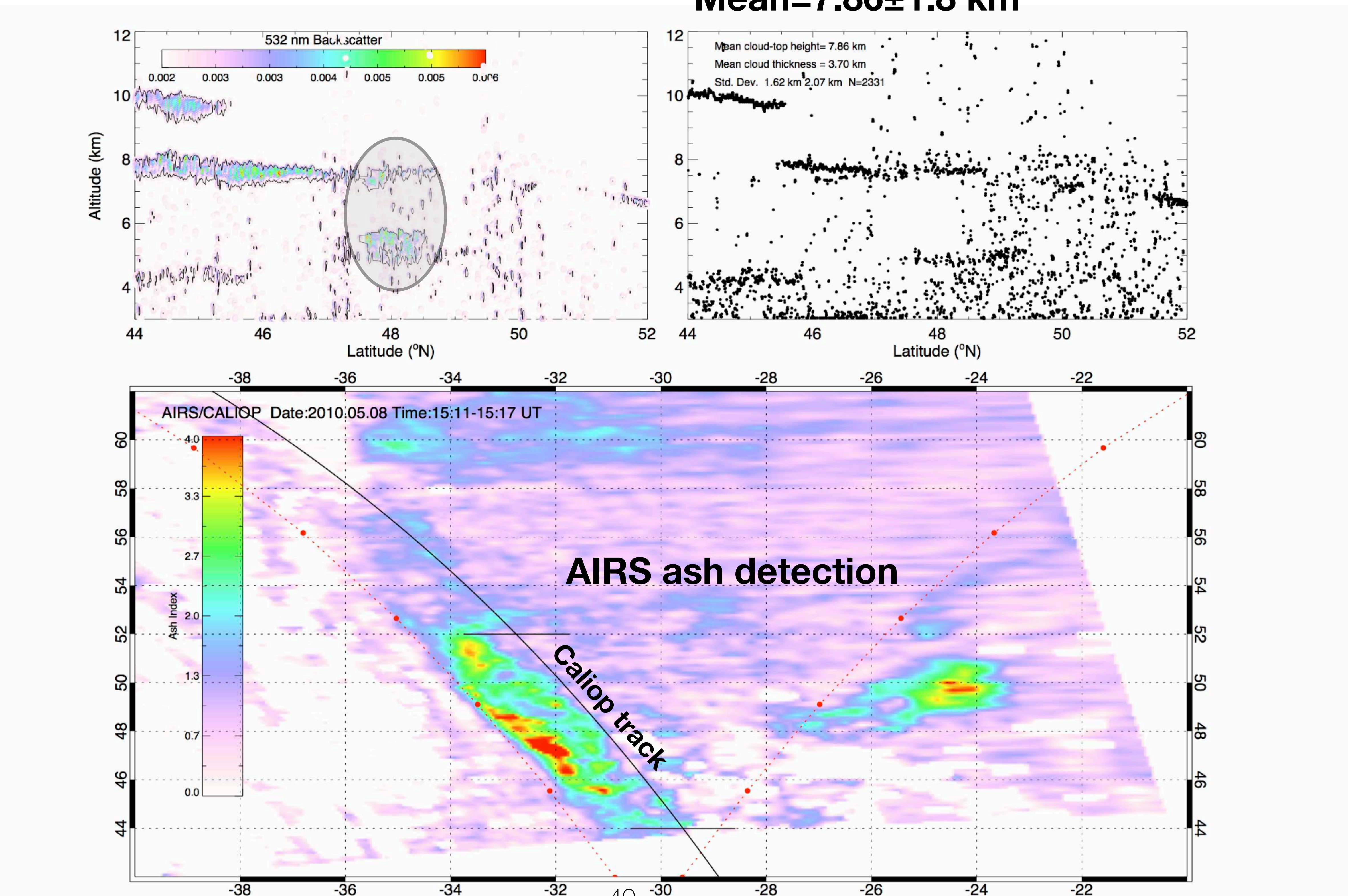

FLEXPART

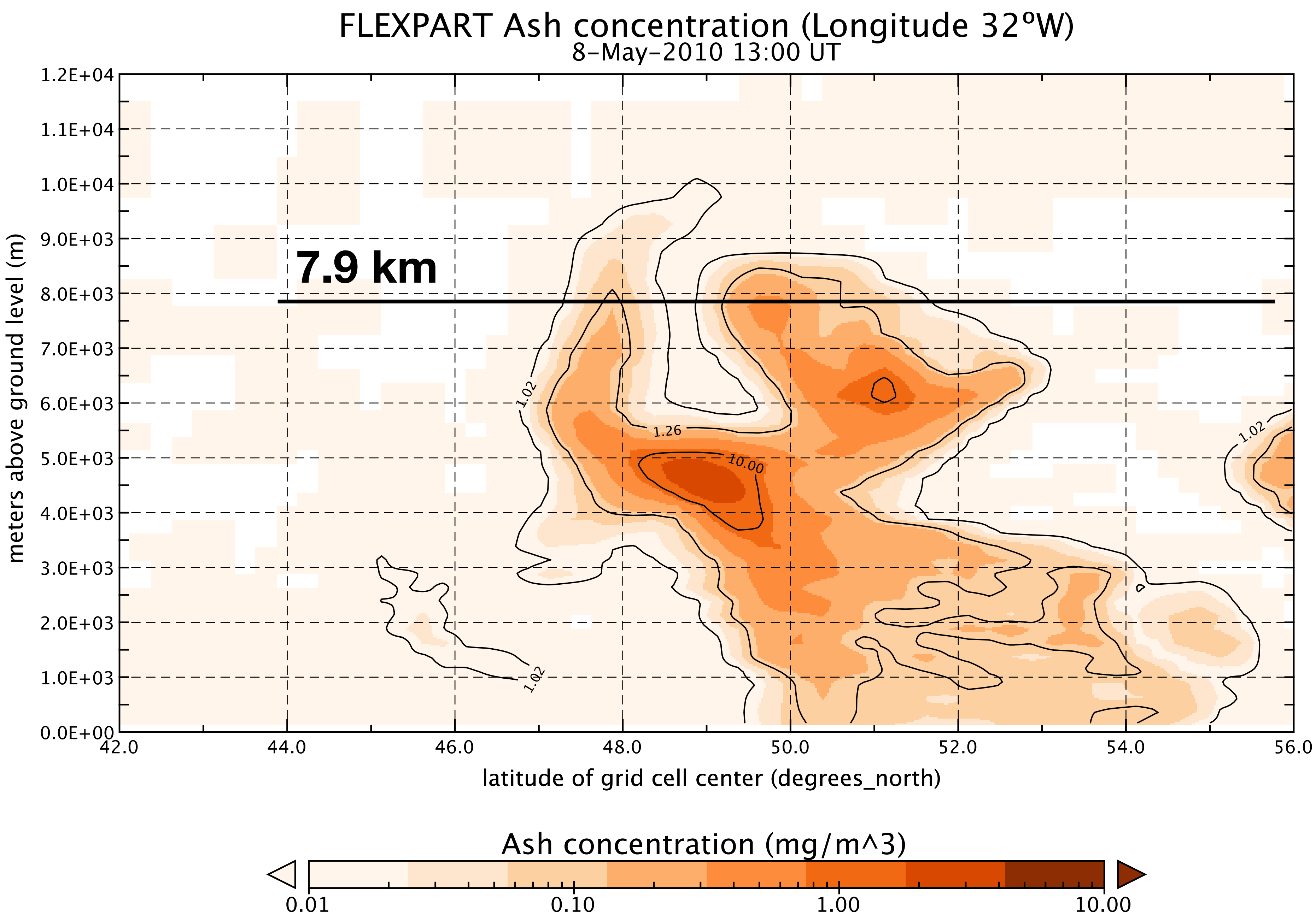
FLEXPART Ash concentration (Longitude 32°W)
8-May-2010 13:00 UT
7.9 km
meters above ground level (m)
latitude of grid cell center (degrees_north)
1.02
1.26
10.00
Ash concentration (mg/m^3)
0.01
0.10
1.00
10.00

Insights

Contrails show that aircraft were crossing the Atlantic while ash was in the vicinity

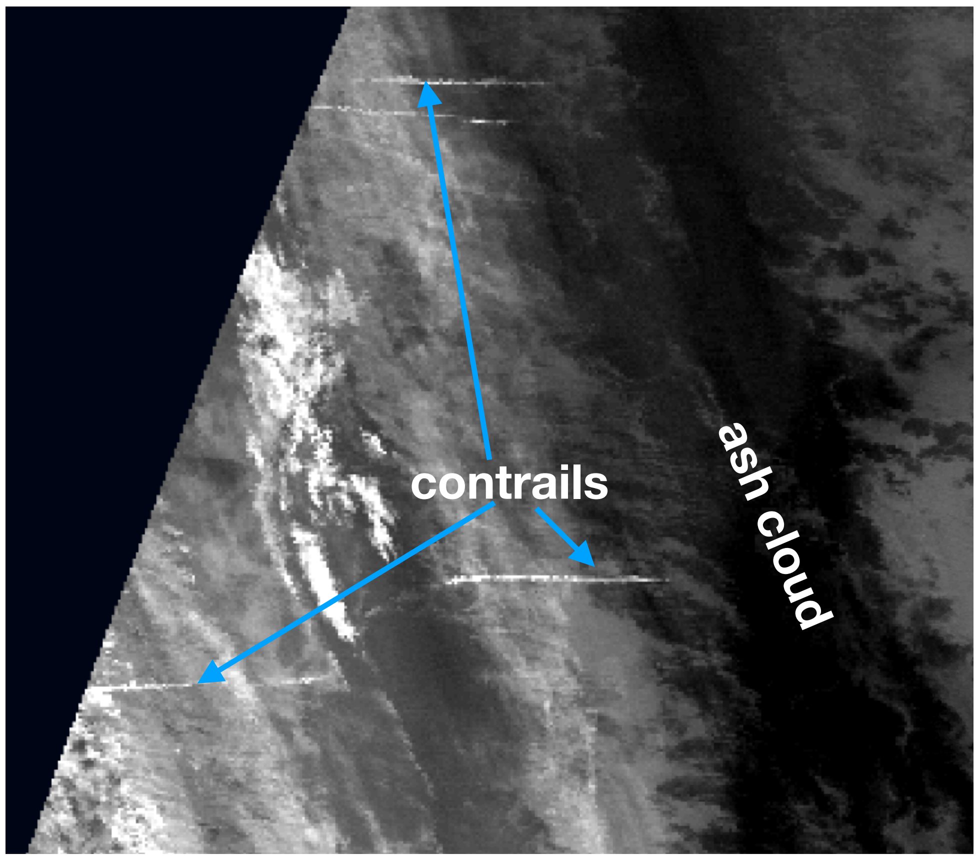

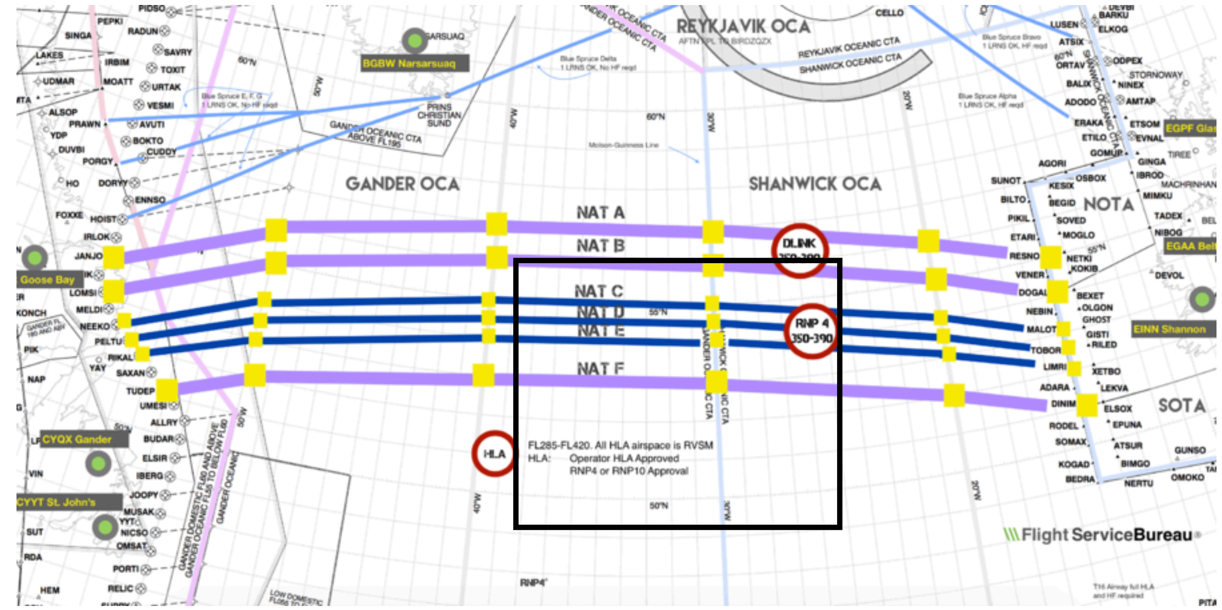

NATS 29,000–41,000 ft (~8.8–12.5 km)

London VAAC advisory suggests ash up to FL350 (35,000 ft ~10.7 km)

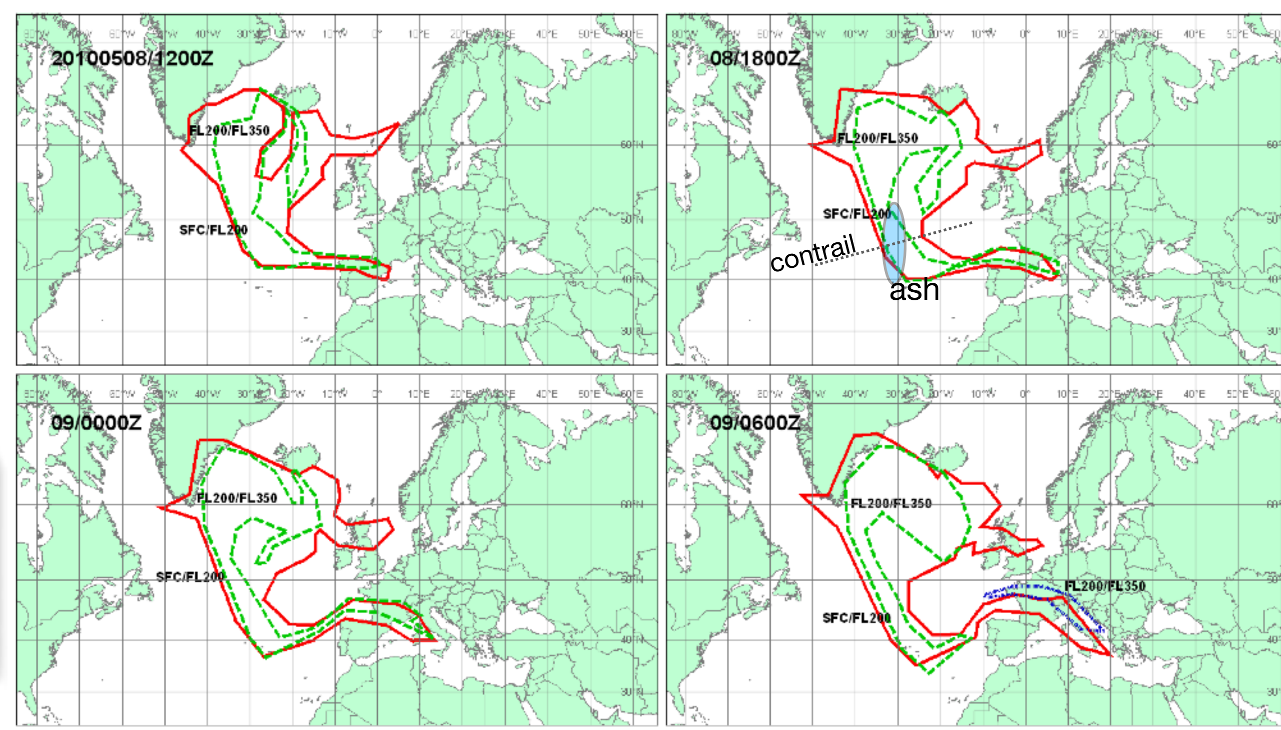

VA ADVISORY
DTG: 20100508/1200Z
VAAC: LONDON
VOLCANO:
EYJAFJALLAJOKULL 1702-02
PSN: N6338 W01937
AREA: ICELAND

SUMMIT ELEV: 1666M
ADVISORY NR: 2010/092
INFO SOURCE: ICELAND MET OFFICE
AVIATION COLOUR CODE: RED
ERUPTION DETAILS: PLUME ERUPTION
CONTINUES, HEIGHTS UP TO FL230.

RMK: ADVISORY NO. NOW UPDATED AND CORRECTED
NXT ADVISORY: 20100508/1800Z

AIRES Pty Ltd

Eruption Rate from Satellite Measurements

Prior art
(using satellite data)

- Cloud shape recognition – pioneering work of Sawada (motivation to identify volcanic clouds in single channel imagery) – 1980's
- Solène Pouget (and co-workers) – 2010 onwards
- Convective clouds – much work in atmospheric sciences based on rapid growth and precipitation onset

Geostationary Satellites

Geo-satellites ideal because of high data repetition

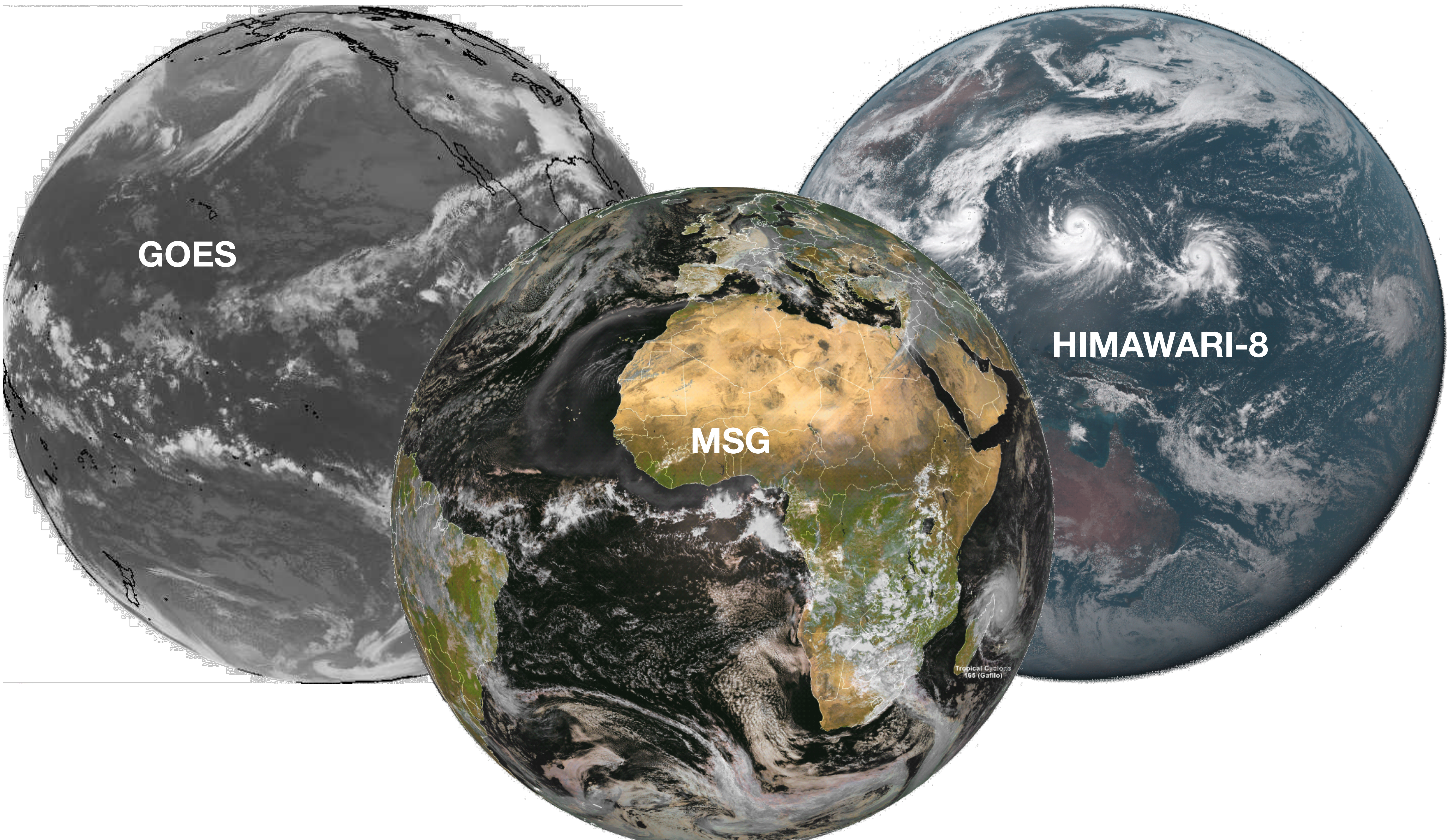

AIRES Pty Ltd

Eruption Rate from Satellite Measurements

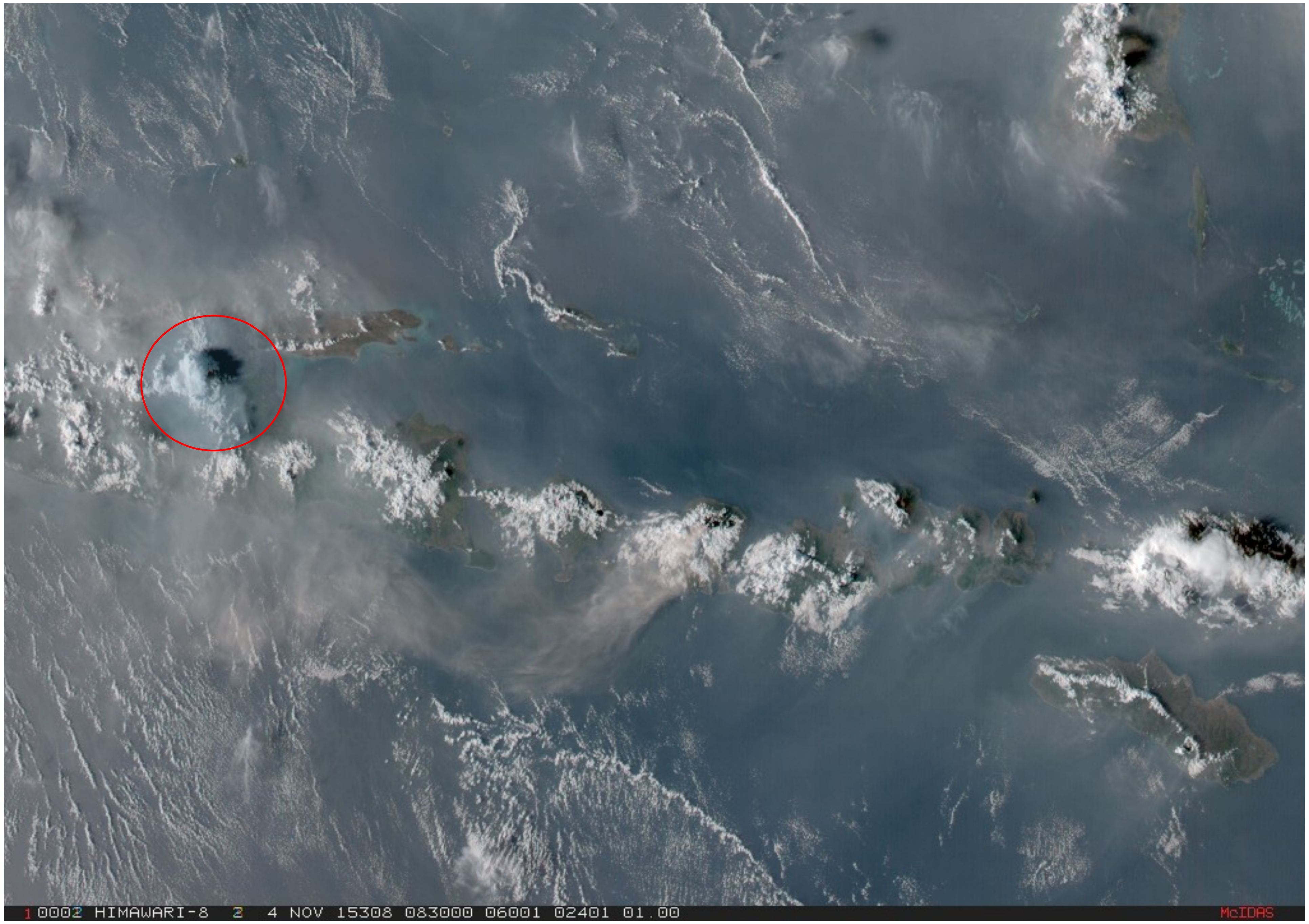

Example of rapid vertical (convective) development of meteorological cloud

AIRES Pty Ltd

Eruption Rate from Satellite Measurements

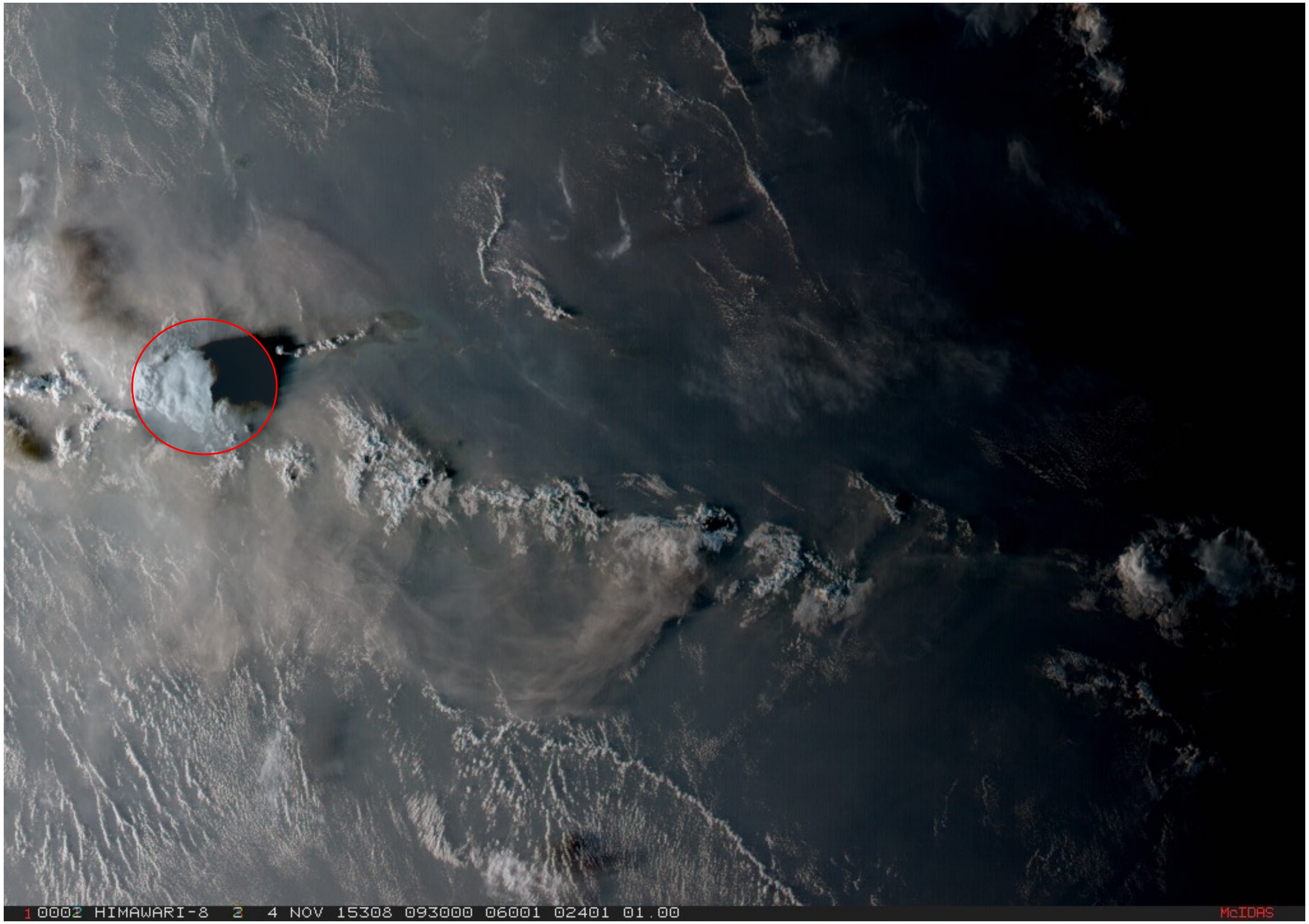

AIRES Pty Ltd

Eruption Rate from Satellite Measurements

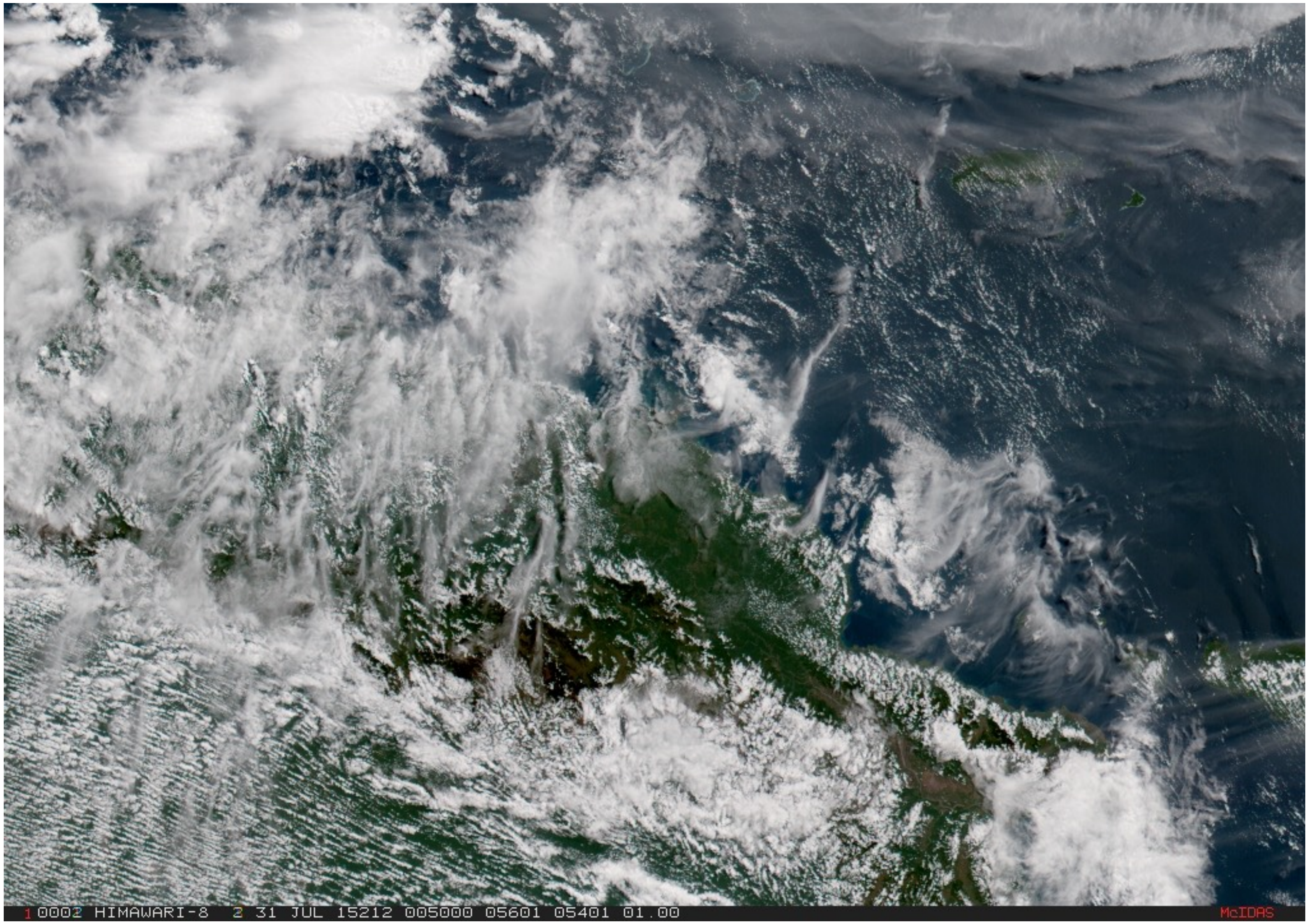

Eruption Rate from Satellite Measurements

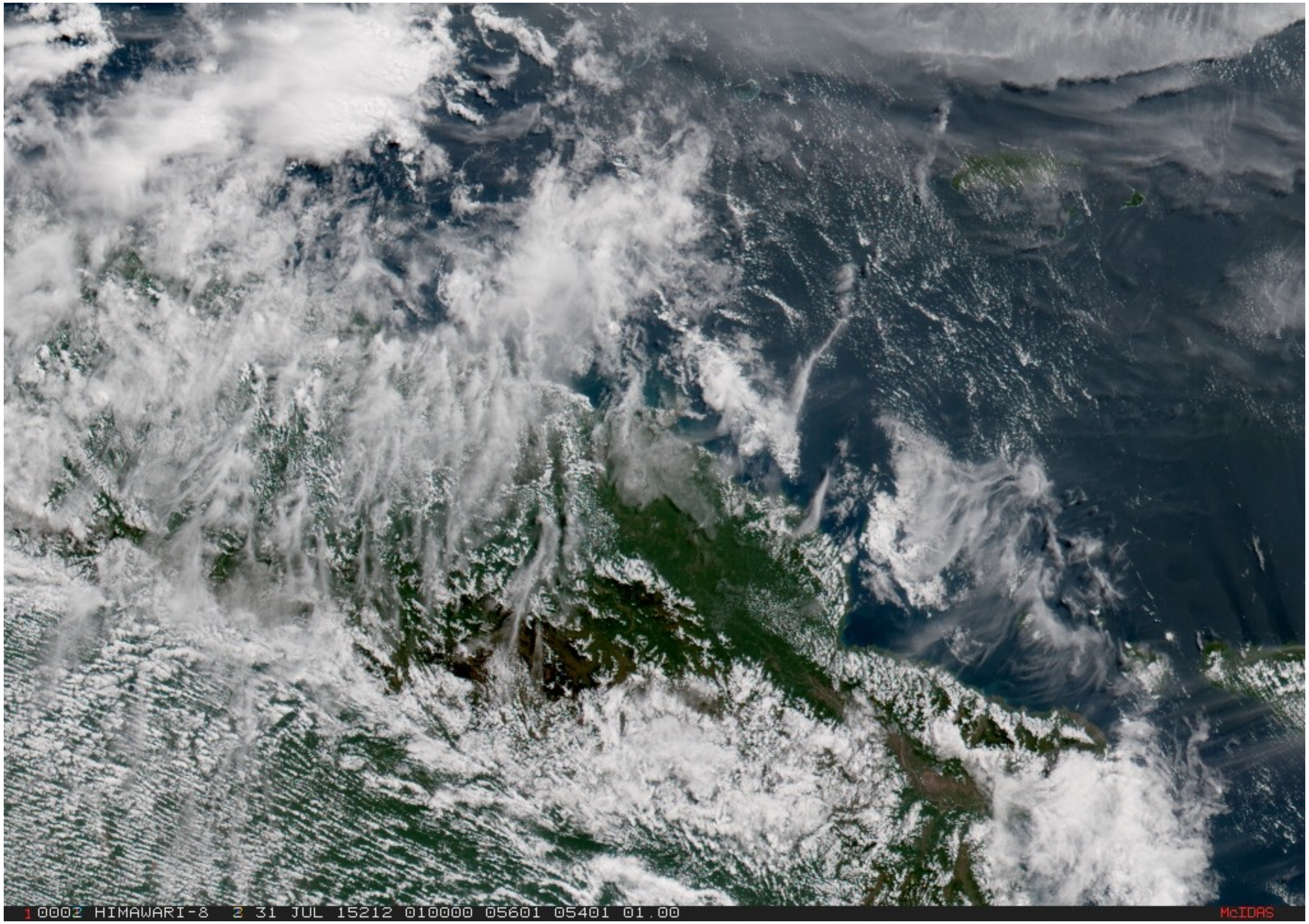

Eruption Rate from Satellite Measurements

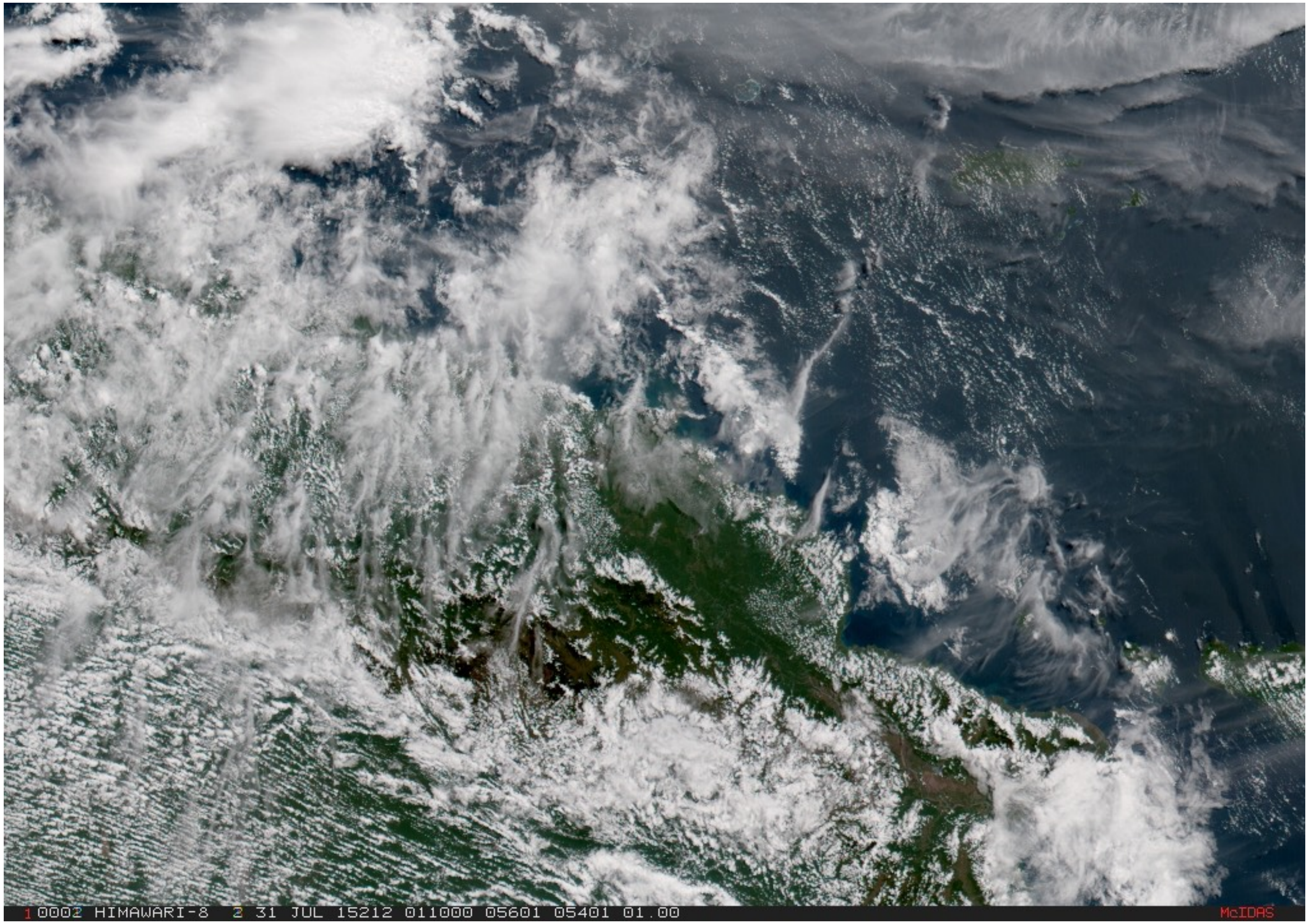

Eruption Rate from Satellite Measurements

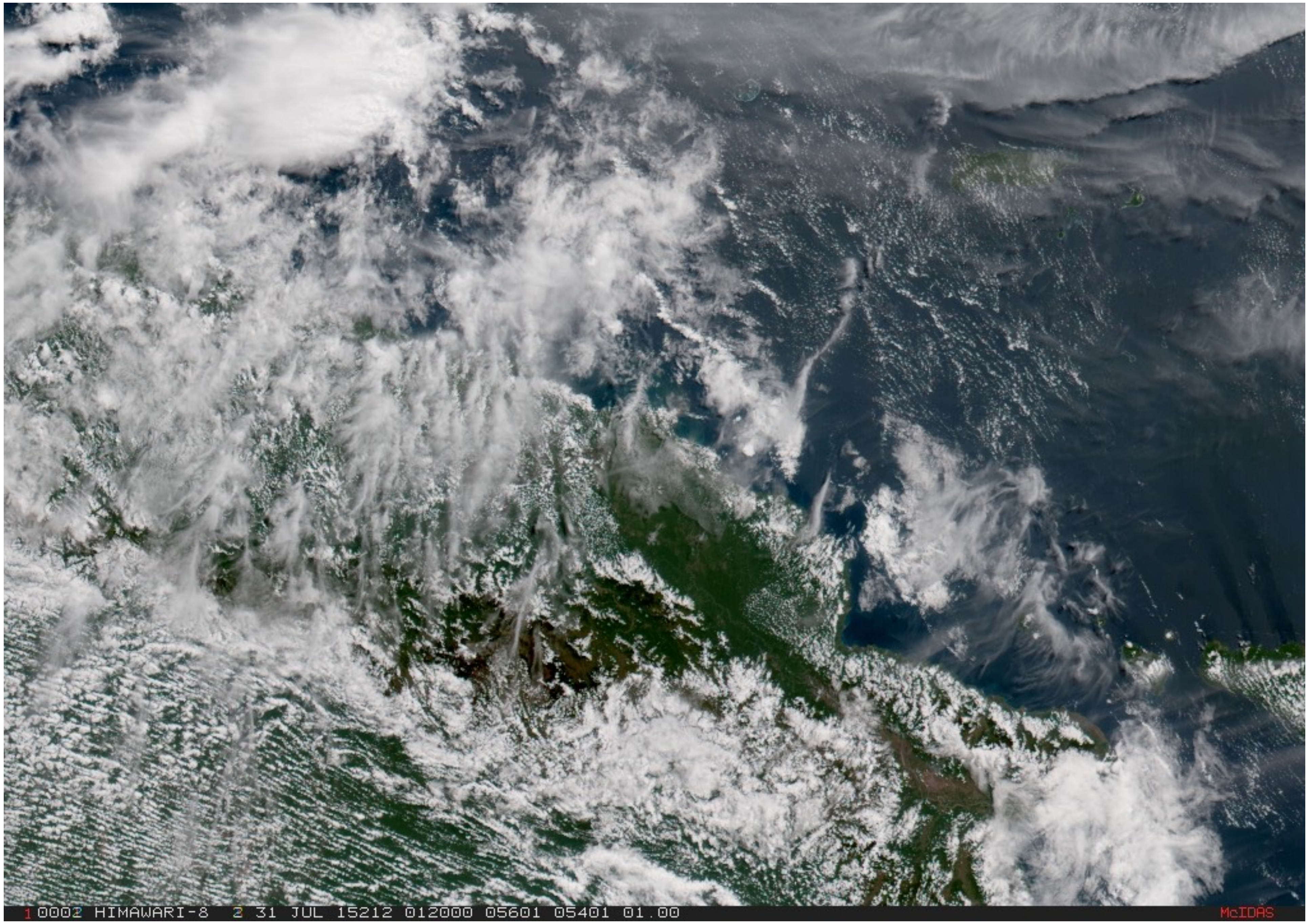

AIRES Pty Ltd

Eruption Rate from Satellite Measurements

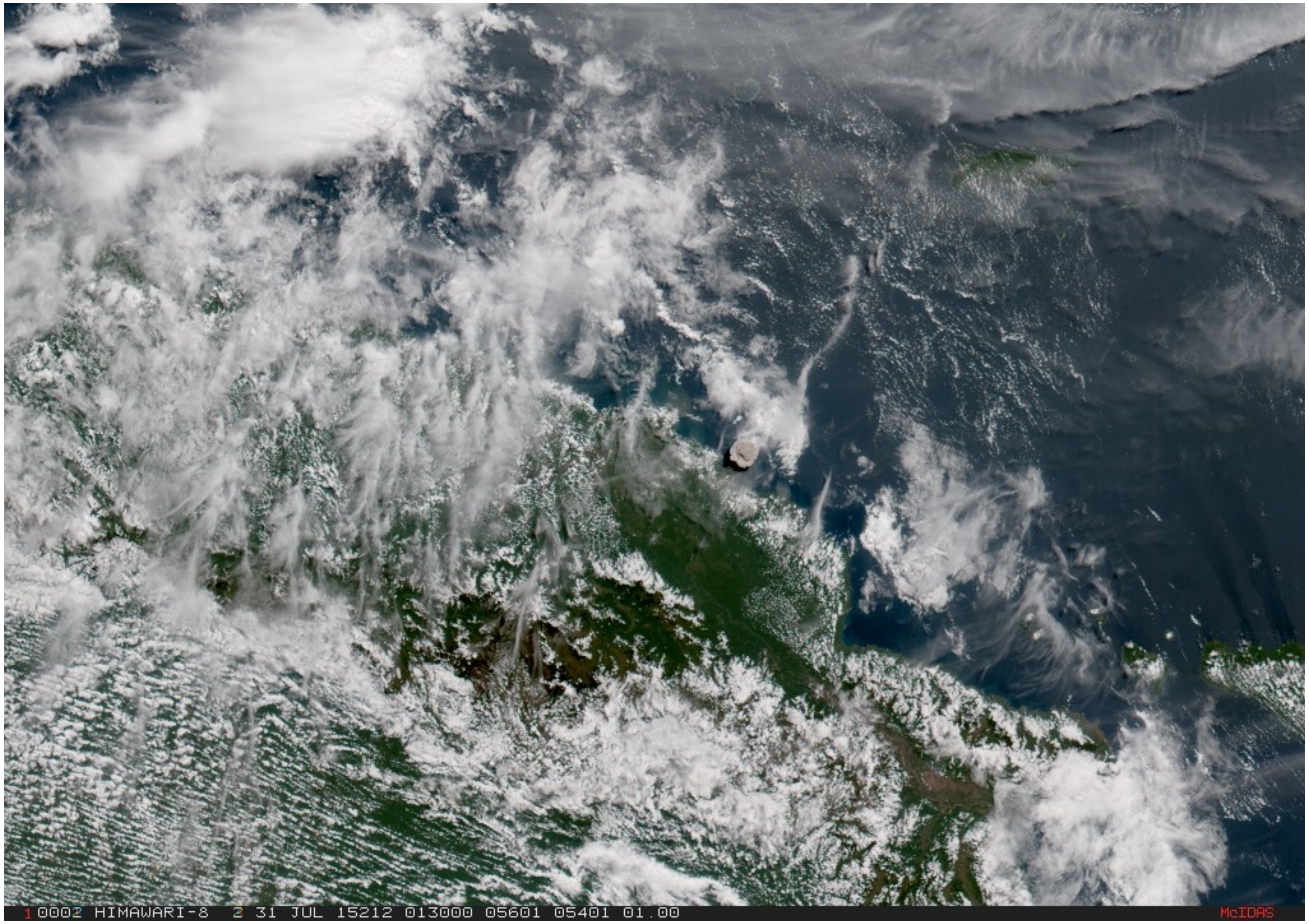

AIRES Pty Ltd

Eruption Rate from Satellite Measurements

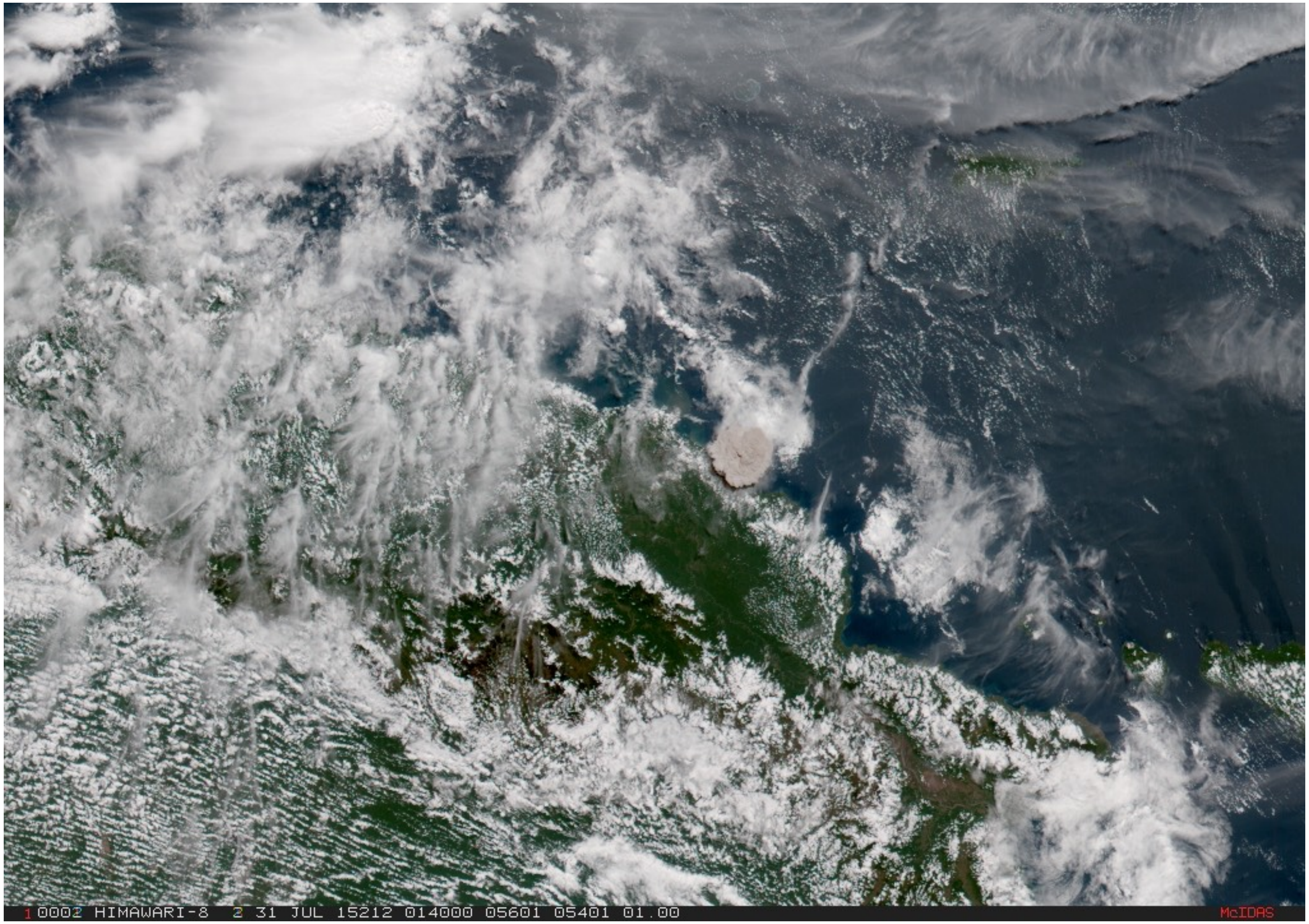

AIRES Pty Ltd

Eruption Rate from Satellite Measurements

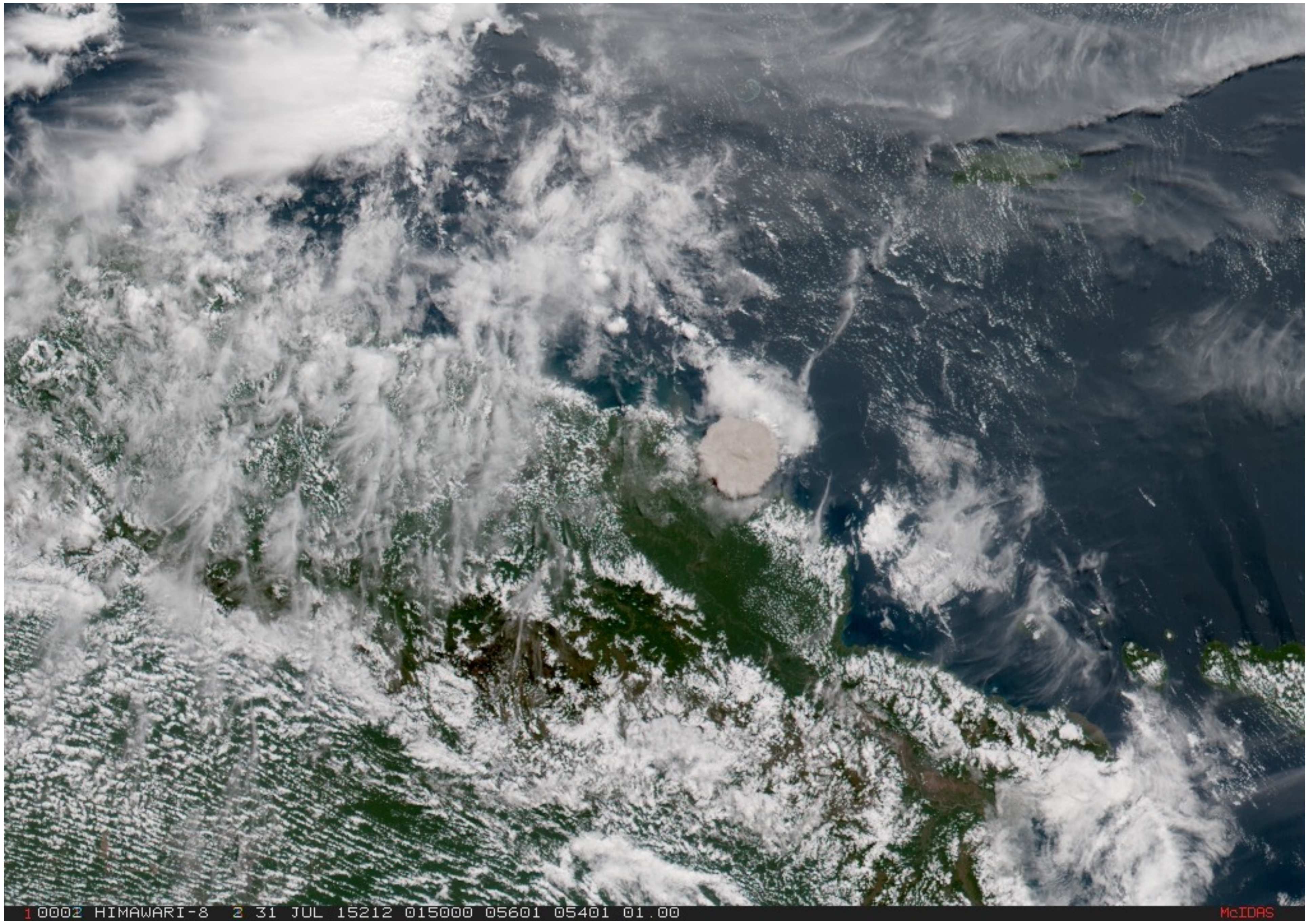

Eruption Rate from Satellite Measurements

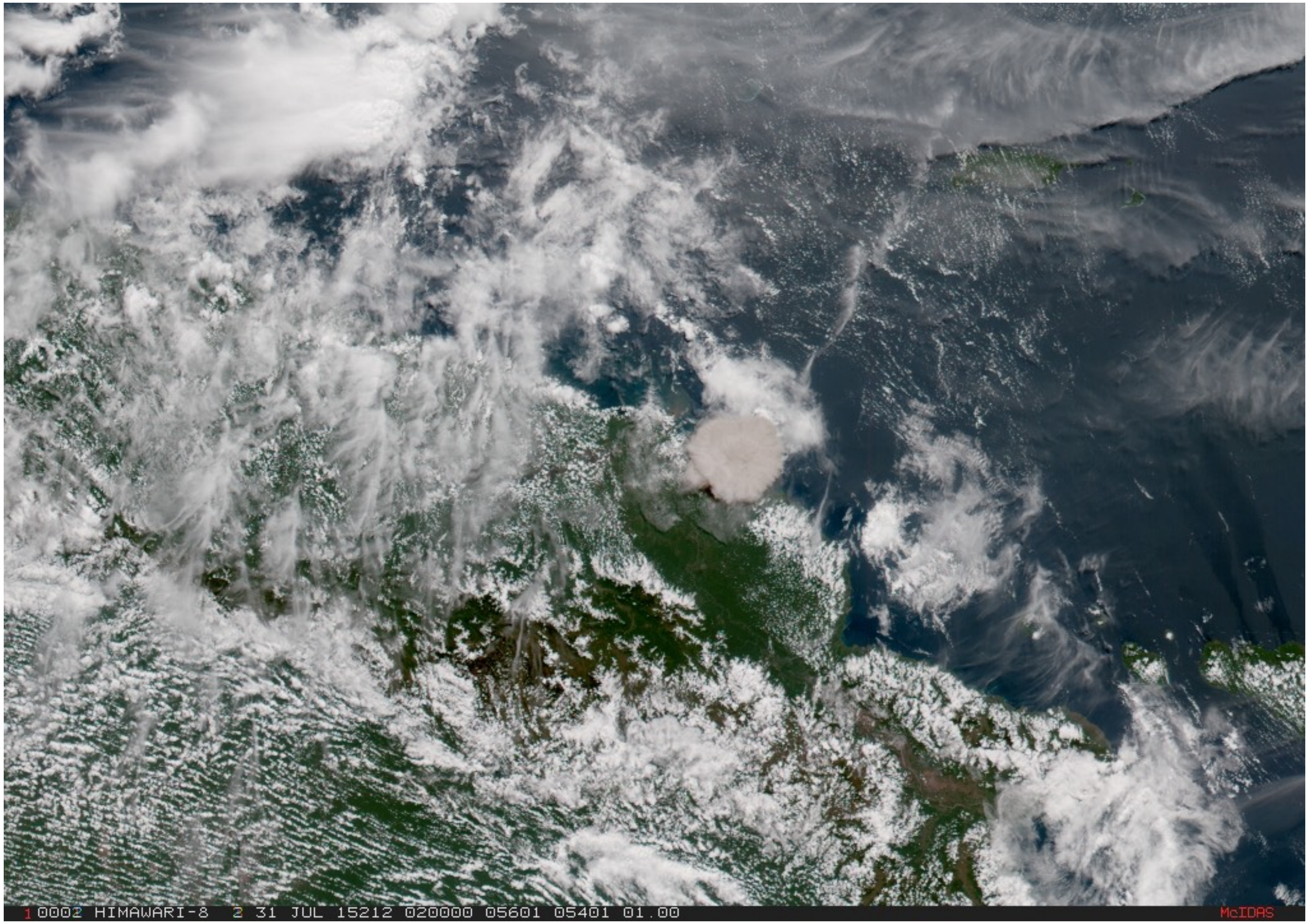

AIRES Pty Ltd

Eruption Rate from Satellite Measurements

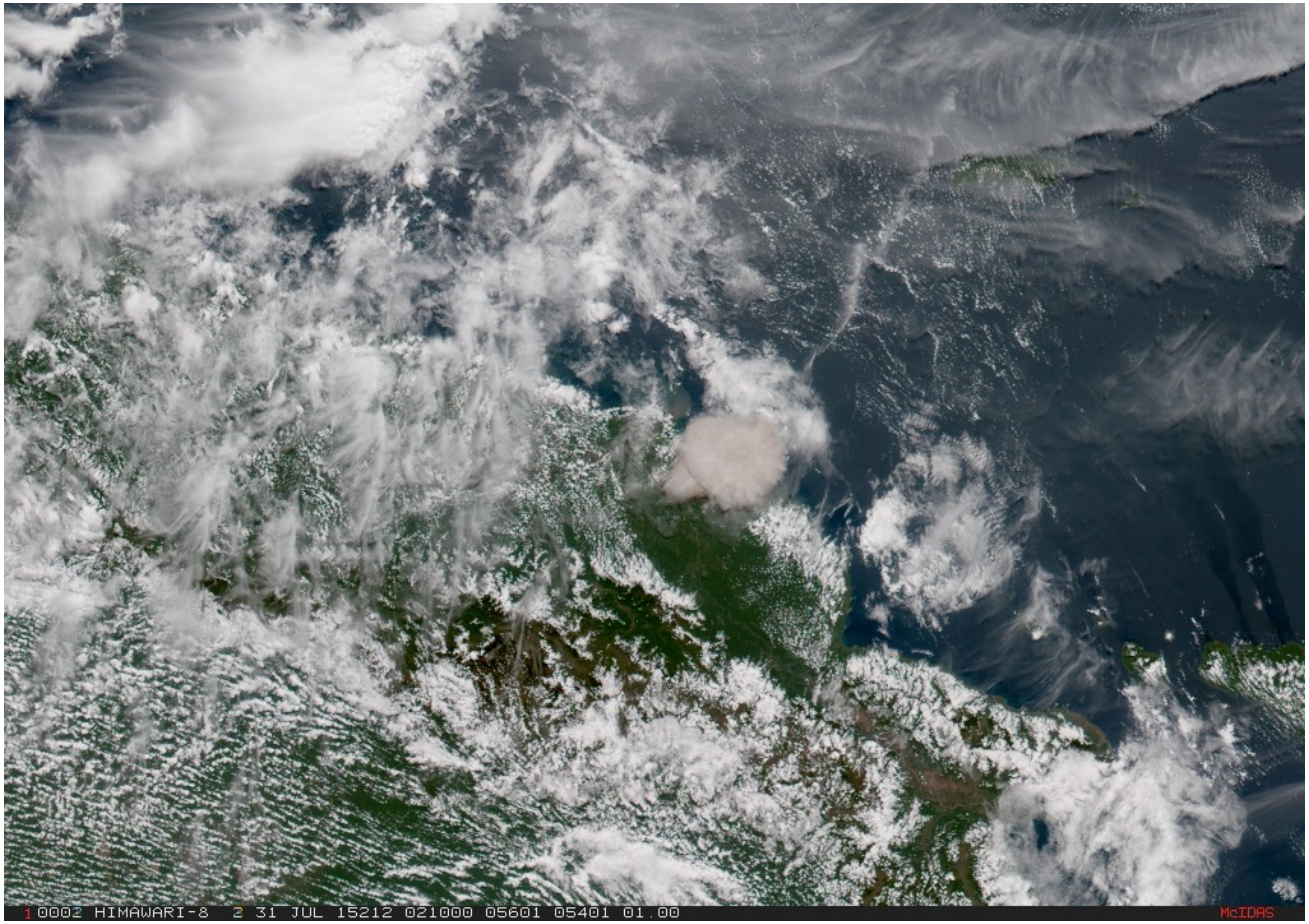

AIRES Pty Ltd

Eruption Rate from Satellite Measurements

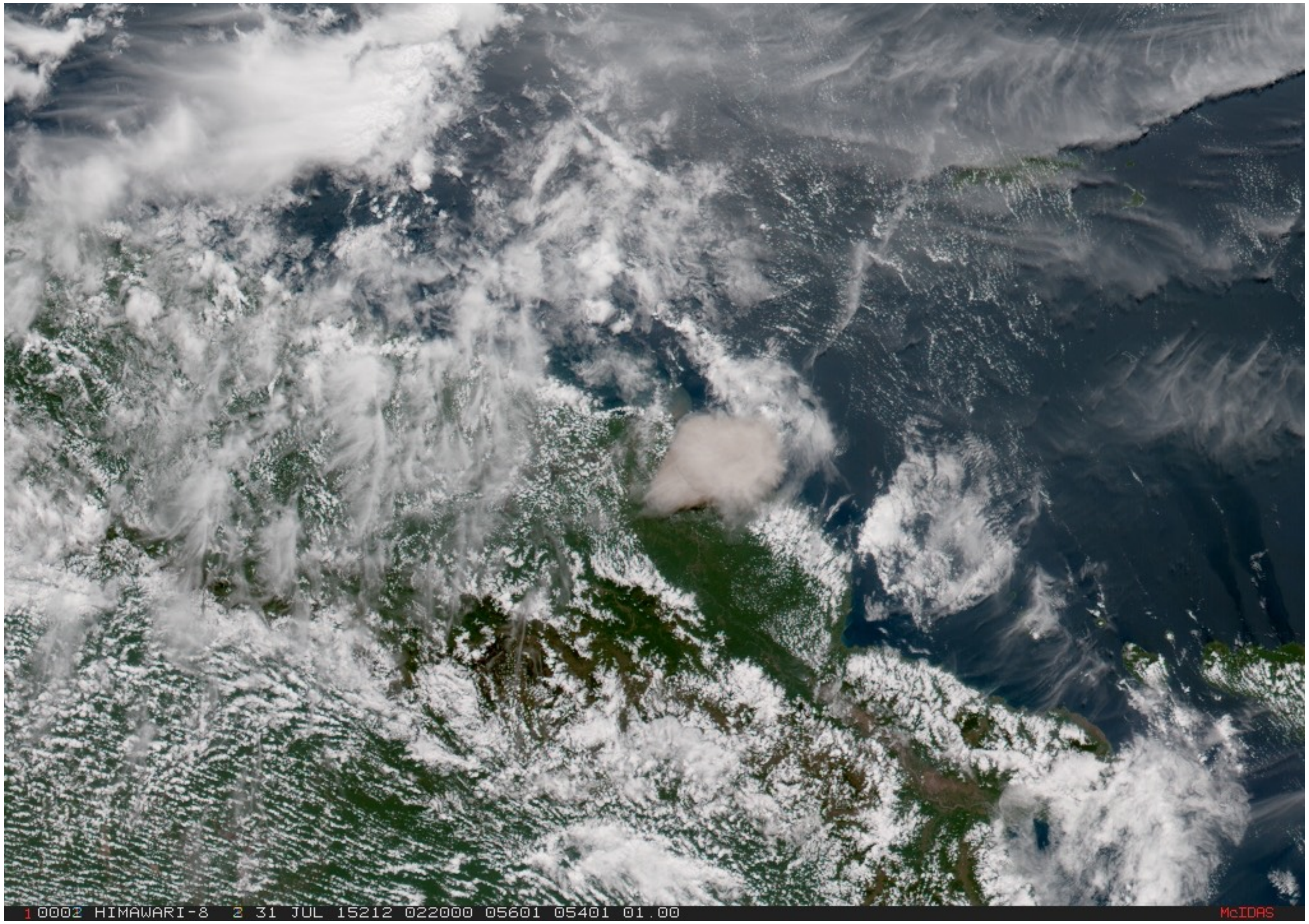

AIRES Pty Ltd

Eruption Rate from Satellite Measurements

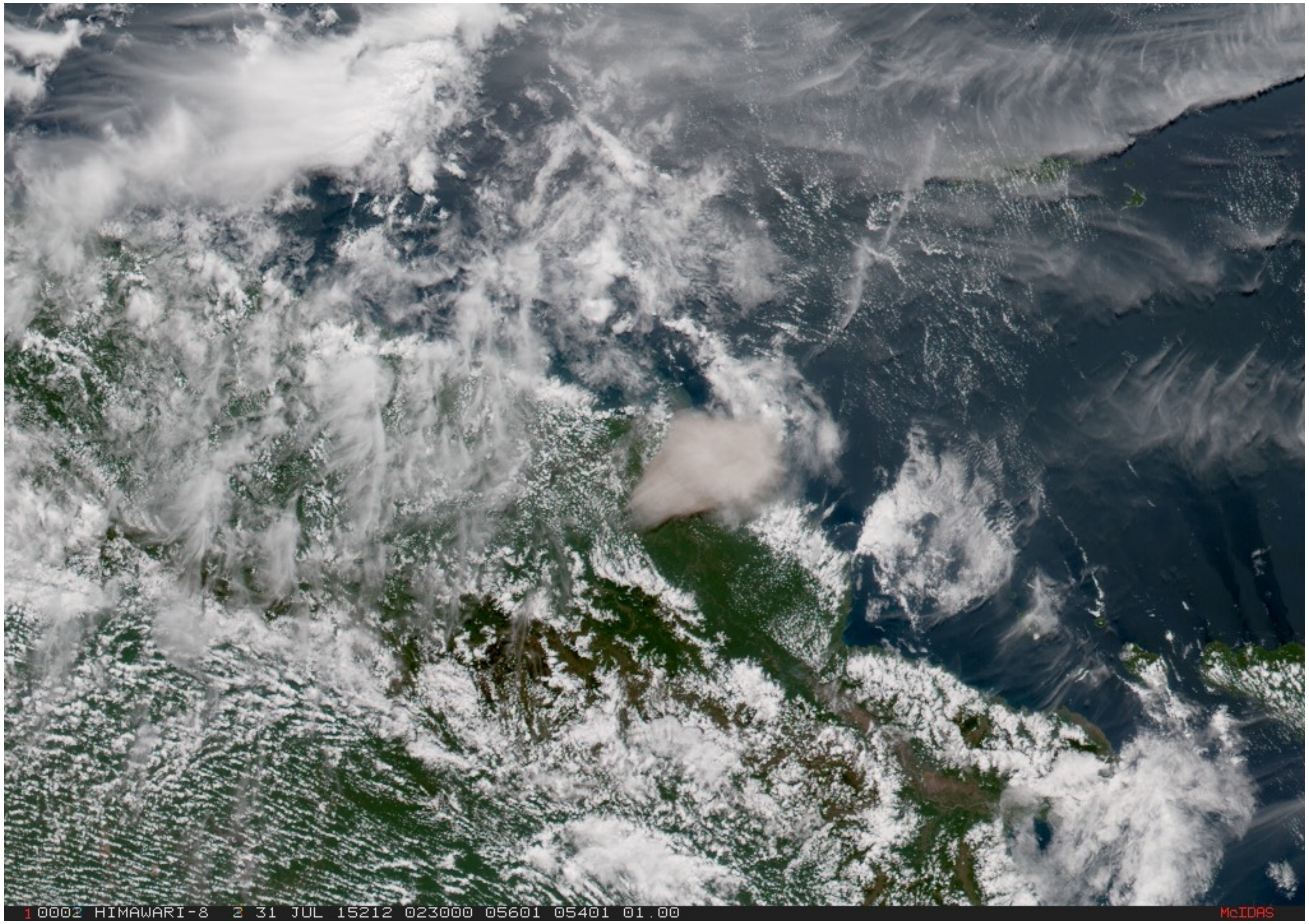

AIRES Pty Ltd

Eruption Rate from Satellite Measurements

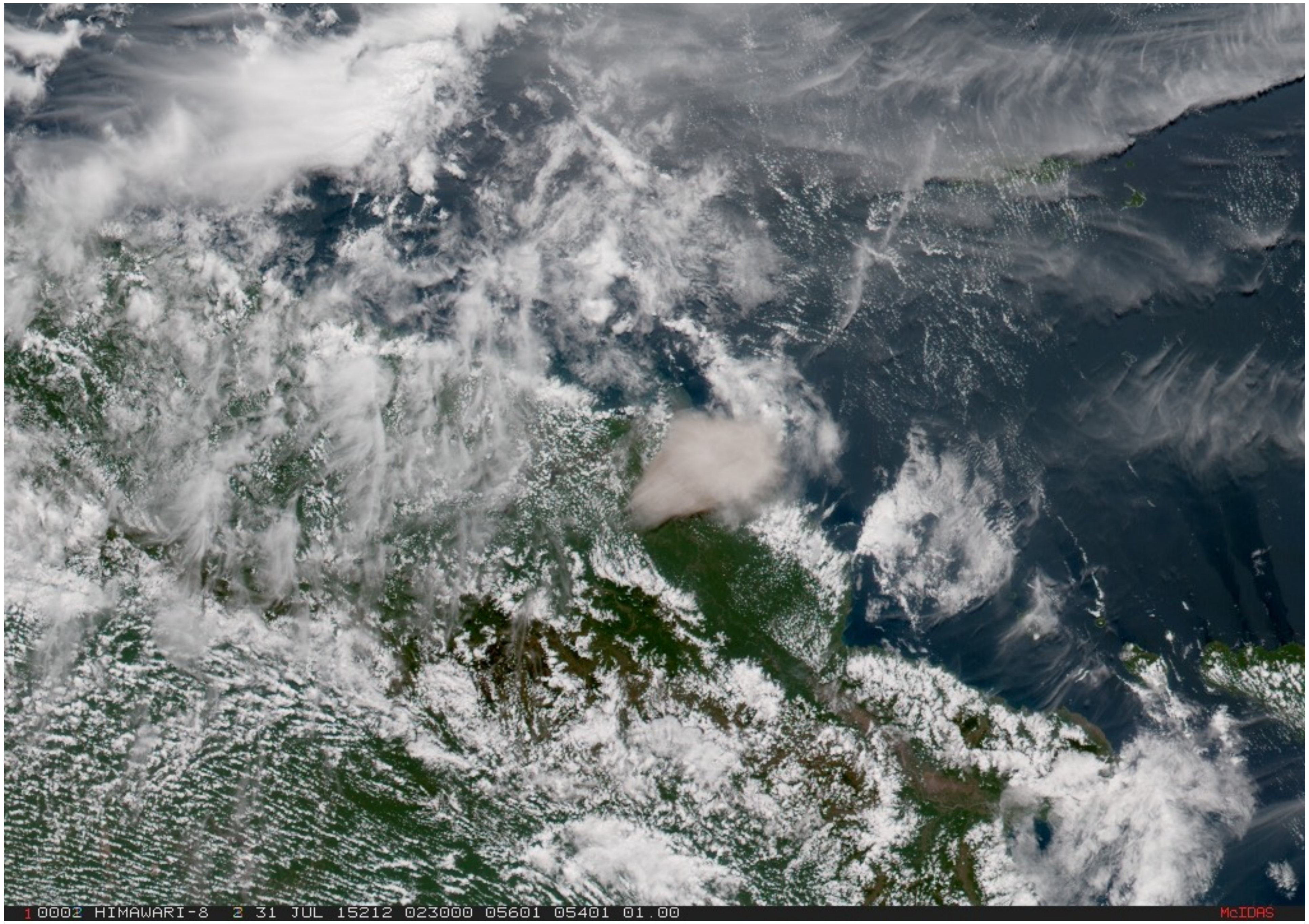

Eruption Rate from Satellite Measurements

Can the rapid spread of the umbrella cloud be used to estimate the eruption rate of the vertical column?

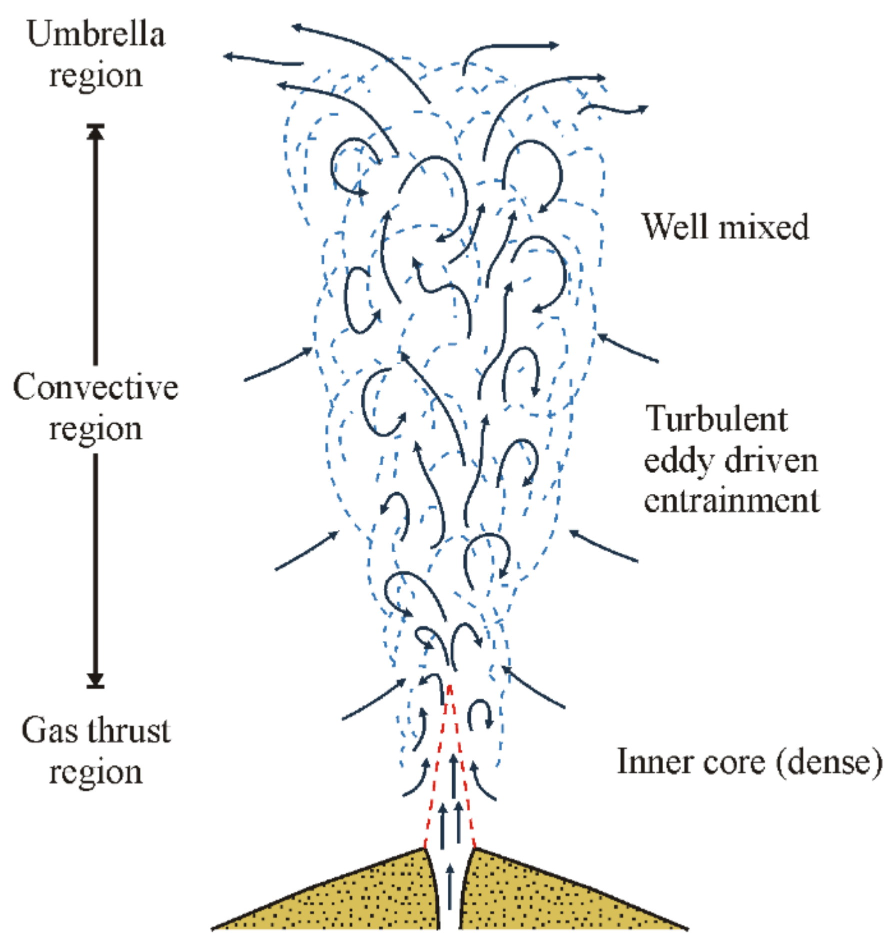

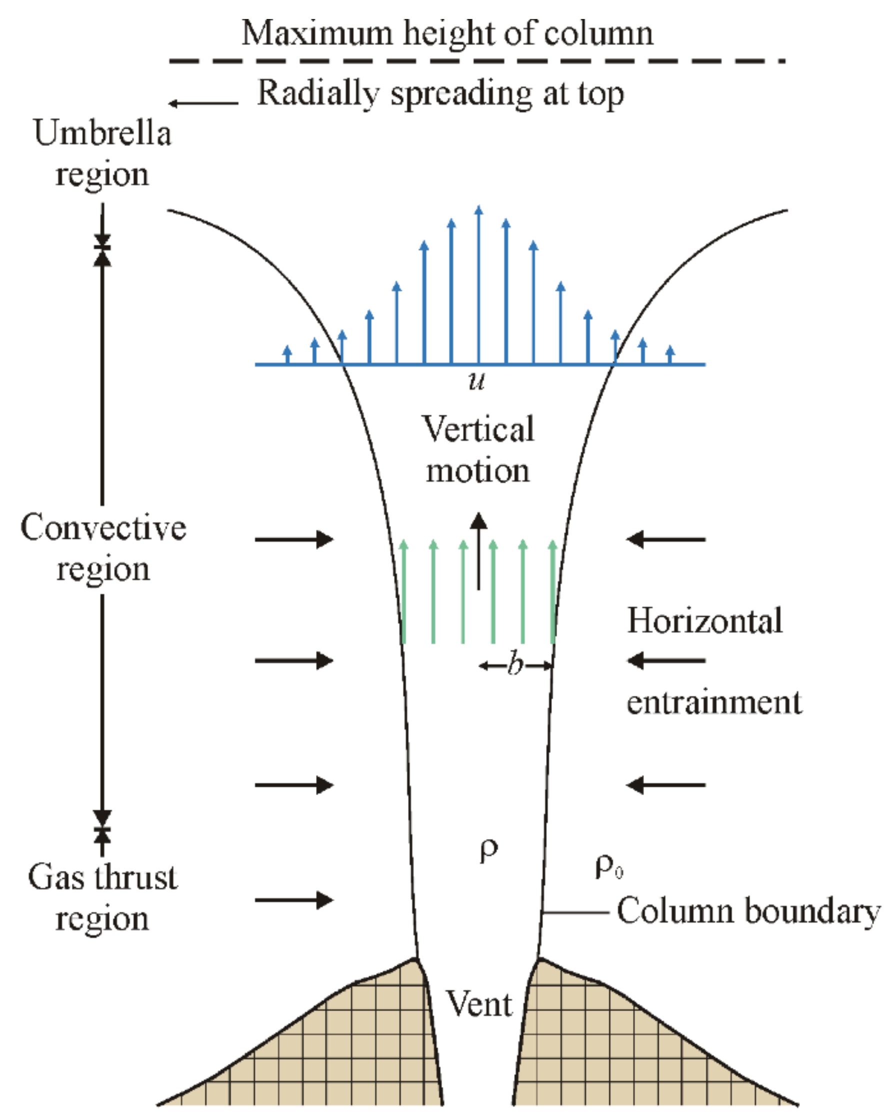

After Agusto Neri

AIRES Pty Ltd

Eruption Rate from Satellite Measurements

Satellites detect many eruption columns from early onset

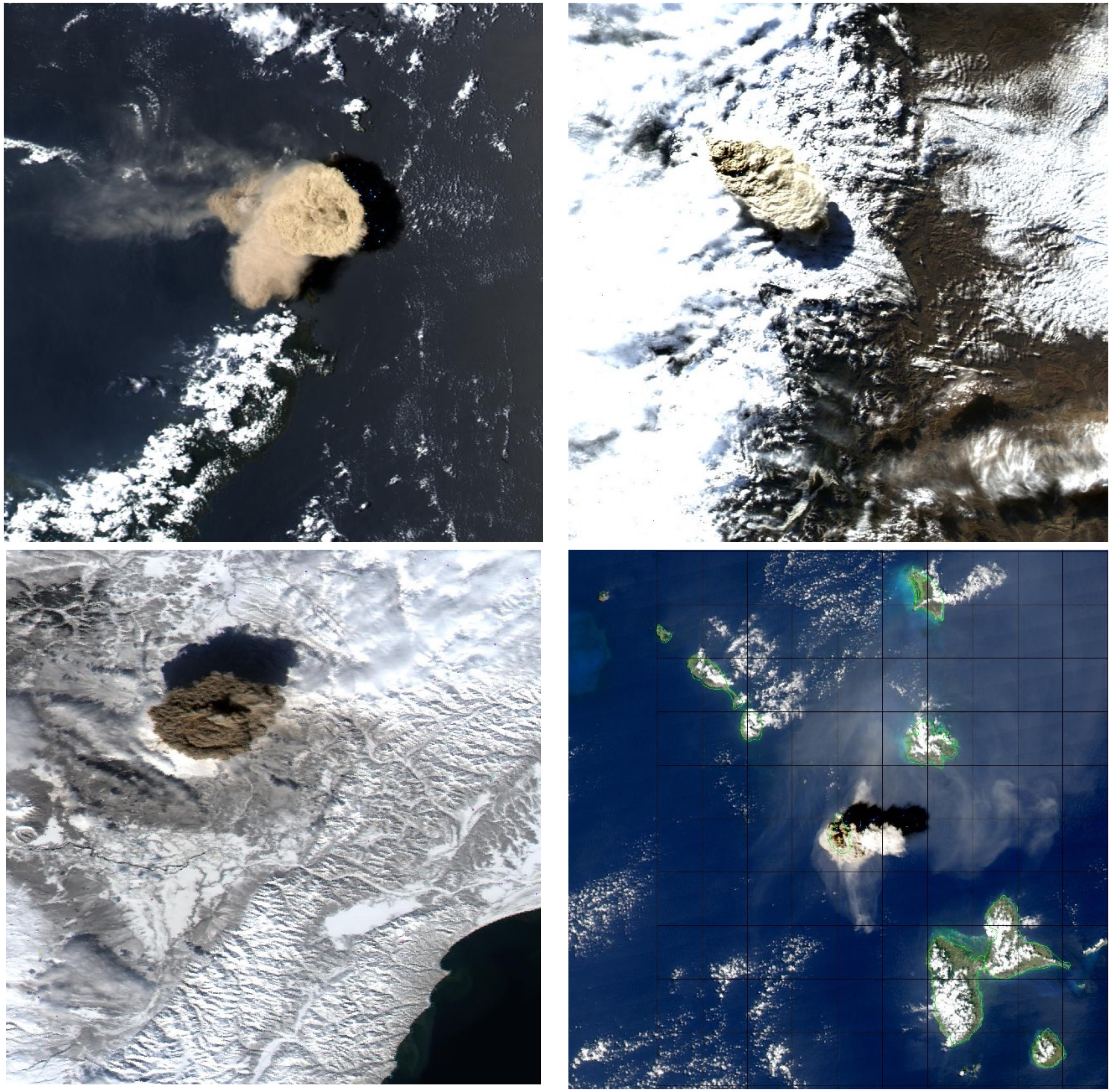

Eruption Rate from Satellite Measurements

Example: Aoba/Ambae eruption – April 2018

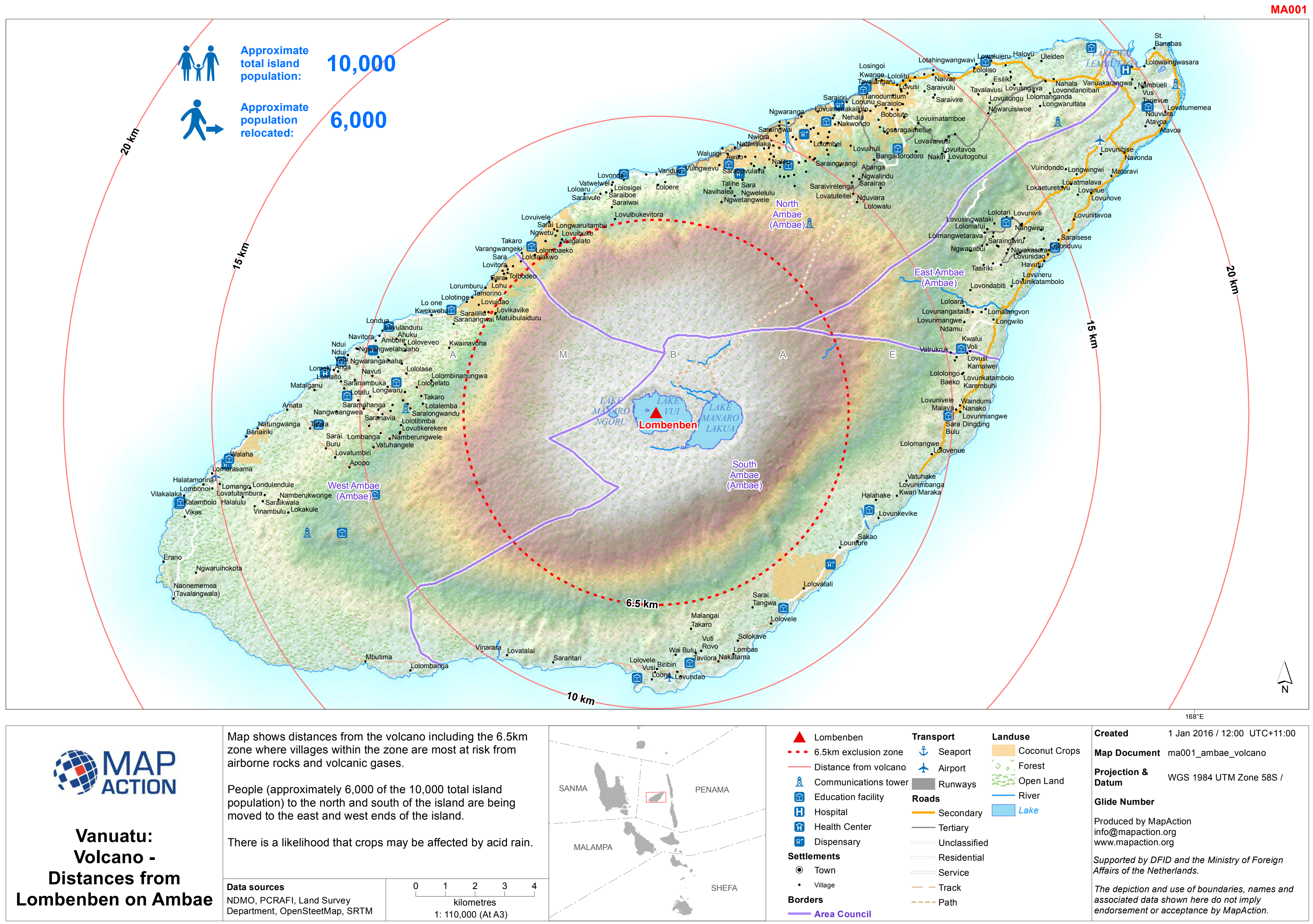

AIRES Pty Ltd

Eruption Rate from Satellite Measurements

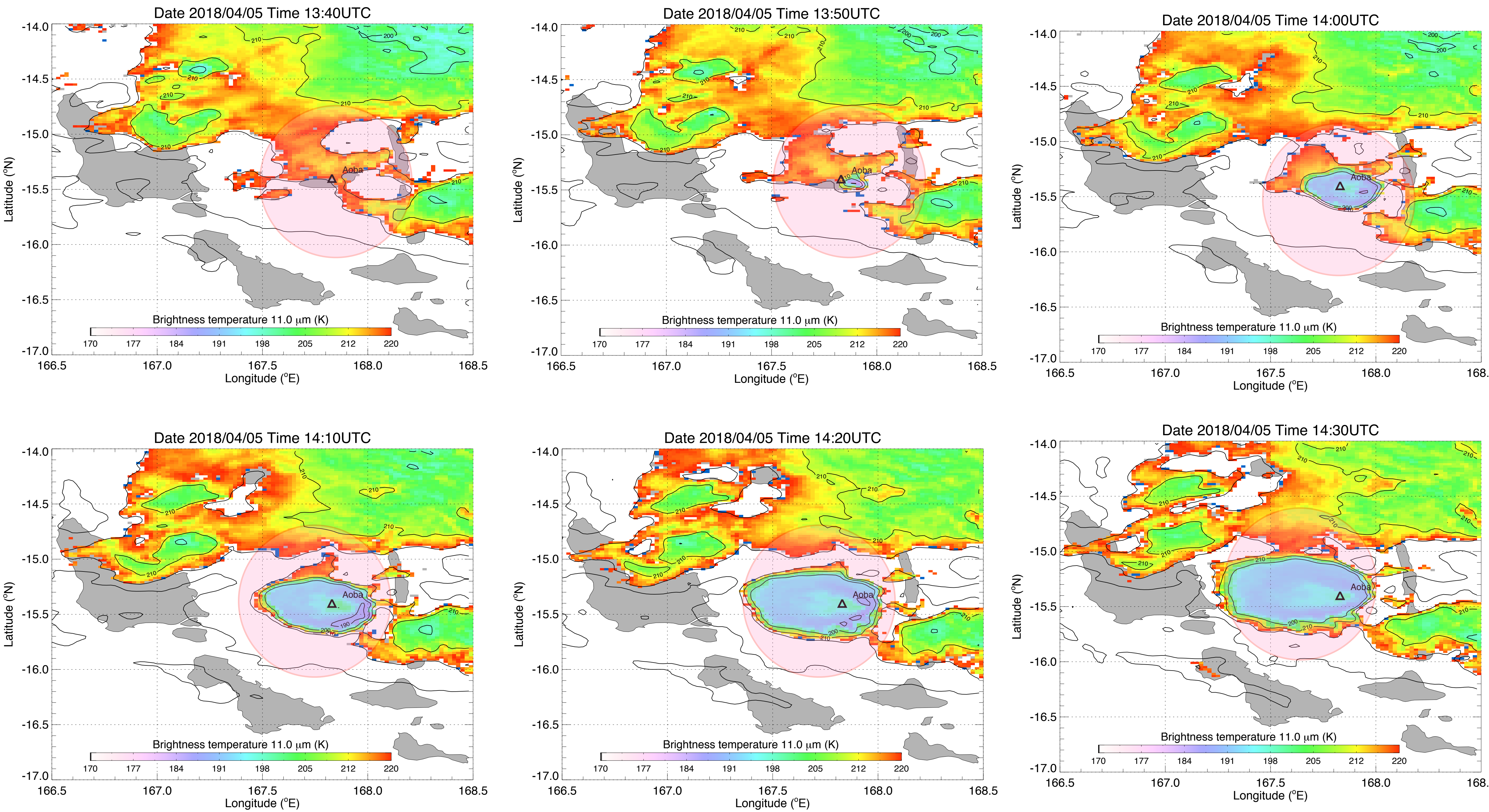

Evolution of the 11 μm brightness temperature at 10 min intervals

AIRES Pty Ltd

Eruption Rate from Satellite Measurements

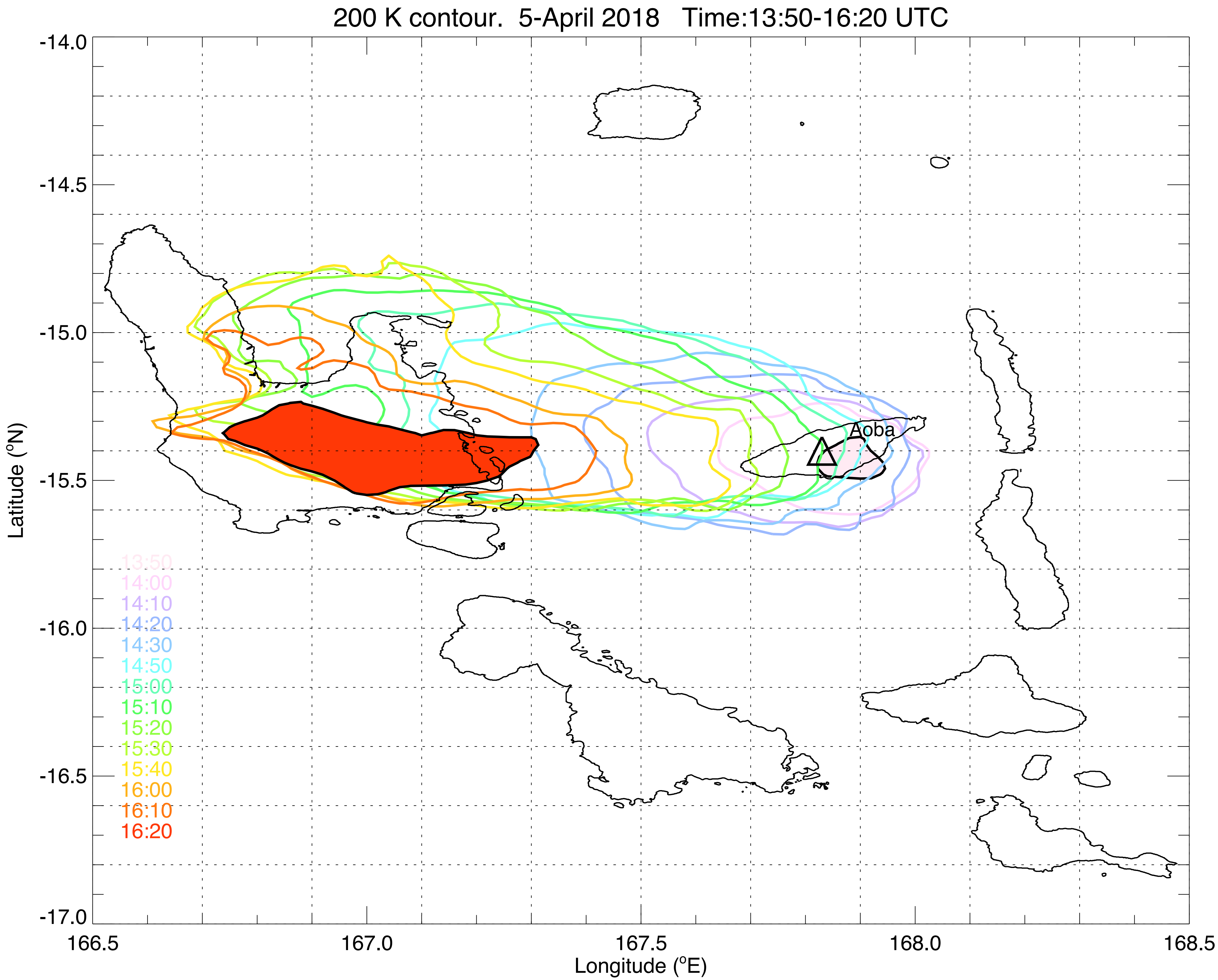

AIRES Pty Ltd

Eruption Rate from Satellite Measurements

The volcanic cloud is easily observed in Himawari-8 and other satellite data. Himawari-8 samples the region at 2 x 2 km^2 spatial resolution in the infrared every 10 minutes. Assuming that the eruption column rises at some vertical ascent rate, unaffected by cross-winds, reaches a neutral buoyancy level and then spreads horizontally, an estimate of the rate of radial spreading can be used to estimate the eruption rate at the top of the cloud, essentially as a consequence of conservation of mass. A common formulation for the increase of the radius of the umbrella cloud is (Sparks et al., 1997; Pouget et al., 2013):

$$r_t = \left(\frac{3\nu N Q_t}{2\pi}\right)^{1/3} t^{2/3}$$

r is the radius

t is time

Q is the volumetric eruption rate

N is the Brunt-Vaisala frequency

ν is a dimensionless constant

Eruption Rate from Satellite Measurements

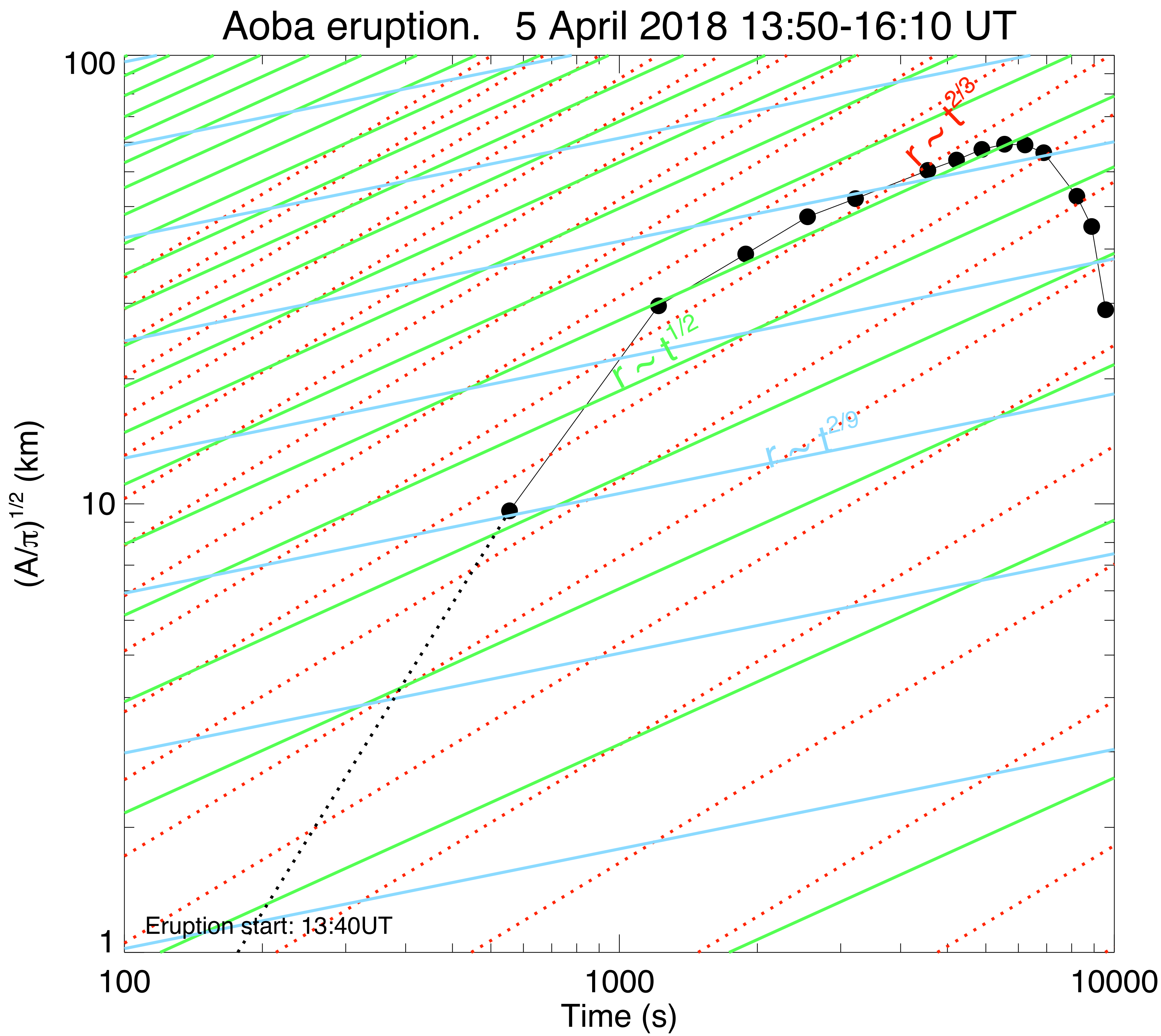

Eruption Rate from Satellite Measurements

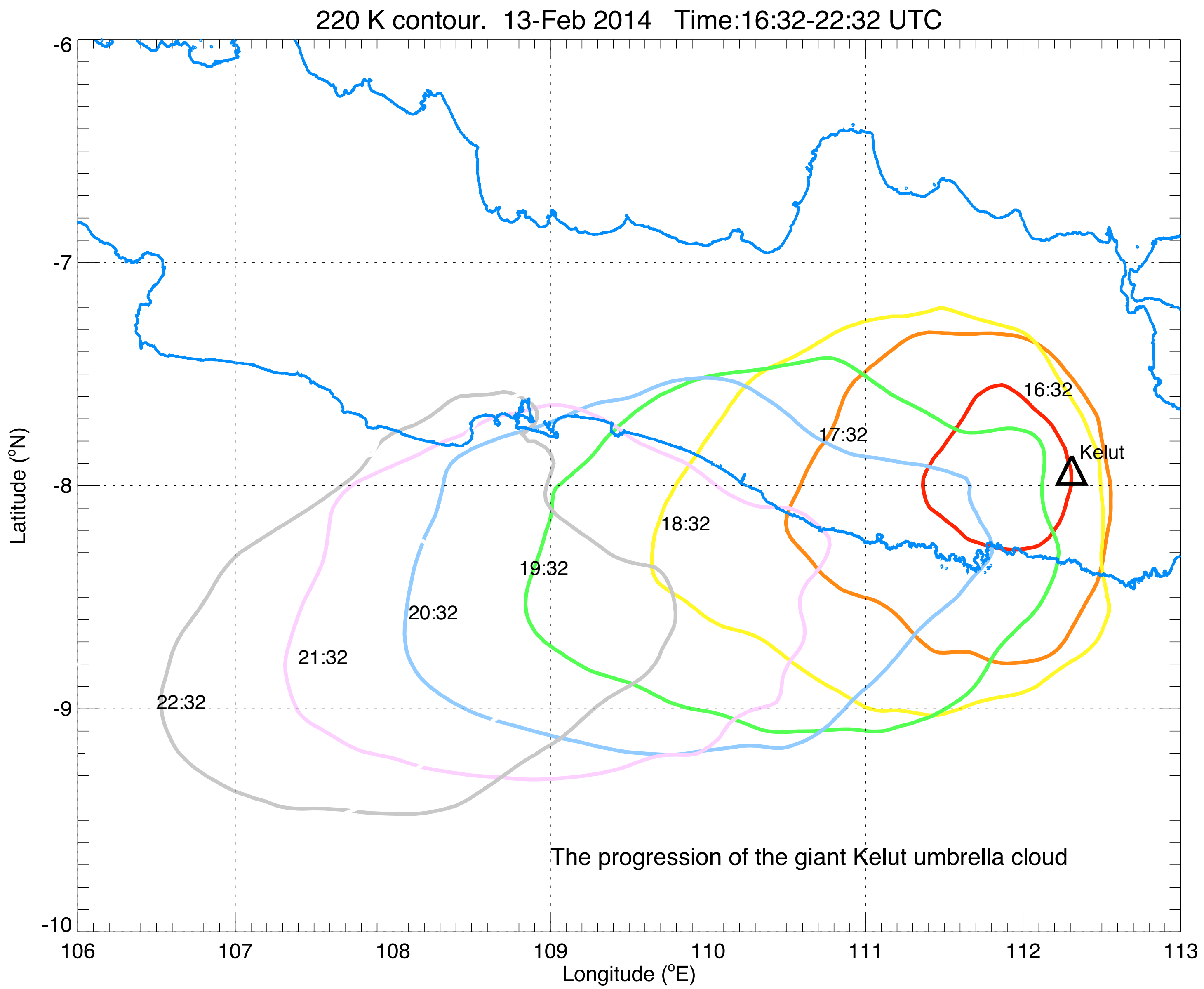

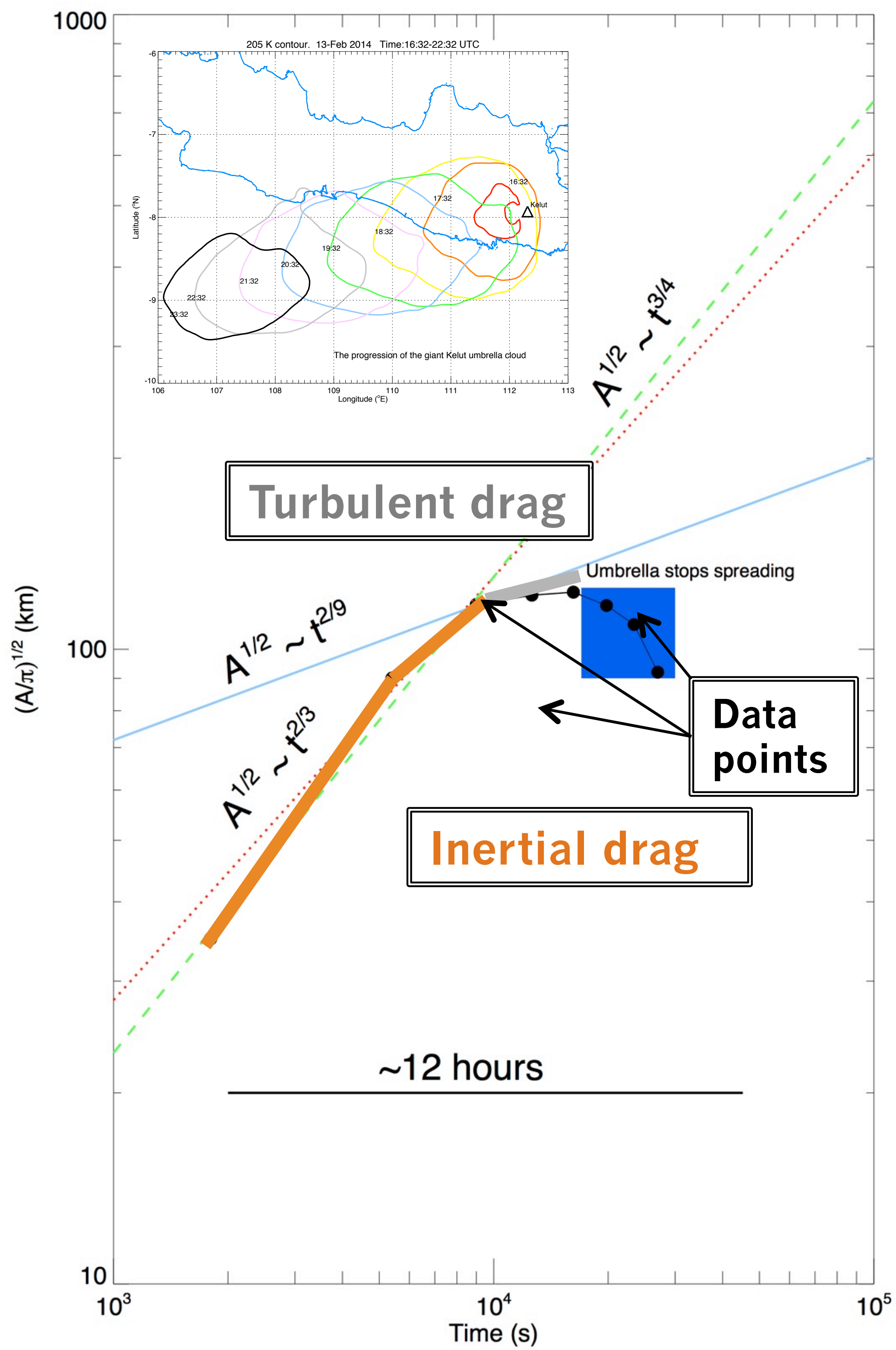

Eruption Rate from Satellite Measurements